# DENDRON AVIDITY PLATFORMS WITH ORTHOGONAL FOCAL POINT COUPLING SITE

**by**

**Daniel Quinn McNerny**

A dissertation submitted in partial fulfillment
of the requirements for the degree of
Doctor of Philosophy
(Chemical Engineering)
in The University of Michigan
2010

Doctoral Committee:

Professor James R. Baker Jr., Chair
Professor Mark M. Banaszak Holl
Associate Professor Joerg Lahann
Associate Professor Michael Mayer

To Erin, Mom and Dad

## ACKNOWLEDGEMENTS

In late 2005, several months after arriving at Michigan, I was without a laboratory and my undergraduate advisor was preparing to contact his collaborators elsewhere on my behalf to find me a new home. 5 years later, I am still at Michigan and have experienced my most rewarding and enjoyable years here. I would like to express my gratitude to the long list of people responsible for this.

I thank my advisor, Dr. James Baker, for giving me the opportunity to work in such a unique multidisciplinary environment and for his help and guidance. I hope I am able to emulate his work ethic and drive to meet goals throughout my professional career. It would be inappropriate of me to go further without acknowledging Prof. Mark Banaszak Holl. While the records will only list him as a member of my dissertation committee, he has served in a much larger capacity by graciously allowing me to work in his chemistry labs, continuously aiding in the growth of my chemistry abilities, and providing advice to assist me in being successful as a student and beyond. I would like to thank my committee members, Prof. Joerg Lahann and Prof. Michael Mayer, for their helpful suggestions during my graduate career.

Working in the Michigan Nanotechnology Institute for Medicine and Biological Sciences (MNIMBS) has brought me into contact with many excellent people; being surrounded by experts in so many different areas is something I doubt I'll ever be able to

replicate. While each of them is intellectually gifted, they are even better people to be associated with- and I'm lucky to call many of them friends.

When I started in MNIMBS another engineering student had also just joined the group. I am fortunate that student was Doug Mullen. His project complimented my own, and coupled with our similar educational backgrounds, identical initials and, according to some nearsighted individuals, similar physical features (I have better hair), many people get us confused. While I always played up the frustration, I always took it as a complement to be mistaken for such a model individual. Doug is a rare friend, as I sure he is to most people he meets, and I feel in debt to his kindness.

I found an equally kind friend in Kevin Landmark, whom I was lucky to share Room 2624 with for our shared time within the group. I owe him for keeping even the most taxing days at work light and humor-filled and for helping me always keep a sense of perspective beyond lab.

Upon joining the lab, Pascale Leroueil immediately became my overprotective big sister. While I will forever remain uncertain to why I deserve her unselfishness, I hope she realizes how much I value her advice, conversation, and love of ridiculously fattening foods.

I am grateful for the assistance and friendship offered by Joey Wallace, in addition to the confocal images in this thesis, since he began his postdoc with the Banaszak Holl group. While I believe few would be able to meet the bar he has set as a young scholar, I have found it most helpful to use him as a role model in preparing for my own postdoc and eventual career. I always enjoyed our conversations, whether they

ranged from planning the institute's certificate program or complaining in our Monday morning quarterback sessions.

As an engineer, my learning curve was likely higher than it would be for most when taking a project containing a substantial percentage of synthetic chemistry. Thankfully, the structure of the institute allowed me to receive training from some remarkable and incredibly patient scientists. Most important was Stassi DiMaggio, who took the task of overseeing Doug and I upon our arrival. While unfortunate circumstances in New Orleans brought her to us, I could not wish for a better teacher. I have missed her stories since her return home, and always look forward to her next visit. Thanks to Dr. Rameshwer Shukla for his invaluable help on my project. I owe him for helping me learn to think more like a chemist and to be able to overcome many of the hurdles that hindered this project in its infancy. I would also like to thank Drs. Istvan Majoros, Xue-min Cheng, and Baohua Huang for their assistance, training, and valuable conversations regarding synthetic chemistry throughout my doctoral studies. Thanks to Dr. Jola Kukowska-Latallo for her assistance and training in the biological studies that contributed to this thesis. Thanks to James Windak of the Chemistry Department for training and assistance on many of the analytical equipment.

Many thanks to Ankur Desai for his tireless contributions to not only my own work, but to the success of everyone within the institute. Our analytical guru is responsible for many of the methods that allow us to evaluate our materials. I regret the inability to be able to properly convey my gratitude for the effort and quality of his work.

I'd like to especially thank Ahleah Rohr, Ajdin Kavara, and Randon H Walker. It was always nice to have an excuse to visit the organometallics lab; while I greatly

appreciate all of the help with the questions I had, I equally enjoyed Ahleah criticizing my barber, Ajdin's sharing his weekly lesson in American pop culture, and Randon's calming influence. Thank you for being a pleasure to know.

I would like to thank the remaining members of MNIMBS that have all contributed to my growth, particularly Prof. Bradford Orr and Dr. Thommey Thomas. I would also like to acknowledge the administrative and support staffs of MNIMBS that help make much of the inter-workings run so smoothly: Gloria Lippens, Mike Parise, and Claire Verweij. Thanks to the many students of MNIMBS and the Banaszak Holl group for their contributions.

Thank you to Annie Mitsak, Linh Luong, Mike Senra, Neil Schweitzer, and Joe Mayne for making much of my time in Ann Arbor, but out of lab, as enjoyable as it has been. I would also like to thank Court Heller, Erik Degelman, Gary Grochmal, and Jessica Graham, who I am lucky to have remained friends with since my departure from Pittsburgh and am happy were able to share much of this experience.

I cannot understate how significant the contributions of my family were in allowing me to achieve the goals I have set for myself. I have been blessed and honored to have a family as caring as I have, from my grandparents to my sister Kate. To Mom and Dad, thank you for giving me every opportunity for success and instilling in me the best parts of you both. My own success is yours as well. I love you dearly.

Finally, and most importantly, I thank my beautiful wife, Erin. While uncredited on any of my published work, she has served as initial reviewer, editor, presentation coach, unlicensed psychiatrist, career counselor, medic, chauffer, and my best friend. My greatest and proudest accomplishment has been marrying you. I love you.

## TABLE OF CONTENTS

## LIST OF FIGURES

## LIST OF ABBREVIATIONS

AF: Alexa Fluor

cHex: Cyclohexane

CuAAC: Copper catalyzed alkyne-azide cycloaddition

DMF: Dimethylformamide

DMSO: Dimethyl sulfoxide

EDC: 1-ethyl-3-(3-dimethylaminopropyl)carbodiimide)

ESI MS: Electrospray Ionization Mass Spectroscopy

EtOAc: Ethyl acetate

HCl: Hydrochloric acid

HPLC: High-pressure/performance Liquid Chromatography

HUVEC: Human Umbilical Vein Endothelial Cells

MALDI TOF: Matrix-assisted laser desorption/ionization time-of-flight

MeCN: Acetonitrile

MeOH: Methanol

MNIMBS: Michigan Nanotechnology Institute for Medicine and Biological Sciences

MTX: Methotrexate

MWCO: Molecular Weight Cut Off

NaOH: Sodium hydroxide

NMR: Nuclear Magnetic Resonance

PAMAM: Poly(amidoamine)

PBS: Phosphate buffered saline

PE: Polyester

PEG: Poly(ethylene glycol)

UPLC: Ultra-performance Liquid Chromatography

## ABSTRACT

This thesis explores the design and synthesis of bifunctional or modular platforms from poly(amidoamine) (PAMAM) dendrons. PAMAM dendrons with an orthogonal focal point are evaluated, testing several click chemistry reactions for high conversion and mild conditions. The orthogonal reaction chemistry used at the dendron focal point gives a precise 1:1 ratio of the attachment of multiple functionalities to a small molecular weight, chemically stable high avidity molecule.

In the first component of the thesis, dendrons were synthesized with c(RGDyK) peptide on the surface to create a scaffold for cellular targeting and multivalent binding. Binary dendron-RGD conjugates were synthesized with a single imaging agent, therapeutic drug, or additional functionalized dendron at the focal point after a copper(I)-catalyzed alkyne-azide cycloaddition (CuAAC) click reaction. The targeted-dendron platform was shown to specifically target $\alpha_V\beta_3$ integrin expressing human umbilical vein endothelial cells (HUVEC) and human glioblastoma cells (U87MG) *in vitro* via flow cytometry. Specific targeting of the dendron-RGD platform was further confirmed by confocal microscopy. Biological activity of the targeted drug conjugate was confirmed via XTT assay.

The remainder of the thesis explores click chemistry reactions that do not require a metal catalyst, which may cause undesired toxicity for some biological applications. Thiol-based click chemistry, specifically the thiol-ene and thiol-yne reactions, is explored

on dendron platforms. The thiol click reactions provide an improved efficiency, compared to CuAAC, by reaching quantitative conversion of the focal point in most cases. The thiol click reactions suffer from some setbacks: the need for a thermal or photoinitiator may prevent the conjugation of some functional ligands and the thiol chemistry is more prone to side reactions.

Finally, strain-promoted alkyne-azide cycloadditions are examined. The ring-strain click chemistry displayed a high degree of orthogonality and quantitative conversion when applied to dendrons. Unfortunately, attempts to build dendrons from a cyclooctyne core were unsuccessful, as traditional growth reactions led to the partial cleavage of the strained ring. However, an alternative convergent synthesis approach is suggested. In general, these studies of orthogonal coupling pathways serve as a framework to selectively combine relevant functions to well-defined modular platforms for many diagnostic and therapeutic applications.

# Chapter 1:
# Introduction

## Dendritic platforms for targeted therapeutics

The narrow therapeutic index of many cytotoxic therapeutics, including doxorubicin, vincristine, cyclophophamide, and paclitaxel, often limits their effectiveness as they must be delivered in sub-optimal dosages to prevent side-effects in the patient (1). To remedy this problem, targeted scaffolds can be used to deliver the drug to the desired location in an increased, local concentration. As a result, the delivered drug is effective only where it is needed and undesired side toxicities are diminished. Examples of drug-targeting systems include nanoparticles, liposomes, micelles, linear polymers, branched polymers, and dendrimers (2).

Dendrimer-based platforms have achieved attention for use in pharmaceutical applications (3-13). Similar to other polymeric carriers, dendrimers can be synthesized to avoid structural toxicity and immunogenicity (14). However, the unique branched structure of the dendrimer allows for the platform to overcome several significant challenges faced associated with other polymeric carriers. Many polymers are highly heterogeneous, making characterization and batch reproducibility of the scaffold difficult. In contrast, the controlled synthesis and growth of dendrimers results in exceptionally low degrees of dispersity (PDI < 1.1) (15, 16) and well-defined average numbers of terminal groups for the conjugation of functional molecules, providing improved reproducibility of the scaffold compared to linear polymers. The ability to

synthesize dendrimers that mimic the size, solubility and globular shape of human proteins makes the technology an ideal choice for many therapeutic and diagnostic applications. Targeted dendrimer delivery platforms have been successfully tested in both *in vitro* and *in vivo* model tumor systems (17-26). Being only 1-10 nanometers in diameter enables dendrimers to efficiently diffuse across the vascular endothelium, internalize into cells, and be rapidly cleared by the kidneys (17, 27). This helps to avoid long-term toxicities and reduces the need for the polymer to be rapidly degraded in the body. The availability of multiple reactive surface groups enables the dendrimer to carry a higher payload of functional molecules, enhancing targeted toxicity; for example, the ability to couple multiple targeting molecules on the polymer provides the opportunity to create a platform with increased binding avidity through polyvalent cell interactions (15).

For a dendrimer to be an appropriate carrier for drug delivery *in vivo*, the polymeric molecules must be non-toxic, non-immunogenic, and be capable of targeting and reaching specific locations by crossing the appropriate barriers while being stable enough to remain in circulation. The vast majority of the dendrimers synthesized and published in literature are insoluble in physiological conditions or are incapable of remaining soluble after the addition of functional molecules and are inappropriate for biological applications. However, several classes of dendrimers have been shown to be useful scaffolds for biomedical applications; examples include polyesters (28, 29), polylysine (30), and polypropyleneimine (PPI or DAB) dendrimers (31, 32).

The most widely studied dendrimers in biomedical applications are poly(amidoamine) (PAMAM) dendrimers. The polyamide backbone synthesized from repeating reactions of methyl acrylate and ethylenediamine helps the macromolecule

maintain water solubility and minimizes immunogenicity (33). PAMAM dendrimers of different generation also are able to mimic the size and properties of globular proteins. However, PAMAM dendrimers offer several advantages over proteins, as proteins are fragile and can be denatured due to exposure to non-physiological temperature, light, or pH conditions (16). The amine-terminated surface of full generation PAMAM dendrimers allows for easy surface modification, enabling the platform to carry and solubilize hydrophobic therapeutic molecules, such as methotrexate (17, 33-36), in physiological conditions. PAMAM dendrimers exhibit little non-specific toxicity if the surface amines have been neutralized or appropriately modified (10, 12, 37-40).

**The perfect polymer's conjugates: far from perfect**

Yet, despite the many research efforts, dendrimer-based products have been slow to reach human trials and much of the excitement surrounding the application of this technology has dissipated. A critical problem that our group believes is stifling the progress of dendrimers is the polydispersity of its conjugates (Figure 1.1); this is a paradox for a platform touted for its uniformity.

Any therapeutic platform conjugated with multiple drug or targeting moieties through an excess of attachment sites can result in a heterogeneous population that becomes more disperse as more functionalities are added. This problem likely leads to unintended variations in biological activity, since the structural platform is not well understood and is difficult to reproduce. So while the dendrimer scaffold can be highly uniform in its number of attachment sites, it will still yield a distribution of conjugated (41, 42). Inadequate mass transport during the conjugation step can promote this

heterogeneity, especially for conjugation chemistries with fast reaction kinetics. This can result in significant portions of the sample either over or under-conjugated, altering the addition of future functionalities.

The degree of heterogeneity is frequently not discussed in published literature and is likely not a consideration in many of the dendritic or nanoparticle platforms. Improved characterization of the material composition is needed and could likely lead to a defined correlation between the distribution of functional components and activity.

The problem in understanding distributions in nanoparticle-ligand systems is in large part due to an inability of most analytical techniques to identify the distributions, instead measuring only the arithmetic mean number of ligands per particle. Efforts from our institute have developed HPLC methods capable of resolving and understanding these distributions (41, 42); however its use to resolve complex distributions may be limited to the few ligands that yield differences in HPLC columns motility once conjugated to the dendrimer.

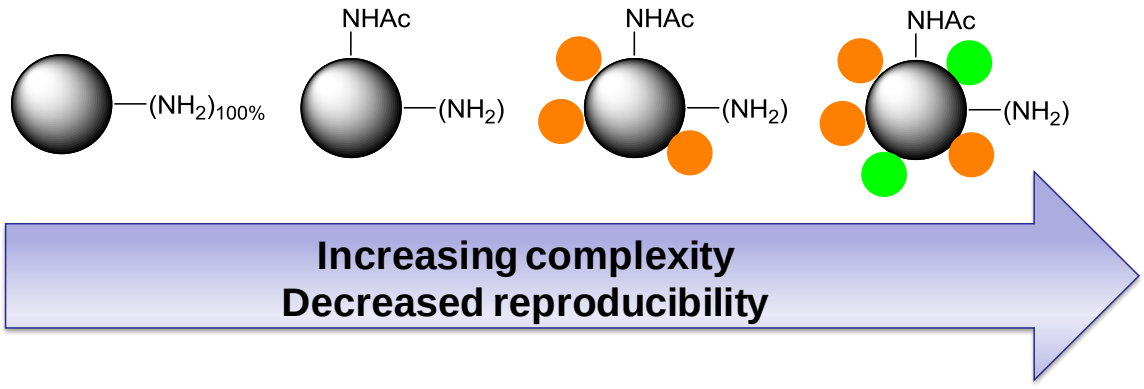


**Figure 1.1.** Polydispersity of the dendrimer platform increases when conjugating multiple functionalities to the surface of a single dendrimer. Ligand distributions are dependent upon distributions of prior conjugated groups, increasing the complexity of the platform while decreasing the reproducibility needed for many biological applications.

**Simplifying distributions on dendritic platforms through orthogonal coupling**

Orthogonal or modular pathways to construct multifunctional dendritic devices have the potential to overcome the ligand polydispersity of conventional dendrimer platforms by providing greater degree of specificity and flexibility in reaction conditions. Mono-functionalized materials can be individually characterized and assembled into more complex structures. Smaller modular units that reduce stochastic distributions or replace them for stoichiometric addition could be designed to ensure quality and improve reproducibility.

Initial work on modular dendritic platforms by Choi employed conjugating oligonucleotides to the terminal surface groups of a dendrimer (43, 44). Dendrimers with the complimentary strand of DNA would then form a binary dumbbell shaped structure. However, the overall yield of these complete structures was minimal, as Choi had to use a vast excess of dendrimer to DNA to prevent multiple oligonucleotides from coupling to a single dendrimer, which could lead to unwanted network formations.

Dendrons are branched polymers much like dendrimers (Figure 1.2). Dendrons differ in that they are wedge-shaped, opposed to spherical, and have a unique reactive site at the focal point. Dendrons are an attractive alternative to dendrimers because they offer an orthogonal coupling at their focal point, providing a single site of attachment per molecule and eliminating complex ligand distributions. In addition, these molecules maintain the branched architecture of dendrimer scaffolds for multivalent targeting (Figure 1.3). Choi's oligonucleotide hybridization strategy was adapted for dendrons by Dematteі et al. (45) who reduced a cystamine core dendrimer to yield cysteamine core dendrons. Oligonucleotides were attached to the focal point, ensuring 1:1 bridging. We

initially planned to expand upon Demattei's oligonucleotide-dendron work with the intention of creating a library of conjugates for targeted drug delivery, but it was ultimately decided that the coupling method was impractical due to A) electrostatic interactions with terminal amines causing the DNA to wrap around the dendron and B) high cost of oligonucleotides. Thus alternative approaches needed to be entertained.

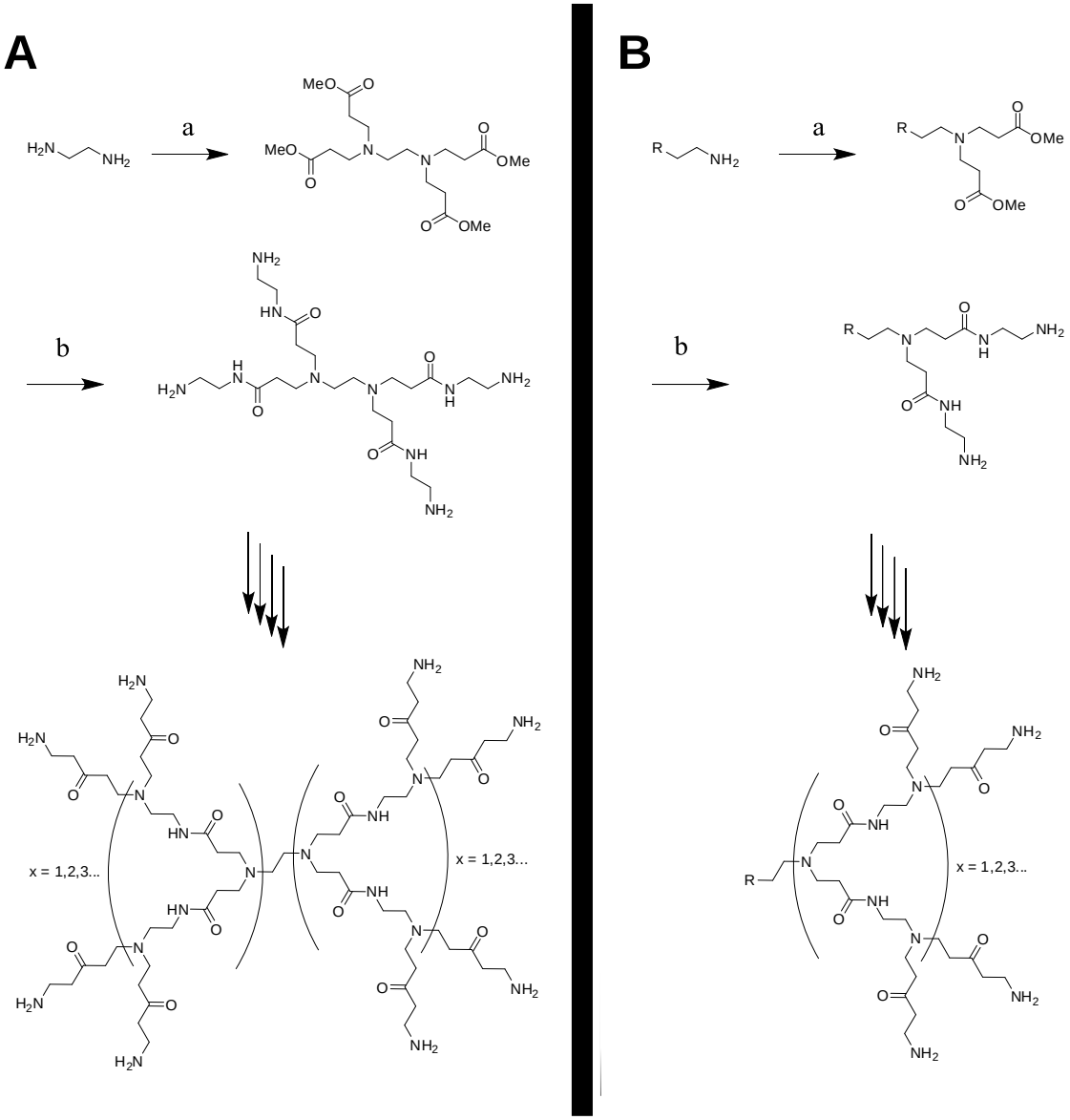


**Figure 1.2.** Growth schemes of A) PAMAM dendrimers and B) PAMAM dendrons. a) excess methyl acrylate, MeOH, b) excess ethylene diamine, MeOH.

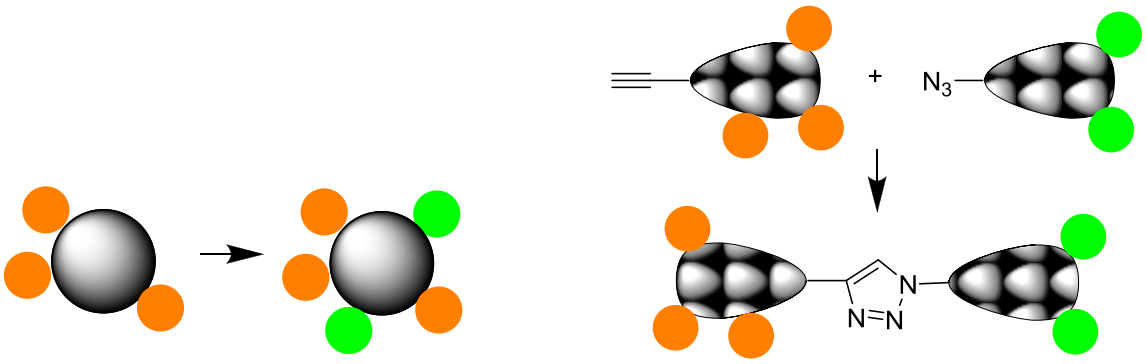


**Figure 1.3.** Dendrons maintain the branched architecture of the dendrimer scaffold for increased payload and multivalent targeting. Orthogonal coupling at the focal point improves quality control by eliminating stacking of complex ligand distributions and allowing the distributions of each module to be independently characterized.

Rather than use complimentary DNA, we explored click chemistry involving well-defined organic synthesis to orthogonally couple dendron focal points. Click chemistry is a class of reactions that provides high versatility and efficiency with mild reaction conditions and an absence of side reactions that eliminates the need for protecting groups. When applied to the focal point of a dendron, click reactions give a precise 1:1 ratio of dendron to functional ligand or dendron, preventing aggregate formation that plagued oligonucleotide-coupled dendrimer platforms. There have been several examples of click chemistry involved in the synthesis and conjugation of dendrimers (46) since Sharpless and co-workers popularized the copper(I)-catalyzed alkyne-azide 1,3-dipolar cycloaddition (CuAAC) (47). Click chemistry has been used to obtain greater control over the synthesis of the dendrimer platforms by minimizing defect structures and reducing the need for purification (48, 49). Click chemistry can also be employed as a means to control the conjugation of desired functionalities to dendritic materials (50-58). The orthogonality of click chemistry provides a means to avoid

incompatible conjugation reactions, minimize the use of protection/deprotection strategies, reduce product heterogeneity and potentially add specific numbers of functional moieties.

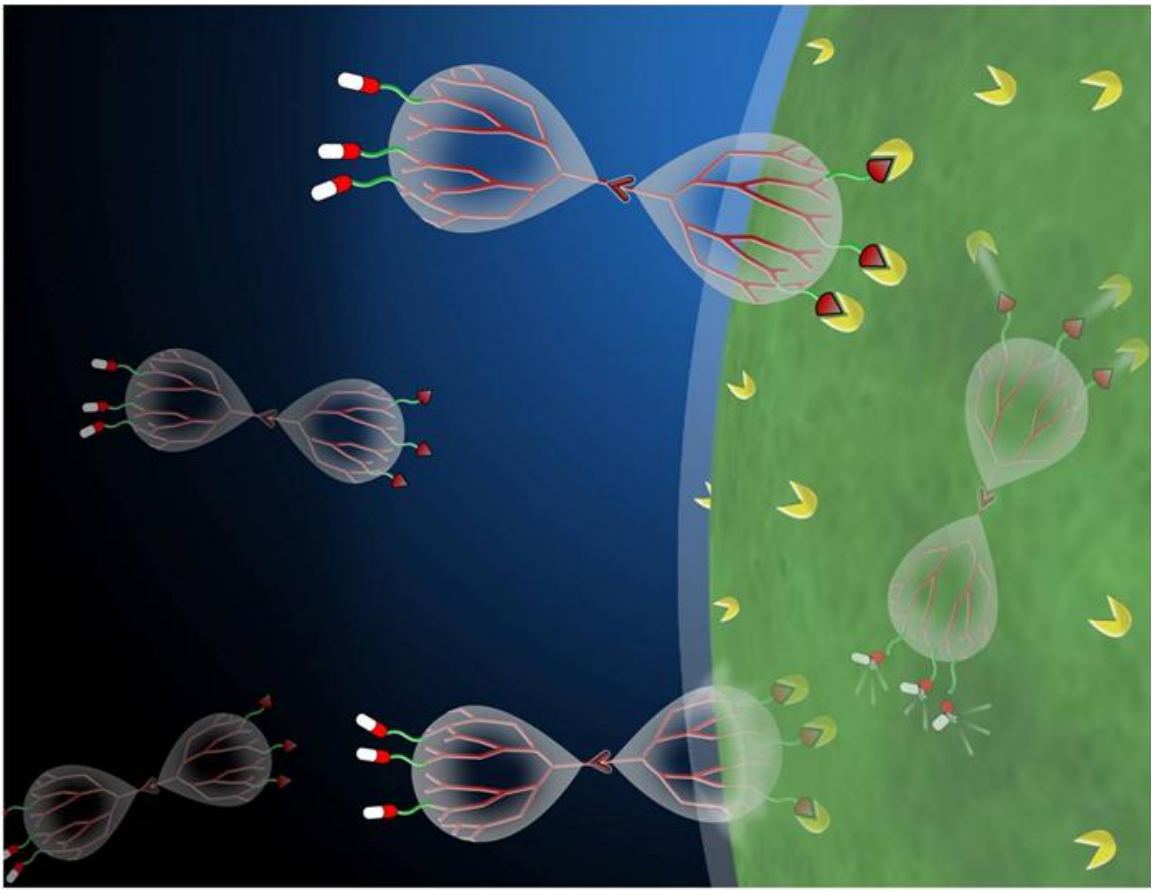

**Figure 1.4.** Representation of bifunctional Janus dendrimers interacting with a cell. One dendron module is conjugated with a targeting ligand that binds to cellular receptors. The second module is loaded with a therapeutic.

**Progress with modular dendrons**

We aim to show in this thesis that although problems remain significant progress has been made towards the efficient, orthogonal conjugation of modular dendrons (Figure 1.4). We will explore the use of multiple click reactions, evaluating their applicability across PAMAM and polyester dendrons (Figure 1.5).

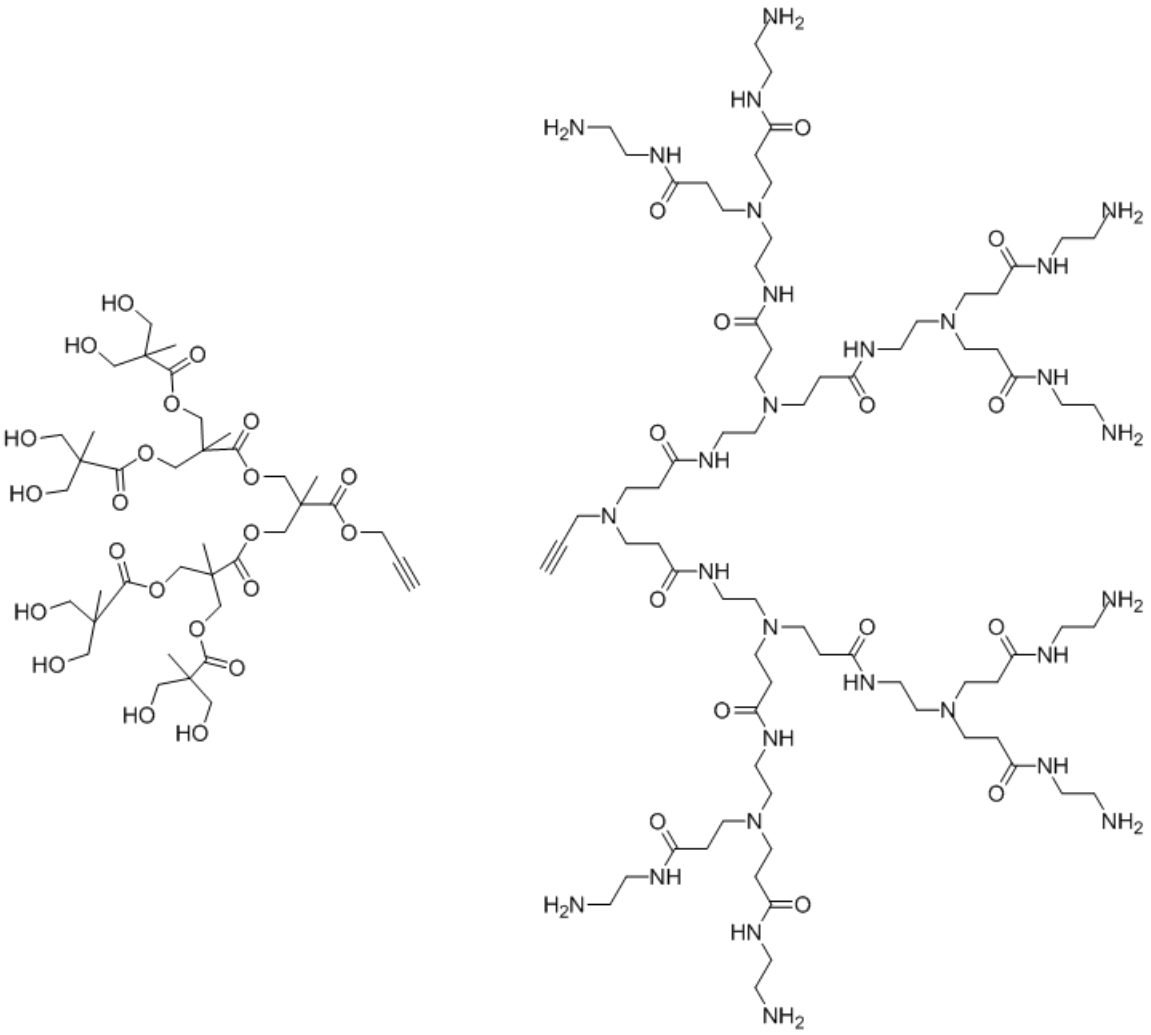

**Figure 1.5.** A polyester dendron, left, based on a 2,2-bis(hydroxymethyl)propanoic acid (bis-MPA) monomer backbone and a poly(amidoamine) (PAMAM) dendron, right.

In Chapter 2, we present the first report of biological activity from a clicked dendron platform. The generation 3 PAMAM dendrons were coupled with c(RGDyK) peptide on the surface to create a scaffold for cellular targeting and multivalent binding (59). Generation 3 dendrons were chosen for this study due to concerns, based on literature (60-62), that the focal point of larger generation material may be blocked by steric hindrance. RGD peptide was explored as the targeting ligand as opposed to folic acid in part because folic acid is markedly hydrophobic and planar molecules that when conjugated to generation 3 dendrons displayed a large amount of aggregates presumably

through pi-stacking of the folate molecules (unpublished data). In contrast, the dendron remained soluble after the addition of multiple RGD to the surface of the molecule.

Binary dendron-RGD conjugates were synthesized via CuAAC with either a single Alexa Fluor 488, biotin, methotrexate drug molecule, or additional functionalized dendron coupled at the focal point. The targeted-dendron platform was shown to specifically target $\alpha_V\beta_3$ integrin expressing human umbilical vein endothelial cells (HUVEC) and human glioblastoma cells (U87MG) *in vitro* via flow cytometry. Specific targeting of the dendron-RGD platform was further confirmed by confocal microscopy. Biological activity of the targeted drug conjugate was confirmed via XTT assay. The orthogonal reaction chemistry used at the dendron focal point gave a precise 1:1 ratio of a variety of functionalities to a small molecular weight dendron (~5-12 kDa) to produce a chemically stable, high-avidity targeted molecule. These studies serve as a framework to specifically combine biologically-relevant molecules having enhanced specific binding activity, and these can serve as a substitute for antibodies in many diagnostic and therapeutic applications.

Despite the successes of the platform, CuAAC displayed less than quantitative reaction efficiencies; it was hypothesized that the reaction was hindered by steric bulk or by complexation of the catalyst with amine terminated materials. To address these problems and to improve the utility of platform synthesis, additional work was performed using click chemistry that did not use metal catalysts. Conjugation of a model system using thiol-based click reactions is highlighted in Chapter 3. Thiol-ene and thiol-yne reactions at the dendron focal point showed improved conversions compared to CuAAC, offering quantitative conversions in most cases. Another approach, using ring-strain

alkyne-azide cycloadditions to dendrons, is highlighted in Chapter 4. The high degree of orthogonality, the vast library of available azide functional ligands, and the highly efficient quantitative conversions makes the strain promoted click chemistry perhaps the most attractive method of dendron focal point conjugation currently available. In general, however, the absence of a contaminant metal catalyst and the higher conversions of the metal-free click chemistry provide final material that is more for *in vivo* therapeutics.

REFERENCES


(1) Allen, T. M. (2002) Ligand-targeted therapeutics in anticancer therapy. Nat.Rev.Cancer. **2**, 750-763

(2) Liu, Y., Miyoshi, H. and Nakamura, M. (2007) Nanomedicine for drug delivery and imaging: A promising avenue for cancer therapy and diagnosis using targeted functional nanoparticles. Int.J.Cancer. **120**, 2527-2537

(3) Boas, U. and Heegaard, P. M. (2004) Dendrimers in drug research. Chem.Soc.Rev. **33**, 43-63

(4) Agarwal, A., Saraf, S., Asthana, A., Gupta, U., Gajbhiye, V. and Jain, N. K. (2008) Ligand based dendritic systems for tumor targeting. Int.J.Pharm. **350**, 3-13

(5) Agarwal, A., Asthana, A., Gupta, U. and Jain, N. K. (2008) Tumour and dendrimers: A review on drug delivery aspects. Journal of Pharmacy and Pharmacology. **60**, 671-688

(6) Cloninger, M. J. (2002) Biological applications of dendrimers. Current Opinion in Chemical Biology. **6**, 742-748

(7) Cheng, Y., Xu, Z., Ma, M. and Xu, T. (2008) Dendrimers as drug carriers: Applications in different routes of drug administration. J.Pharm.Sci. **97**, 123-143

(8) Dufès, C., Uchegbu, I. F. and Schätzlein, A. G. (2005) Dendrimers in gene delivery. Advanced Drug Delivery Reviews. **57**, 2177-2202

(9) Gillies, E. R. and Frechet, J. M. J. (2005) Dendrimers and dendritic polymers in drug delivery. Drug Discovery Today. **10**, 35-43

(10) Lee, C. C., MacKay, J. A., Frechet, J. M. J. and Szoka, F. C. (2005) Designing dendrimers for biological applications. Nature Biotechnology. **23**, 1517-1526

(11) Liu, M. and Frechet, J. M. (1999) Designing dendrimers for drug delivery. Pharm.Sci.Technolo Today. **2**, 393-401

(12) Svenson, S. and Tomalia, D. A. (2005) Dendrimers in biomedical applications—reflections on the field. Advanced Drug Delivery Reviews. **57**, 2106-2129

(13) Svenson, S. (2009) Dendrimers as versatile platform in drug delivery applications. Eur.J.Pharm.Biopharm. **71**, 445-462

(14) McNerny, D. Q., Leroueil, P. R. and Baker, J. R. (2010) Understanding specific and nonspecific toxicities: A requirement for the development of dendrimer-based pharmaceuticals. Wiley Interdiscip.Rev.Nanomed Nanobiotechnol. **2**, 249-259

(15) Hong, S., Leroueil, P. R., Majoros, I. J., Orr, B. G., Baker, J. R.,Jr and Banaszak Holl, M. M. (2007) The binding avidity of a nanoparticle-based multivalent targeted drug delivery platform. Chem.Biol. **14**, 107-115

(16) Esfand, R. and Tomalia, D. A. (2001) Poly(amidoamine) (PAMAM) dendrimers: From biomimicry to drug delivery and biomedical applications. Drug Discov.Today. **6**, 427-436

(17) Kukowska-Latallo, J. F., Candido, K. A., Cao, Z., Nigavekar, S. S., Majoros, I. J., Thomas, T. P., Balogh, L. P., Khan, M. K. and Baker, J. R.,Jr. (2005) Nanoparticle targeting of anticancer drug improves therapeutic response in animal model of human epithelial cancer. Cancer Res. **65**, 5317-5324

(18) Quintana, A., Raczka, E., Piehler, L., Lee, I., Myc, A., Majoros, I., Patri, A. K., Thomas, T., Mule, J. and Baker, J. R.,Jr. (2002) Design and function of a dendrimer-based therapeutic nanodevice targeted to tumor cells through the folate receptor. Pharm.Res. **19**, 1310-1316

(19) Thomas, T. P., Patri, A. K., Myc, A., Myaing, M. T., Ye, J. Y., Norris, T. B. and Baker, J. R.,Jr. (2004) In vitro targeting of synthesized antibody-conjugated dendrimer nanoparticles. Biomacromolecules. **5**, 2269-2274

(20) Thomas, T. P., Majoros, I. J., Kotlyar, A., Kukowska-Latallo, J. F., Bielinska, A., Myc, A. and Baker, J. R.,Jr. (2005) Targeting and inhibition of cell growth by an engineered dendritic nanodevice. J.Med.Chem. **48**, 3729-3735

(21) Wiener, E. C., Brechbiel, M. W., Brothers, H., Magin, R. L., Gansow, O. A., Tomalia, D. A. and Lauterbur, P. C. (1994) Dendrimer-based metal chelates: A new class of magnetic resonance imaging contrast agents. Magn.Reson.Med. **31**, 1-8

(22) Shukla, R., Thomas, T. P., Peters, J., Kotlyar, A., Myc, A. and Baker Jr, J. R. (2005) Tumor angiogenic vasculature targeting with PAMAM dendrimer-RGD conjugates. Chem.Commun.(Camb). **(46)**, 5739-5741

(23) Shukla, R., Thomas, T. P., Peters, J. L., Desai, A. M., Kukowska-Latallo, J., Patri, A. K., Kotlyar, A. and Baker, J. R.,Jr. (2006) HER2 specific tumor targeting with dendrimer conjugated anti-HER2 mAb. Bioconjug.Chem. **17**, 1109-1115

(24) Barth, R. F., Soloway, A. H., Adams, D. M. and Alam, F. (1992) Delivery of boron-10 for neutron capture therapy by means of monoclonal antibody-starburst dendrimer immunoconjugates.

(25) Malik, N., Evagorou, E. G. and Duncan, R. (1999) Dendrimer-platinate: A novel approach to cancer chemotherapy. Anticancer Drugs. **10**, 767-776

(26) Malik, N., Wiwattanapatapee, R., Klopsch, R., Lorenz, K., Frey, H., Weener, J. W., Meijer, E. W., Paulus, W. and Duncan, R. (2000) Dendrimers: Relationship between structure and biocompatibility in vitro, and preliminary studies on the biodistribution of 125I-labelled polyamidoamine dendrimers in vivo. J.Control.Release. **65**, 133-148

(27) Kong, G., Braun, R. D. and Dewhirst, M. W. (2000) Hyperthermia enables tumor-specific nanoparticle delivery: Effect of particle size. Cancer Res. **60**, 4440-4445

(28) Padilla De Jesus, O. L., Ihre, H. R., Gagne, L., Frechet, J. M. and Szoka, F. C.,Jr. (2002) Polyester dendritic systems for drug delivery applications: In vitro and in vivo evaluation. Bioconjug.Chem. **13**, 453-461

(29) Morgan, M. T., Carnahan, M. A., Immoos, C. E., Ribeiro, A. A., Finkelstein, S., Lee, S. J. and Grinstaff, M. W. (2003) Dendritic molecular capsules for hydrophobic compounds. J.Am.Chem.Soc. **125**, 15485-15489

(30) Bourne, N., Stanberry, L. R., Kern, E. R., Holan, G., Matthews, B. and Bernstein, D. I. (2000) Dendrimers, a new class of candidate topical microbicides with activity against herpes simplex virus infection. Antimicrob.Agents Chemother. **44**, 2471-2474

(31) Hollins, A. J., Benboubetra, M., Omidi, Y., Zinselmeyer, B. H., Schatzlein, A. G., Uchegbu, I. F. and Akhtar, S. (2004) Evaluation of generation 2 and 3 poly(propylenimine) dendrimers for the potential cellular delivery of antisense oligonucleotides targeting the epidermal growth factor receptor. Pharm.Res. **21**, 458-466

(32) Wang, S. J., Brechbiel, M. and Wiener, E. C. (2003) Characteristics of a new MRI contrast agent prepared from polypropyleneimine dendrimers, generation 2. Invest.Radiol. **38**, 662-668

(33) Majoros, I. J., Myc, A., Thomas, T., Mehta, C. B. and Baker, J. R.,Jr. (2006) PAMAM dendrimer-based multifunctional conjugate for cancer therapy: Synthesis, characterization, and functionality. Biomacromolecules. **7**, 572-579

(34) Majoros, I. J., Thomas, T. P., Mehta, C. B. and Baker, J. R.,Jr. (2005) Poly(amidoamine) dendrimer-based multifunctional engineered nanodevice for cancer therapy. J.Med.Chem. **48**, 5892-5899

(35) Patri, A. K., Kukowska-Latallo, J. F. and Baker, J.,James R. (2005) Targeted drug delivery with dendrimers: Comparison of the release kinetics of covalently conjugated drug and non-covalent drug inclusion complex. Advanced Drug Delivery Reviews. **57**, 2203-2214

(36) Patri, A. K., Majoros, I. J. and Baker, J. R. (2002) Dendritic polymer macromolecular carriers for drug delivery. Current Opinion in Chemical Biology. **6**, 466-471

(37) Majoros, I. J., Keszler, B., Woehler, S., Bull, T. and Baker, J. R. (2003) Acetylation of poly(amidoamine) dendrimers. Macromolecules. **36**, 5526-5529

(38) Hong, S. P., Bielinska, A. U., Mecke, A., Keszler, B., Beals, J. L., Shi, X. Y., Balogh, L., Orr, B. G., Baker, J. R. and Holl, M. M. B. (2004) Interaction of poly(amidoamine) dendrimers with supported lipid bilayers and cells: Hole formation and the relation to transport. Bioconjugate Chemistry. **15**, 774-782

(39) Hong, S. P., Leroueil, P. R., Janus, E. K., Peters, J. L., Kober, M. M., Islam, M. T., Orr, B. G., Baker, J. R. and Holl, M. M. B. (2006) Interaction of polycationic polymers with supported lipid bilayers and cells: Nanoscale hole formation and enhanced membrane permeability. Bioconjugate Chemistry. **17**, 728-734

(40) Leroueil, P. R., Hong, S. Y., Mecke, A., Baker, J. R., Orr, B. G. and Holl, M. M. B. (2007) Nanoparticle interaction with biological membranes: Does nanotechnology present a janus face? Accounts of Chemical Research. **40**, 335-342

(41) Mullen, D. G., Desai, A. M., Waddell, J. N., Cheng, X. M., Kelly, C. V., McNerny, D. Q., Majoros, I. J., Baker, J. R.,Jr, Sander, L. M., Orr, B. G. and Banaszak Holl, M. M. (2008) The implications of stochastic synthesis for the conjugation of functional groups to nanoparticles. Bioconjug.Chem. **19**, 1748-1752

(42) Mullen, D. G., Fang, M., Desai, A., Baker, J. R., Orr, B. G. and Banaszak Holl, M. M. (2010) A quantitative assessment of nanoparticle-ligand distributions: Implications for targeted drug and imaging delivery in dendrimer conjugates. ACS Nano. **4**, 657-670

(43) Choi, Y., Thomas, T., Kotlyar, A., Islam, M. T. and Baker, J. R.,Jr. (2005) Synthesis and functional evaluation of DNA-assembled polyamidoamine dendrimer clusters for cancer cell-specific targeting. Chem.Biol. **12**, 35-43

(44) Choi, Y., Mecke, A., Orr, B. G., Banaszak Holl, M. M. and Baker, J. R. (2004) DNA-directed synthesis of generation 7 and 5 PAMAM dendrimer nanoclusters. Nano Letters. **4**, 391

(45) DeMattei, C. R., Huang, B. and Tomalia, D. A. (2004) Designed dendrimer syntheses by self-assembly of single-site, ssDNA functionalized dendrons. Nano Letters. **4**, 771

(46) McNerny, D. Q., Mullen, D. G., Majoros, I. J., Holl, M. M. B. and Jr, J. R. B. (2009) Dendrimer synthesis and functionalization by click chemistry for biomedical

applications. In Click Chemistry for Biotechnology and Materials Science (Lahann, J., ed. ), pp. 177-193

(47) Kolb, H. C., Finn, M. G. and Sharpless, K. B. (2001) Click chemistry: Diverse chemical function from a few good reactions. Angew.Chem.Int.Ed Engl. **40**, 2004-2021

(48) Joralemon, M. J., O'Reilly, R. K., Matson, J. B., Nugent, A. K., Hawker, C. J. and Wooley, K. L. (2005) Dendrimers clicked together divergently. Macromolecules. **38**, 5436-5443

(49) Killops, K. L., Campos, L. M. and Hawker, C. J. (2008) Robust, efficient, and orthogonal synthesis of dendrimers via thiol-ene "click" chemistry. J.Am.Chem.Soc. **130**, 5062-5064

(50) Wyszogrodzka, M. and Haag, R. (2008) A convergent approach to biocompatible polyglycerol "click" dendrons for the synthesis of modular core-shell architectures and their transport behavior. Chemistry. **14**, 9202-9214

(51) Wu, P., Malkoch, M., Hunt, J. N., Vestberg, R., Kaltgrad, E., Finn, M. G., Fokin, V. V., Sharpless, K. B. and Hawker, C. J. (2005) Multivalent, bifunctional dendrimers prepared by click chemistry. Chem.Commun.(Camb). **(46)**, 5775-5777

(52) Haridas, V., Lal, K. and Sharma, Y. K. (2007) Design and synthesis of triazole-based peptide dendrimers. Tetrahedron Lett. **48**, 4719

(53) Fernandez-Megia, E., Correa, J., Rodriguez-Meizoso, I. and Riguera, R. (2006) A click approach to unprotected glycodendrimers†. Macromolecules. **39**, 2113-2120

(54) Dijkgraaf, I., Rijnders, A. Y., Soede, A., Dechesne, A. C., van Esse, G. W., Brouwer, A. J., Corstens, F. H., Boerman, O. C., Rijkers, D. T. and Liskamp, R. M. (2007) Synthesis of DOTA-conjugated multivalent cyclic-RGD peptide dendrimers via 1,3-dipolar cycloaddition and their biological evaluation: Implications for tumor targeting and tumor imaging purposes. Org.Biomol.Chem. **5**, 935-944

(55) Gopin, A., Ebner, S., Attali, B. and Shabat, D. (2006) Enzymatic activation of second-generation dendritic prodrugs: Conjugation of self-immolative dendrimers with poly(ethylene glycol) via click chemistry. Bioconjug.Chem. **17**, 1432-1440

(56) Mariano Ortega-Muñoz, Javier Lopez-Jaramillo, Fernando Hernandez-Mateo,Francisco Santoyo-Gonzalez,. (2006) Synthesis of glyco-silicas by cu(I)-catalyzed ldquoClick-chemistryrdquo and their applications in affinity chromatography. Advanced Synthesis & Catalysis. **348**, 2410-2420

(57) Urbani, C. N., Bell, C. A., Lonsdale, D., Whittaker, M. R. and Monteiro, M. J. (2008) Self-assembly of amphiphilic polymeric dendrimers synthesized with selective degradable linkages. Macromolecules. **41**, 76-86

(58) Ornelas, C., Broichhagen, J. and Weck, M. (2010) Strain-promoted alkyne azide cycloaddition for the functionalization of poly(amide)-based dendrons and dendrimers. J.Am.Chem.Soc. **132**, 3923-3931

(59) McNerny, D. Q., Kukowska-Latallo, J., Mullen, D. G., Wallace, J. M., Desai, A. M., Shukla, R., Huang, B., Banaszak Holl, M. M. and Baker, J. R. (2009) RGD dendron bodies; synthetic avidity agents with defined and potentially interchangeable effector sites that can substitute for antibodies. Bioconjug.Chem. **20**, 1853-1859

(60) Lee, J. W., Kim, H. J., Han, S. C., Kim, J. H. and Jin, S. H. (2008) Designing poly(amido amine) dendrimers containing core diversities by click chemistry of the propargyl focal point poly(amido amine) dendrons. Journal of Polymer Science Part a-Polymer Chemistry. **46**, 1083-1097

(61) Lee, J. W., Kim, J. H., Kim, H. J., Han, S. C., Kim, J. H., Shin, W. S. and Jin, S. H. (2007) Synthesis of symmetrical and unsymmetrical PAMAM dendrimers by fusion between azide- and alkyne-functionalized PAMAM dendrons. Bioconjug.Chem. **18**, 579-584

(62) Lee, J. W., Kim, J. H. and Kim, B. K. (2006) Synthesis of azide-functionalized PAMAM dendrons at the focal point and their application for synthesis of PAMAM-like dendrimers. Tetrahedron Letters. **47**, 2683-2686

## Chapter 2:
## Synthesis and in vitro evaluation of bifunctional, RGD-conjugated PAMAM dendrons; synthetic avidity agents with orthogonal coupling by copper(I)-catalyzed 1,3-dipolar cycloaddition

### Background

To increase the utility of the dendritic scaffold, orthogonal and modular pathways can be used to construct binary devices with coupling specificity while maintaining flexibility in their content. Research pursuing such pathways to create multi-functional dendritic devices has been sparse: dendrimers with unique surface groups that can be employed for modular synthesis via click chemistry (1), complimentary oligonucleotide hybridization (2), or orthogonal functionalization (3). Dendrons with a bis-MPA backbone have been utilized by exploiting the unique reactive site at the focal point to create bi-functional materials (4). Modular approaches offer the potential to construct unique bi-molecular combinations for specific targeting applications from a library of functionalized mono-substituted dendrons in a versatile manner that overcomes the inefficiencies of step-wise conjugations on a single dendritic macromolecule. The central advantage of these techniques is that they provide increased homogeneity products by reducing the complexity of ligand distributions created by multi-functional platforms.

Herein, we present the synthesis and evaluation of *in vitro* biological activity for a high-avidity targeted, PAMAM dendron platform (Figure 2.1). This is the first report of a clicked dendron platform displaying biological activity. The functionalized

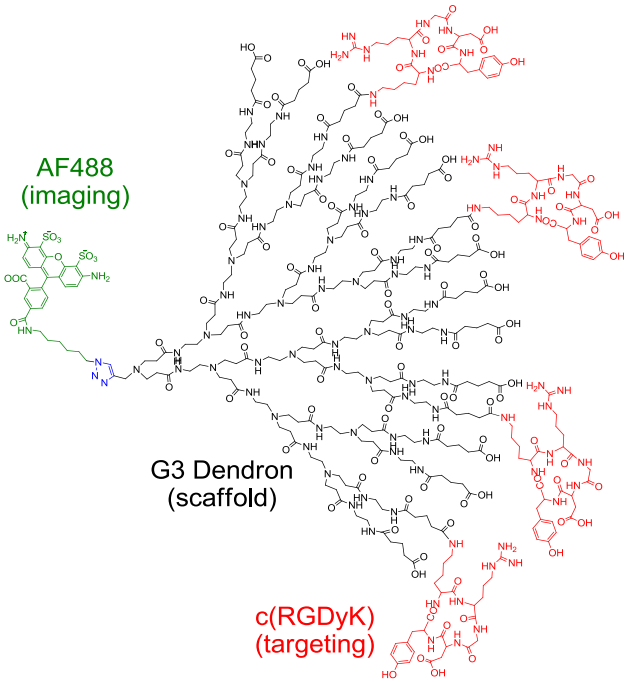


**Figure 2.1.** Dendron conjugate AF-G3$(COOH)_{11.9}(RGD)_{4.1}$ **(4)** where Alexa Fluor 488 is conjugated to the dendron focal point via a 1,3-dipolar cycloaddition. The targeting moiety, c(RGDyK) peptide, is conjugated to the carboxylated surface of the dendron.

PAMAM dendron can maintain the binding specificity and multivalency of previous dendritic models (5, 6) while creating an orthogonally coupled bi-functional molecule more suitable for specific therapeutic applications. Binary devices were synthesized using a unique alkyne group functionalized at the dendron focal point. The alkyne is reacted with an azide-functionalized dye, biotin, therapeutic molecule or a second dye-conjugated dendron in a copper-catalyzed alkyne-azide 1,3-dipolar cycloaddition (CuAAC), the most common reaction in a class of synthetic approaches referred to as click chemistry (7). This strategy is attractive because it provides high versatility and yields while utilizing mild reaction conditions and avoiding alterations to neighboring functional groups and the need for protecting groups. Additionally, other materials can be easily functionalized with either alkyne or azide substitutions and the 1,2,3-triazole product generated through this synthesis is very stable. The Cu(I) catalysis dramatically

lowers the activation barrier, eliminating the need for either high temperatures or pressures with the Huisgen 1,3-dipolar cycloaddition, while forming regioselective 1,4-triazoles.

The platform itself gives a precise 1:1 ratio of the attachment of multiple functionalities, preventing aggregate formation. A dendron with multiple Arg-Gly-Asp (RGD) adhesion ligands on the surface and an additional function at the focal point can specifically target $\alpha_V\beta_3$ integrin expressing human umbilical vein endothelial cells (HUVEC) and human glioblastoma cells (U87MG), displaying the biological utility of the platform. The dendron-RGD platform also successfully inhibits tumor growth when conjugated to a therapeutic drug, such as methotrexate (MTX). Thus, the ability to conjugate specific and varied effector sites to the dendron periphery to generate a high avidity binding agent and use orthogonal reaction chemistry at the focal point to add additional functionalities makes these "dendro–bodies" an attractive alternative to antibodies for targeting applications.

**Experimental procedures**

**General.** Alexa Fluor 488 azide and Prolong Gold mounting agent were obtained from Invitrogen. c(RGDyK) peptide was obtained from Peptide International. Biotin-dPEG$_{3+4}$-azide was obtained from Quanta Biodesign. Sephadex G15 and G25 were obtained from GE Life Sciences. Spectra/Por 7 dialysis membrane (MWCO 1000) was obtained from Spectrum Laboratories. NeutrAvidin-Dylight 405 was obtained from Pierce. All other chemicals were obtained from Sigma. All purified reaction products

were characterized by $^{1}H$ NMR, HPLC, and matrix-assisted laser desorption-ionization time-of-flight (MALDI-TOF) mass spectrometry.

**Synthesis of alkyne-G3-PAMAM dendron (1).** Alkyne-G3-PAMAM dendron was prepared as previously reported (8) and analyzed by $^{1}H$ and $^{13}C$ NMR and MALDI-TOF. MS (MALDI): 3479 Da; calculated for $C_{153}H_{305}N_{61}O_{30}$: 3479.45 Da.

**Synthesis of alkyne-G3(COOH)$_{16}$ (2).** Glutaric anhydride (0.0164 g, 0.1437 mmol) dissolved in anhydrous MeOH (0.8 mL) was added dropwise to a solution of **1** (0.0200 g, 0.0057 mmol) and triethylamine ($Et_3N$) (0.0186 g, 0.1838 mol) in anhydrous MeOH (0.2 mL) while stirring, and the reaction mixture was allowed to stir for 24 hours at room temperature. All solvent was removed *in vacuo*, and the reaction material was dissolved in $H_2O$, purified on a G-15 Sephadex column and lyophilized. MS (MALDI): 5305 Da; calculated for $C_{233}H_{401}N_{61}O_{78}$: 5305.04 Da.

**Synthesis of alkyne-G3(COOH)$_{11.9}$(RGD)$_{4.1}$ (3).** 1-(3-(dimethylamino)propyl)-3-ethylcarbodiimide HCl (EDC) (0.0838 g, 0.4373 mmol) was allowed to react with **2** (0.0145 g, 0.0027 mmol) in 1:1 $H_2O$/DMSO (2 mL) for 2 hours to form an active ester. c(RGDyK) (0.0169 g, 0.0273 mmol) in 4:1 $H_2O$/DMSO (1.25mL) was added dropwise to the EDC and dendron solution and stirred for 2 days at room temperature. The DMSO was removed via dialysis in $H_2O$ for 1 hour. The resulting solution was lyophilized, redissolved in $H_2O$, and purified on a G-15 Sephadex column, then again lyophilized. MS (MALDI): 5300-12000 Da (broad).

**Synthesis of AF-G3(COOH)$_{11.9}$(RGD)$_{4.1}$ (4).** A mixture of azide-functionalized Alexa Fluor 488 (0.00022 g, 0.0002 mmol) and **3** (0.0015 g, 0.0002 mmol) in $H_2O$ (1 mL) in the presence of copper(II) sulfate (2.5 x $10^{-5}$ g, 0.0001 mmol) and sodium ascorbate (4.0 x $10^{-5}$ g, 0.0002 mmol) was stirred for 36 hours at room temperature. The solution was purified on a G-25 Sephadex column and lyophilized. MS (MALDI): 5300-12600 Da (broad).

**Synthesis of MTX-azide (5).** Methotrexate (0.0238 g, 0.05237 mmol) was dissolved in DMF (1 mL) and cooled in a water/ice bath. *N*-Hydroxysuccinimide (0.0067 g, 0.0576 mmol) and EDC (0.0110 g, 0.0576 mmol) were added, and the resulting mixture was stirred in the ice bath for 30 min to give a white precipitate. A solution of 11-azido-3,6,9-trioxaundecan-1-amine (0.0120 g, 0.0550 mmol) in DMF (0.5 mL) was added, and the resulting mixture was allowed to warm to room temperature and stirred for 24 h. The mixture was poured into water (50 mL) and washed with chloroform (50 mL x 3). The aqueous layer was lyophilized and further purified on a G-25 Sephadex column. MS: 654.7 Da; calculated for $C_{28}H_{38}N_{12}O_7$: 654.68 Da.

**Synthesis of MTX-G3(COOH)$_{11.9}$(RGD)$_{4.1}$ (6).** A mixture of **5** (0.0019 g, 0.0029 mmol) and **3** (0.0025 g, 0.0003 mmol) in $H_2O$ (1 mL) in the presence of copper(II) sulfate (2.5 x $10^{-5}$ g, 0.0001 mmol) and sodium ascorbate (4.0 x $10^{-5}$ g, 0.0002 mmol) was stirred for 36 hours at room temperature. The solution was purified on a G-25 Sephadex column and lyophilized. MS (MALDI): 5300-12600 Da (broad).

**Synthesis of biotin-G3(COOH)$_{11.9}$(RGD)$_{4.1}$ (7).** A mixture of biotin-dPEG$_{3+4}$-azide (0.0045 g, 0.0006 mmol) and **3** (0.0080 g, 0.0001 mmol) in 1:1 DMSO/$H_2O$ (1 mL) in the presence of copper(II) sulfate (2.5 x $10^{-5}$ g, 0.0001 mmol) and sodium ascorbate (4.0 x $10^{-5}$ g, 0.0002 mmol) was stirred for 36 hours at room temperature. The solution was purified on a G-25 Sephadex column and lyophilized. MS (MALDI): 5300-12700 Da (broad).

**Synthesis of azide-G2-PAMAM dendron (8).** Azide-G2-PAMAM dendron was prepared as previously reported (9) and analyzed by $^1$H and MALDI-TOF. MS (MALDI): 1698.1 Da; calculated for $C_{73}H_{148}N_{32}O_{14}$: 1698.16 Da.

**Synthesis of azide-G2(AF)$_2$(OH)$_{24}$ (9).** Alexa Fluor 488 sulfodichlorophenol ester (0.0050 g, 0.0061 mmol) dissolved in 0.5 mL DMF was added dropwise to **8** (0.0028 g, 0.0015 mmol) in 0.5 mL 0.1 M sodium bicarbonate buffer while stirring, and the reaction mixture was allowed to stir for 24 hours at room temperature. Solvent was removed *in vacuo*, and the resulting product was dissolved in 2 mL $H_2O$. Glycidol (0.0112 g, 0.1506 mmol) was added to the solution and the mixture was allowed to stir for 24 hours at room temperature. The solution was purified on a G-25 Sephadex column and lyophilized. MS (MALDI): 3000-7000 Da (broad).

**Synthesis of (OH)$_{24}$(AF)$_2$G2-G3(COOH)$_{11.9}$(RGD)$_{4.1}$ co-dendron (10).** A mixture of **9** (0.0030 g, 0.0009 mmol) and **3** (0.0044 g, 0.0006 mmol) in $H_2O$ (1 mL) in the presence of copper(II) sulfate (2.5 x $10^5$ g, 0.0001 mmol) and sodium ascorbate (4.0 x

$10^5$ g, 0.0002 mmol) was stirred for 36 hours at room temperature. The solution was first purified on a G-25 Sephadex column and lyophilized. The product was further purified via HPLC to remove excess azide-G2(AF)(OH). MS (MALDI): 5000-29000 Da (broad), 17500 Da maximum.

**Cell Culture and incubation with the dendron.** HUVEC cells were obtained from Invitrogen (Cascade Biologics). U87MG and KB cells were obtained from American Type Tissue Collection (Manasass, VA). HUVEC cells (cat. # C-015-10C), U87MG and KB cells were grown and maintained according to the supplier's protocol. Compounds were prepared in non-supplemented cell culture medium (Medium 200) and incubated in cell suspensions for 2 hours at 37 $^{o}$C in a 5% $CO_2$ incubator. Blocking experiments were run by pre-incubating the cells with a 200 equivalent excess of c(RGDyK) for 10 minutes at room temperature prior to incubation.

**Flow Cytometry.** Cells were washed with 5mL of PBS, spun at 150 X G for 7 minutes, and re-suspended in 1 mL of PBS prior to being analyzed. Cells were examined quantitatively for dendron uptake via a flow cytometer (Beckman Coulter Epics XL-MCL). The FL1 fluorescence of 10000 cells was measured and the mean fluorescence of cells was quantified.

**Confocal Microscopy.** HUVEC cells were seeded and grown on 35 mm glass-bottomed culture dishes (MatTek Corp., Ashland, MA). After 2 days, cells were treated with 0.5 μM co-dendron **10** or biotin-conjugated dendron **7**. Blocked samples were run

by pre-incubating the cells with a 200 equivalent excess of c(RGDyK) for 10 minutes at room temperature prior to incubation. After the 2 hour incubation period, biotin-conjugated dendron **7** treated cells were treated with 4 mg/mL BSA for 30 minutes to limit non-specific binding followed by treatment with 0.5 μM NeutrAvidin-Dylight 405 for 30 minutes. Media was aspirated from the cells, washed 3 times with PBS, and fixed with 2% paraformaldehyde. The samples were again aspirated, washed 3 times, and aspirated before mounting with Prolong Gold and a cover slip was added. Samples were imaged using an Olympus FluoView 500 Laser Scanning confocal microscope using a 60X, 1.5 NA oil immersion objective. Fluorescence and differential interference contrast (DIC) images were collected simultaneously using either an argon laser with 488 nm excitation or a solid state diode laser with 405 nm excitation and *Fluo*V*iew* software.

**Cytotoxicity Assay.** For cytotoxicity experiments, cells were seeded in 96-well microtiter plates (2500 cells/well) in Medium 200. The cells were treated in triplicate with different concentrations of free MTX or dendron conjugates for 72 hours with a replenishing of 100 μL medium and the conjugates after 48 hours. A colorimetric XTT assay (Invitrogen) was performed following the vendor's protocol. An aliquot of 30 μL of XTT working solution prepared according to manufacturer instructions was added to each well using a multichannel pipette followed by the addition of 20 μL of PBS. After 1 hour incubation in the dark at 37 °C, the absorbance at 490 nm was recorded using a plate reader. 690 nm was selected as a reference wavelength. Cell viability was calculated based on optical density (OD) from untreated cells. Statistical significance was assessed

using Two-Way ANOVA with posthoc Bonferroni tests checking for main effects of conjugate and concentration. P-values less than 0.05 were considered significant.

**Results and Discussion**

The surface amines of the G3 PAMAM dendron **1** were allowed to react with excess glutaric anhydride in MeOH, in the presence of $Et_3N$ as base, to form carboxylic acids (Figure 2.2 i). The reaction yielded carboxyl terminal groups and eliminates potential nonspecific charge interactions with the cell plasma membrane caused by primary amines. $^1$H NMR spectroscopy confirmed complete conversion of the primary amines and formation of dendron **2** by the loss of methylene peaks ($–CH_2CH_2NH_2$) at δ 2.80 and 3.30 ppm and the formation of new methylene peaks ($-NHCO(CH_2)_3COOH$) at δ 1.84, 2.21, and 2.27 ppm.

The targeting moiety, RGD peptide, was conjugated to the carboxylated surface of the PAMAM dendron (Figure 2.2 ii). RGD binds to the $\alpha_V\beta_3$ integrin found on the luminal surface of endothelial cells during angiogenesis (10, 11). This makes the $\alpha_V\beta_3$ integrin a unique marker that differentiates newly formed capillaries in the tumor vasculature from their mature counterparts (12-14). Antiangiogenic therapies, such as ones that employ RGD targeting, prevent neovascularization by inhibiting differentiation, migration and proliferation of endothelial cells (15).

The surface carboxyl groups were activated with EDC, followed by the addition of 12 equivalents of c(RGDyK) to give dendron **3**. The product was purified by size exclusion chromatography and lyophilized. The $^1$H NMR spectrum of the dendron-RGD body shows some of the aliphatic signals of the peptide overlap with the aliphatic signals

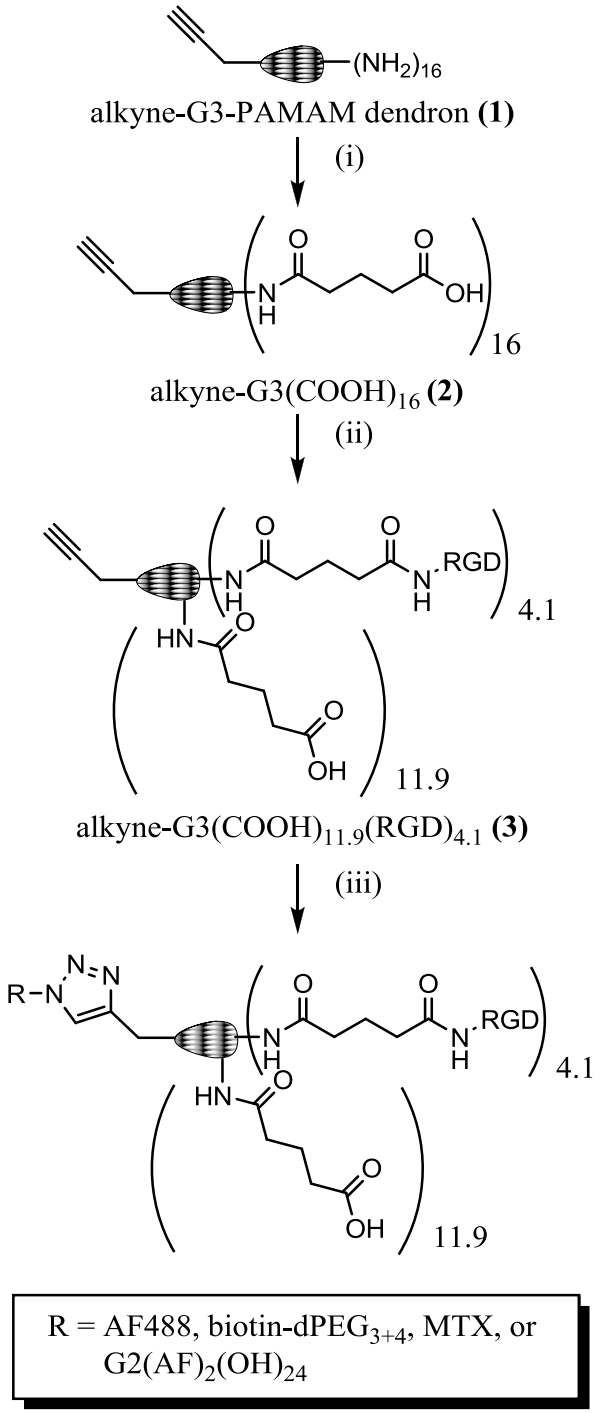


**Figure 2.2**. Reaction scheme for creating click-conjugated dendrons employed in the *in vitro* studies. (i) glutaric anhydride, MeOH, 24 hrs, r.t. (ii) EDC, c(RGDyK), $H_2O$/DMSO, 2 days, r.t. (iii) Alexa Fluor 488 azide OR biotin-$dPEG_{3+4}$-azide OR MTX-azide **(5)** OR azide-$G2(AF)_2(OH)_{24}$ **(9)**, sodium ascorbate, copper (II) sulfate, $H_2O$, 36 hours, r.t.

of the dendron; however, using the peak integration values in the aromatic region from the phenyl ring of the peptide, an average of 4.1 attached RGD per dendron was calculated.

The dendron AF-G3$(COOH)_{11.9}(RGD)_{4.1}$ **4** (Figure 2.2 iii) was synthesized by the reaction of azide-functionalized Alexa Fluor 488 with **3** in a copper-catalyzed 1,3-dipolar cycloaddition. Alexa Fluor 488 was chosen as the fluorescent label for detection of conjugates by flow cytometry because it is brighter than fluorescein conjugates and more resistant to photobleaching. The products were purified via size exclusion chromatography and lyophilized. The characteristic triazole proton peak of a successful click reaction ($\delta$ 8.10 ppm) partially overlaps with the peaks for Alexa Fluor 488. The crowded aromatic region of the NMR spectra proved to be a shortcoming of the copper-catalyzed cycloaddition, as it was impossible to accurately quantify the degree of conversion.

The specific binding of **4** to $\alpha_V\beta_3$ integrin expressing HUVEC and U87MG cells was examined via flow cytometry (Figure 2.3). KB cells, which express lower levels of $\alpha_V\beta_3$ integrin, were also evaluated. Cells were treated with dendron-RGD conjugates at final concentrations of 0.25, 0.50, 1, 2, and 4 $\mu$M, either with or without preincubation with 200 fold molar equivalences of free RGD peptide. Specificity and dose dependency of dendron bodies to integrin expressing cells were evaluated after the 2 hour incubation at 37 °C. The addition of excess free peptide to inhibit the uptake of the binary dendron by HUVEC and U87MG cells significantly blocked uptake. The inability to completely inhibit binding of the dendron may be due to a higher avidity of the dendron conjugate when compared to free RGD.

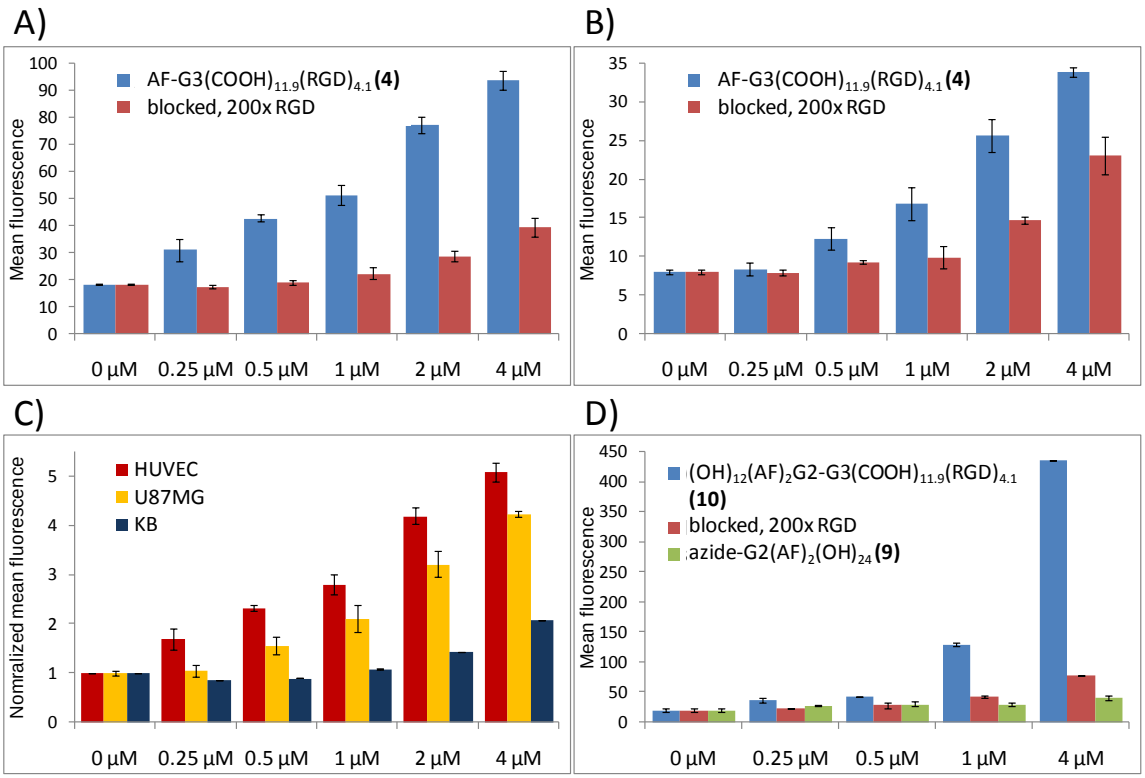


**Figure 2.3**. Dose dependent uptake and specific targeting of binary dendrons determined via flow cytometry, with mean fluorescence plotted against the concentration of the dendron conjugate. Specific targeting of AF-G3(COOH)$_{11.9}$(RGD)$_{4.1}$ **(4)** was displayed in human umbilical vein endothelial cells (HUVEC) (A), and U87MG human glioblastoma cells (B). Blocking of **4** at all tested concentrations with a 200-fold molar excess of c(RGDyK) confirms specific targeting of the $\alpha_V\beta_3$ integrin by the dendron. A cell-line comparison between HUVEC, U87MG, and $\alpha_V\beta_3$ integrin deficient KB cells (C) shows dendron uptake is greater in cell lines with increased $\alpha_V\beta_3$ integrin expression, demonstrating the active targeting capability of the binary dendron. A significant increase in mean fluorescence was displayed for a co-dendron structure capable of carrying additional dye, (OH)$_{24}$(AF)$_2$G2-G3(COOH)$_{11.9}$(RGD)$_{4.1}$ **(10)**, in HUVEC (D). The specific uptake of the co-dendron was confirmed by inhibition with free RGD as well as from a non-targeted control, azide-G2(AF)$_2$(OH)$_{24}$ **(9)**. Error bars indicate standard deviation as computed from the half-peak coefficient of variation.

A co-dendron structure, (OH)$_{24}$(AF)$_2$G2-G3(COOH)$_{11.9}$(RGD)$_{4.1}$ **10** was created by reacting an Alexa Fluor 488 conjugated dendron **9** with an azide focal point with **3**. The product was purified via HPLC to remove excess **9**. The HPLC shows that a significant percentage of the starting material was unreacted. Reaction conditions should

be optimized in the future. The co-dendron structure offers an increased carrying capacity for conjugates, including the Alexa Fluor 488 used in this study. NMR of **9** showed an average of 2 Alexa Fluor 488 molecules attached per dendron, thus it was expected to emit a stronger signal when conjugated to **3** compared to a single dye at the focal point.

The specific binding of co-dendron **10** to $\alpha_V\beta_3$ integrin expressing HUVEC cells was determined via flow cytometry (Figure 2.3 D). The co-dendron treated samples show the expected increase in mean fluorescence compared to mono-dye conjugated **4**. Specific binding could be significantly blocked (Figure 2.4), but again the higher avidity dendron conjugate out-competed free RGD. Non-targeted control **9** showed minimal non-specific uptake.

The specific binding evaluated by flow cytometry was confirmed by confocal microscopy. HUVEC cells were treated with 0.5 μM **10** or biotin-conjugated **7** and incubated for 2 hours. The biotin-conjugate was detected by the addition of an avidin-functionalized dye. Confocal images confirm the uptake of the dendrons (Figure 2.5 B, D), as seen from the punctuate pattern within the cytoplasm. Partial inhibition of the dendron conjugates by preincubation with free RGD was also established (Figure 2.5 C, E).

A drug conjugate, **6** was synthesized to show the therapeutic potential of the platform. MTX was reacted with 11-azido-3,6,9-trioxaundecan-1-amine to yield an azide-functional drug. The resulting MTX-azide was then attached to the dendron at the focal point via click chemistry. The inhibition of cell growth induced by the dendron conjugates was tested by XTT colorimetric assay. **6** and free MTX showed comparable

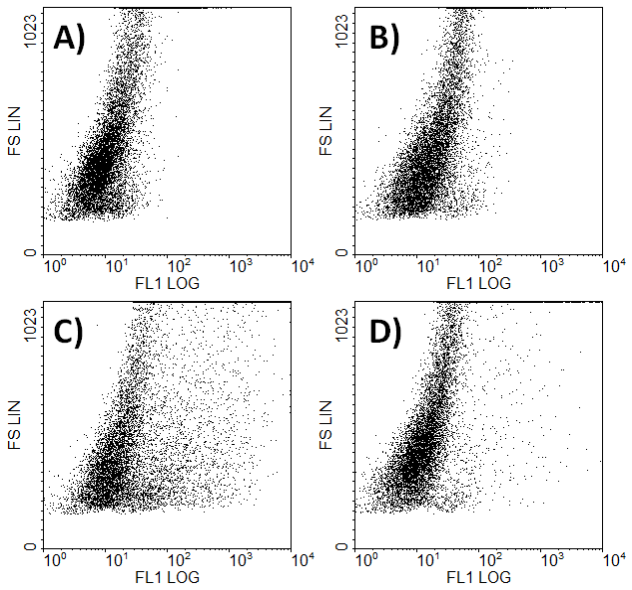


**Figure 2.4**. Flow cytometry plot of fluorescence versus forward scatter for $(OH)_{24}(AF)_2G2\text{-}G3(COOH)_{11.9}(RGD)_{4.1}$ **(10)** at 4 µM. The co-dendron conjugate (C) shows a significant broadening in cell population compared to the untreated control (A). When pre-incubated with a 200-fold molar excess of free RGD (D), **10** is partially blocked, but out-competes the excess monomeric RGD. The non-targeted control (B), azide-$G2(AF)_2(OH)_{24}$ **(9)**, shows no significant change in cell population when compared to the control.

cytotoxicity to HUVEC cells after 3 days (Figure 2.6). Cell numbers were between 55-80% for all **6** and free MTX treated samples at concentrations greater than 0.125 µM. The effects of **6** and MTX were not significantly different at these concentrations. **6** had a significantly greater effect on cell viability versus **3** for concentrations greater than 0.125 µM. **6** has an approximately equivalent concentration of MTX compared to free drug; the drug-conjugated dendron **6** treatments may have slightly lower drug concentration due to any remaining uncoupled dendron. The similar toxicities of **6** and free MTX show that the dendron scaffold is effective at delivering a therapeutic to cells.

We have shown that by exploiting the initiation point as a unique binding site in PAMAM dendrons, selective coupling reactions can yield highly defined binary devices that exhibit the ability to bind to specific cells. Employing a 1,3-dipolar cycloaddition to

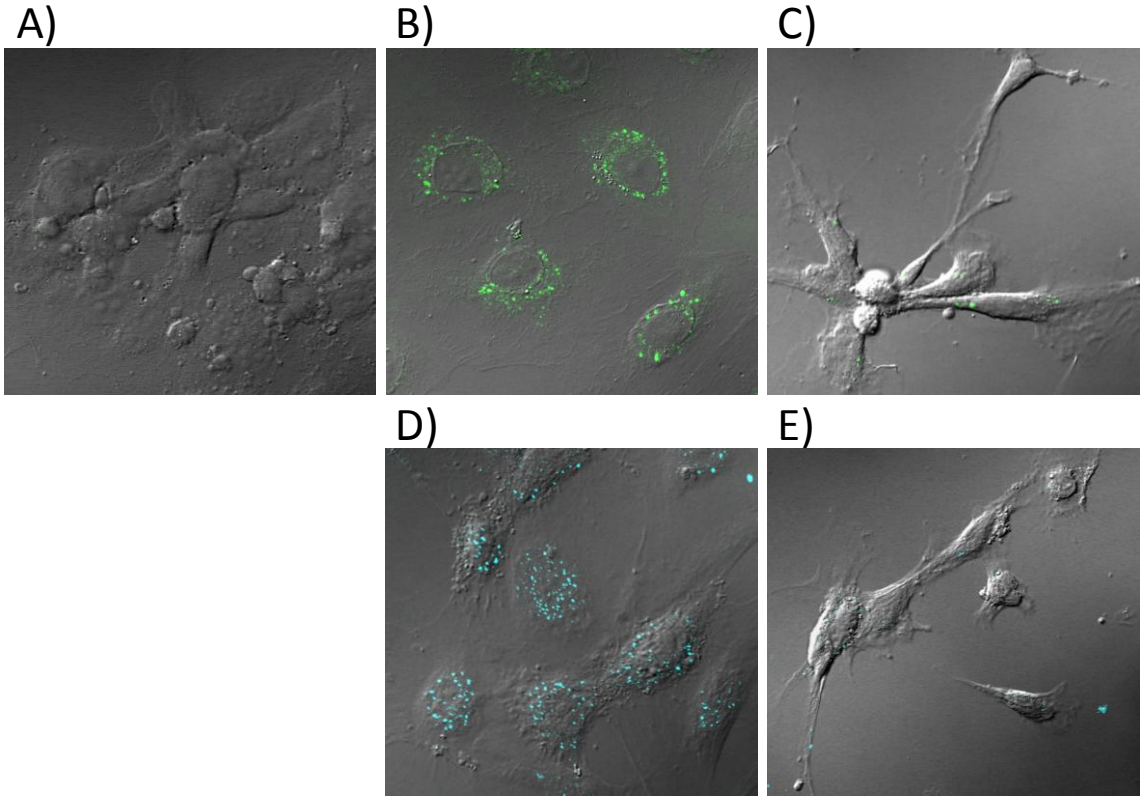


**Figure 2.5**. Confocal images of HUVEC cells either untreated (A) or treated with 0.5 µM $(OH)_{24}(AF)_2$G2-G3$(COOH)_{11.9}(RGD)_{4.1}$ **(10)** (B-C) or biotin-G3$(COOH)_{11.9}(RGD)_{4.1}$ **(7)** (D-E) dendron for 2 hours. Samples C and E were pre-incubated with 100 µM c(RGDyK). Biotin-conjugated dendrons were detected by the addition of NeutrAvidin-Dylight 405.

the focal point of the dendron allows for additional functional moieties to be added in a precise manner without altering other molecules on the dendron. The prototype molecule, synthesized **4**, successfully displayed specific targeting to $\alpha_V\beta_3$ integrin, behaving similarly to RGD conjugates on previously studied multifunctional G5 PAMAM dendrimers (5, 6) that lack the same degree of synthetic control. Detection can be enhanced by attaching an additional dendron with an increased carrying capacity, shown with **10**. The dendron can be combined with biotin, allowing it to interact with a variety of avidin-functionalized molecules. **6** was shown to successfully inhibit the growth of HUVEC cells similarly to free drug. The PAMAM dendron platform has

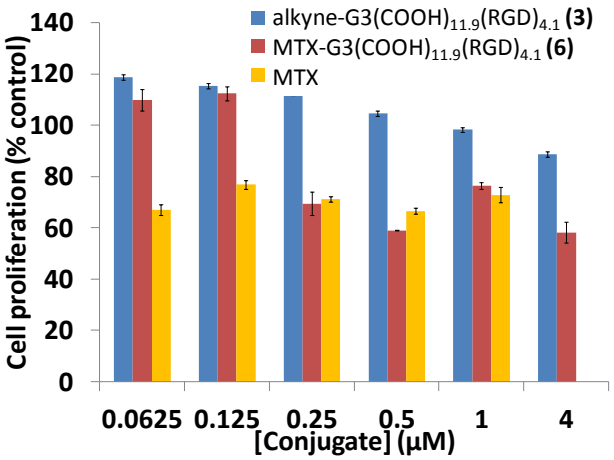


**Figure 2.6**. The antiproliferative effect of MTX-G3(COOH)$_{11.9}$(RGD)$_{4.1}$ **(6)**. The dose-dependent inhibition of cell growth of **6** was compared to free MTX and alkyne-G3(COOH)$_{11.9}$(RGD)$_{4.1}$ control **(3)** using a XTT assay. The cells were treated with different concentrations of free MTX or dendron conjugates for 72 hours with a replenishing of 100 μL medium and the conjugates after 48 hours. **6** and MTX were determined to not be significantly different for concentrations greater than or equal to 0.25 μM. The effects of **6** and MTX were not significantly different for concentrations greater than 0.125 μM. **6** had a significantly greater effect on cell viability versus **3** for concentrations greater than 0.125 μM.

potential to be important in targeted delivery chemistry, as our binary device can serve as a framework to selectively attach diagnostic and imaging agents, therapeutics, or other biologically relevant moieties and surfaces. In addition, coupling a second functionalized dendron or dendrimer to the dendron could address other applications requiring the delivery of multiple drugs or imaging agents.

The methodology of using click chemistry to create modular dendritic platforms is attractive, though can be improved upon. The removal of toxic copper catalyst is highly intensive and may limit the applicability of the platform for other biological systems. Additionally, the claims that copper-catalyzed click chemistry is a universal system offering quantitative yields were not supported using the PAMAM platform. While the mechanism for this was not explored, it has been hypothesized that steric bulk around the focal point significantly hinders reaction conversions (16). The Weck group

argued that copper complexation to polyamide dendrimers likely prevented quantitative yields (17). We can argue that a similar fate occurs in our analogous system.

**Acknowledgments:** Jolanta F. Kukowska-Latallo, Douglas G. Mullen, Joseph M. Wallace, Ankur M. Desai, Rameshwer Shukla, Baohua Huang, Mark M. Banaszak Holl, and James R. Baker Jr. made essential contributions to the work in this chapter.

## Chapter 2 Appendix

**Figure S2.1: $^{1}$H NMR spectrum of alkyne-G3-PAMAM dendron (1)**

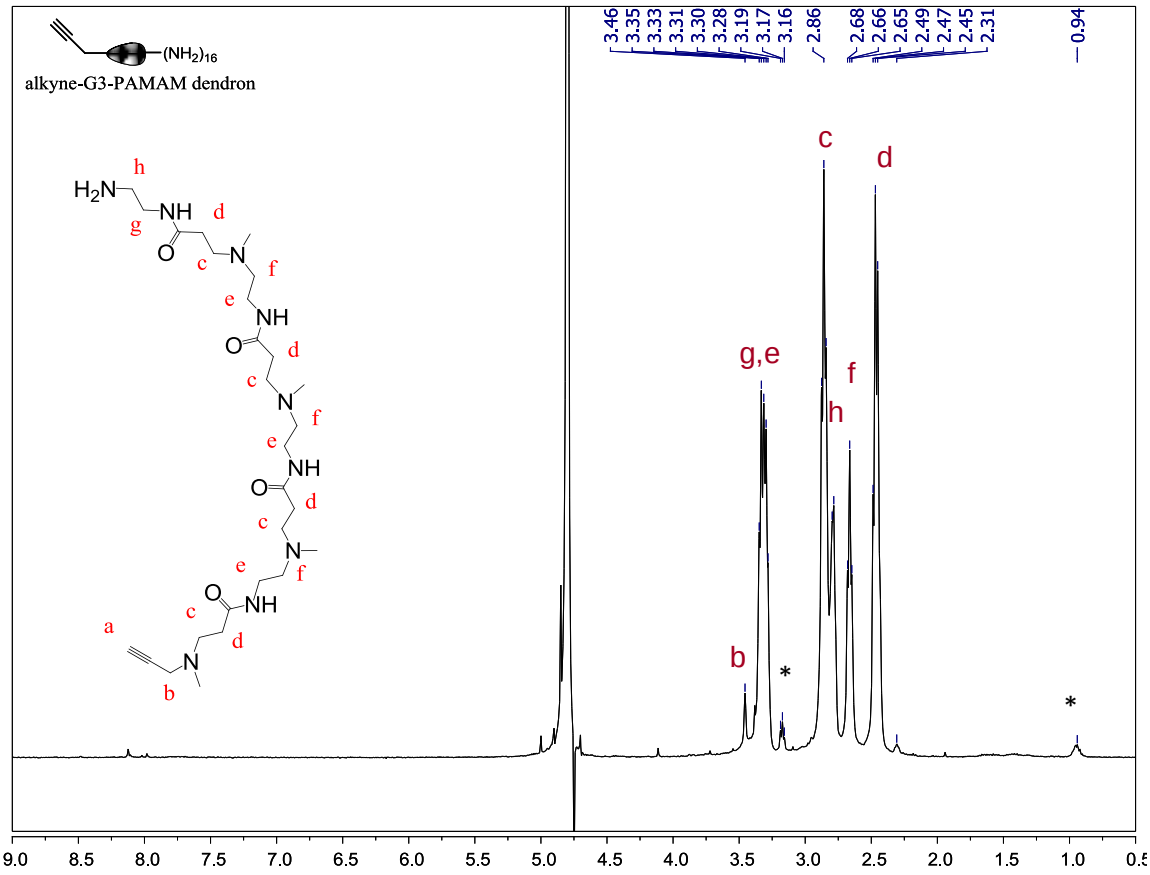


$^{1}$H NMR (400 MHz, $D_2O$): δ = 3.46 (s, 2H, N-C*H*$_2$-CH, "b"), 3.43-3.20 (m, 64H, NH-C*H*$_2$-CH$_2$-NH$_2$, NH-C*H*$_2$-CH$_2$-N, "g and e"), 2.86 (m, 60H, N-C*H*$_2$-CH$_2$-CO, "c"), 2.78 (m, 28H, NH-CH$_2$-C*H*$_2$-NH$_2$, "h"), 2.66 (t, 28H, NH-CH$_2$-C*H*$_2$-N, "f"), 2.47 (m, 60H, N-CH$_2$-C*H*$_2$-CO, "d").

* denotes residual 1-butanol used in azeotropic removal of excess ethylenediamine.

Proton "a", found at 2.61 ppm for smaller generation dendrons, is likely buried within peaks assigned "f", or "d".

**Figure S2.2: $^{1}$H NMR spectrum of alkyne-G3(COOH)$_{16}$ dendron (2)**

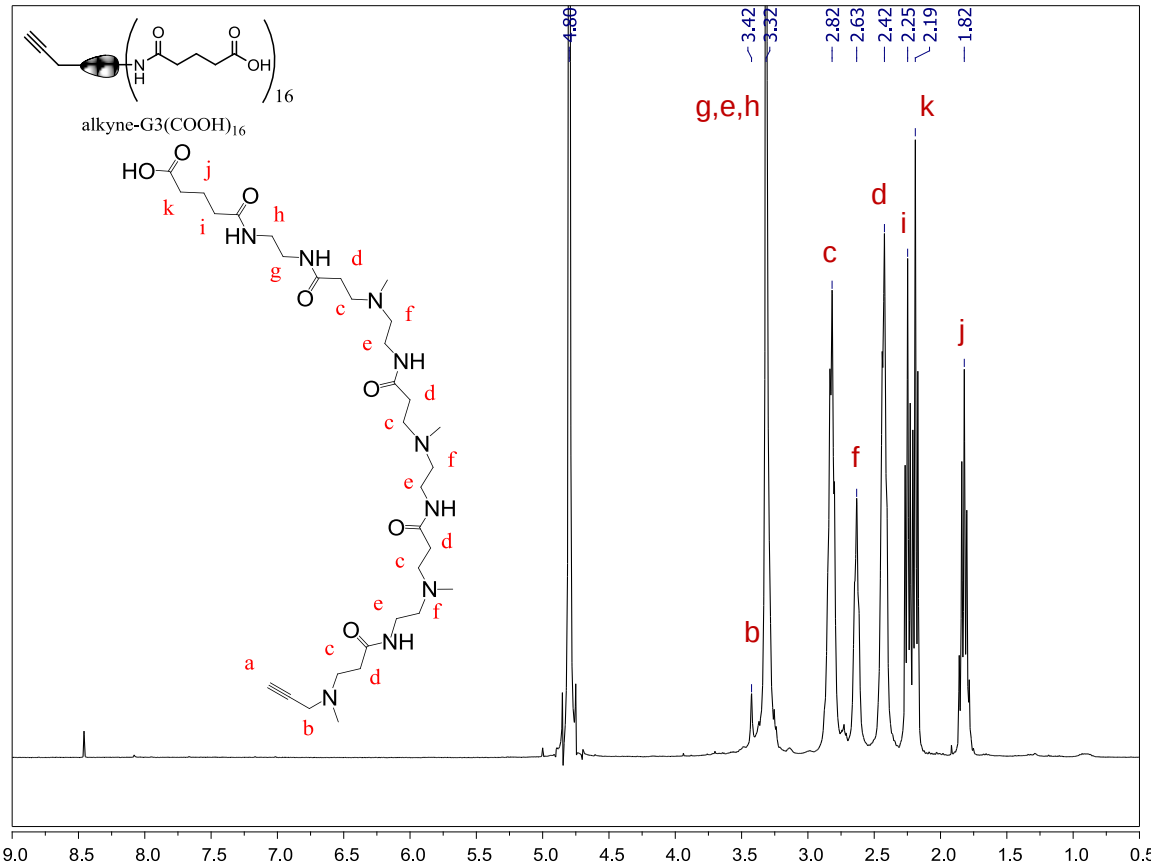


$^{1}$H NMR (400 MHz, $D_2O$): δ = 3.42 (s, 2H, N-C*H*$_2$-CH, "b"), 3.32 (m, 92H, NH-C*H*$_2$-$CH_2$-$NH_2$, NH-C*H*$_2$-$CH_2$-N, NH-$CH_2$-C*H*$_2$-$NH_2$, "g, e, and h"), 2.82 (m, 60H, N-C*H*$_2$-$CH_2$-CO, "c"), 2.62 (t, 28H, NH-$CH_2$-C*H*$_2$-N, "f"), 2.42 (m, 60H, N-$CH_2$-C*H*$_2$-CO, "d"), 2.25 (t, 32H, CO-C*H*$_2$-$CH_2$-$CH_2$-CO-OH, "i"), 2.19 (t, 32H, CO-$CH_2$-$CH_2$-C*H*$_2$-CO-OH), "k", 1.84 (qt, 32H, CO-$CH_2$-C*H*$_2$-$CH_2$-CO-OH, "j").

Proton "a" is overlapping with dendron peaks in the 2.75-2.50 ppm range.

**Figure S2.3: $^{1}$H NMR spectrum of alkyne-G3(COOH)$_{11.9}$(RGD)$_{4.1}$ dendron (3)**

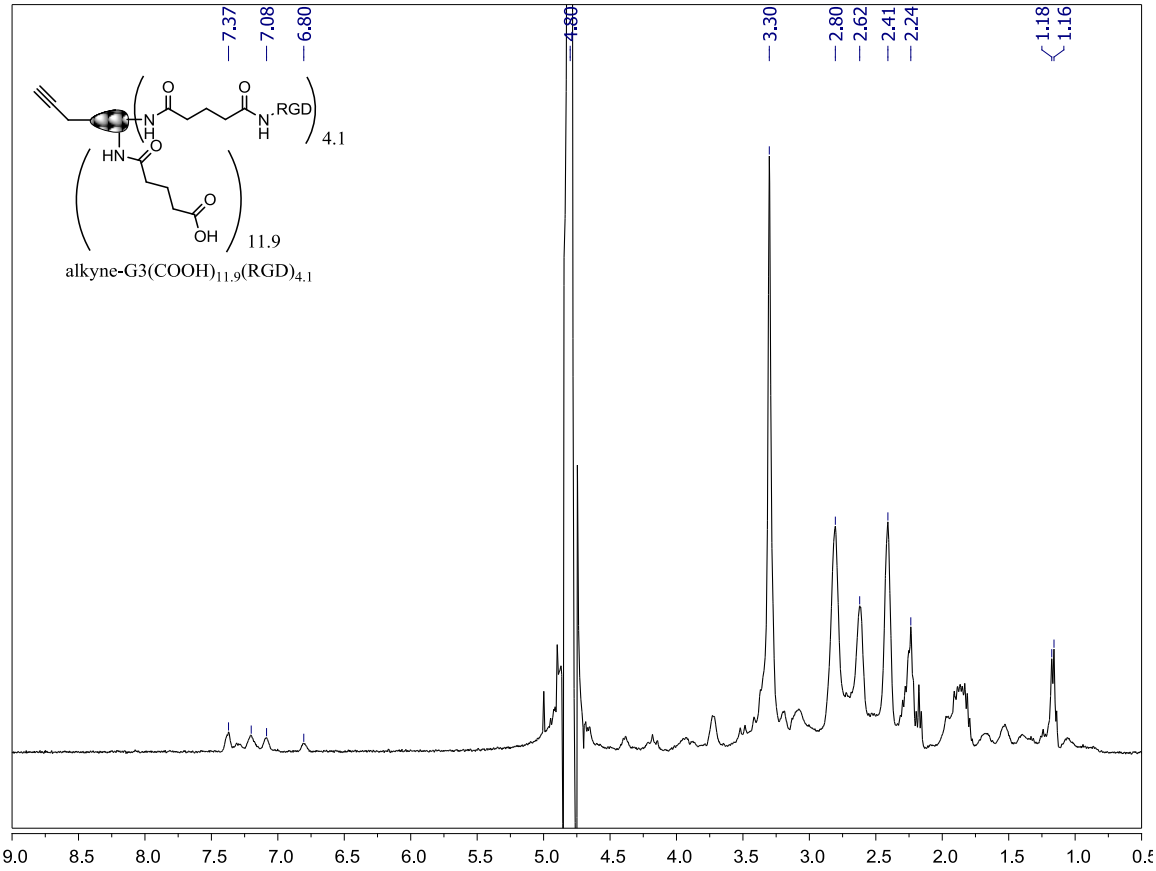


$^{1}$H NMR (400 MHz, $D_2O$): δ =

Dendron backbone: 3.42 (s, 2H, N-C*H*$_2$-CH), 3.30 (m, 92H, NH-C*H*$_2$-CH$_2$-NH$_2$, NH-C*H*$_2$-CH$_2$-N, NH-CH$_2$-C*H*$_2$-NH$_2$), 2.80 (m, 60H, N-C*H*$_2$-CH$_2$-CO, ), 2.62 (b, 28H, NH-CH$_2$-C*H*$_2$-N), 2.41 (b, 60H, N-CH$_2$-C*H*$_2$-CO), 2.24 (b, 48H, CO-C*H*$_2$-CH$_2$-CH$_2$-CO-OH, CO-CH$_2$-CH$_2$-C*H*$_2$-CO-OH, from unreacted glutarate terminal groups "i an k"), 2.10-1.75 (m, 48H, "j" and "i', j', and k'" from conjugated glutarate terminal groups).

Conjugated RGD: 7.40-6.80 (16.4 H, aromatic RGD protons), 4.40 (8.2H), 4.20 (8.2H), 3.72 (8.2H), 3.10, 1.70 (8.2H), 1.53 (8.2H), 1.35 (8.2H) 1.17 (16.4H). Additional peaks are overlapping with peaks from the dendron backbone.

**Figure S2.4: $^{1}$H NMR spectrum of AF-G3(COOH)$_{11.9}$(RGD)$_{4.1}$ dendron (4)**

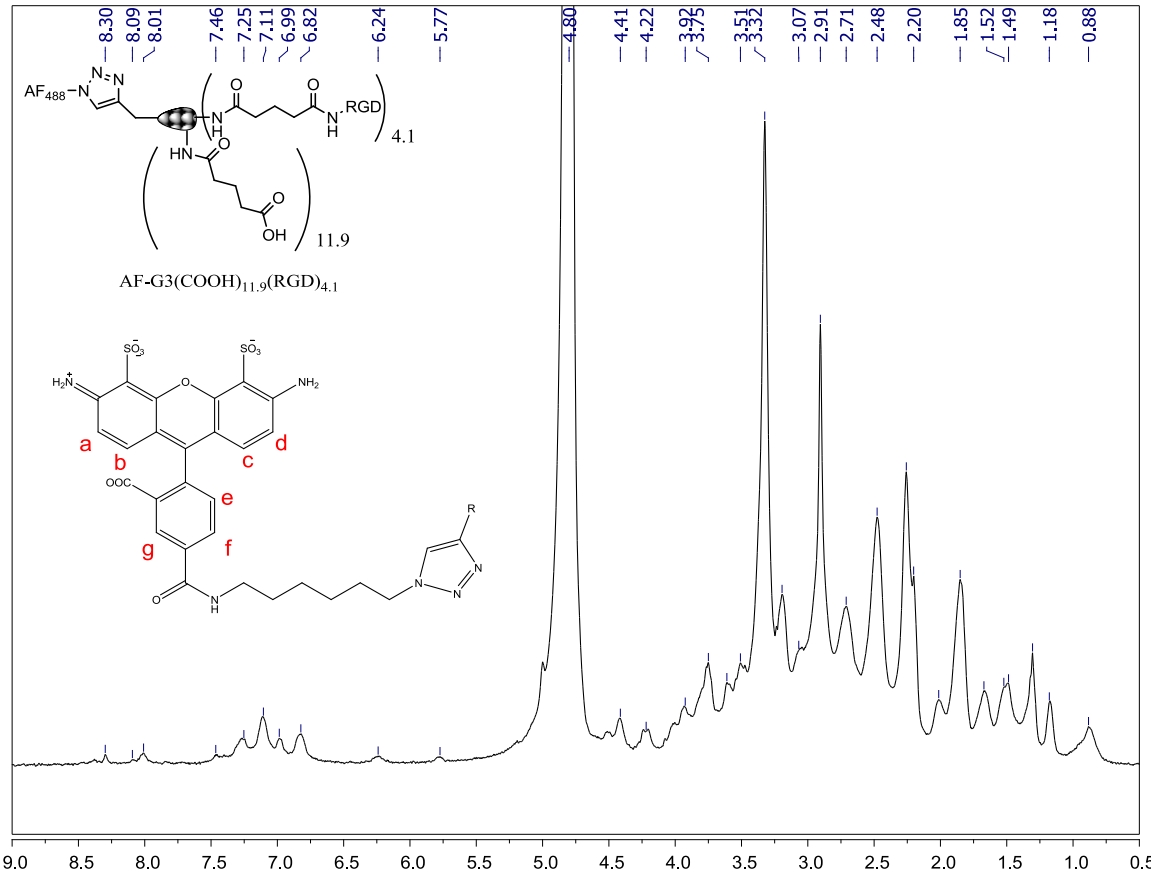


***R = G3(COOH)$_{11.9}$(RGD)$_{4.1}$***

$^{1}$H NMR (500 MHz, $D_2O$):

Aromatic Alexa Fluor 488 peaks at 8.30 (~0.65H, "g"), 8.09 (~0.65H, "f"), and 7.46 (~0.65H, "e") can be resolved. Peaks "b" and "c" (expected at 7.17) and "a" and "d" (expected at 6.94) are overlapped by the aromatic RGD peaks.

Peaks from the $(CH_2)_6$ spacer are overlapped with the aliphatic dendron and RGD peaks.

**Figure S2.5: $^{1}$H NMR spectrum of MTX-azide (5)**

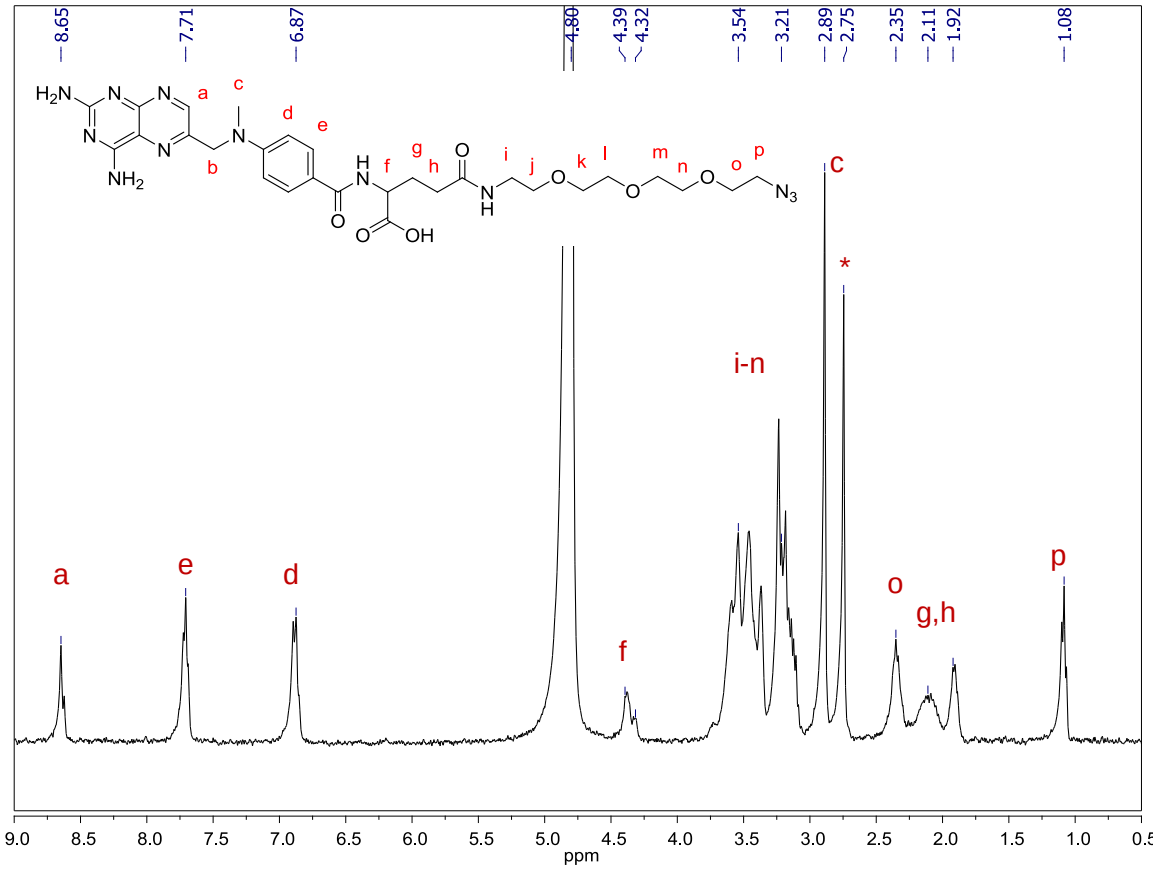


$^{1}$H NMR (500 MHz, $D_2O$): δ = 8.65 (1H, N-CH-C, “a”), 7.71 (d, 2H, C-C-CH-CH-C-CO, “e”), 6.87 (d, 2H, C-C-CH-CH-C-CO, “d”), 4.40-4.30 (b, 1H, NH-C*H*C-CH2, “f”), 3.7-3.05 (m, O-CH2-CH2-O, “i-n”), 2.89 (s, N-$CH_3$, “c”), 2.35 (b, 2H, O-C*H*$_2$-$CH_2$-$N_3$, “o”), 2.11 (b, 2H, CH-C*H*$_2$-$CH_2$-CO, “g”), 1.92 (b, 2H, CH-$CH_2$-C*H*$_2$-CO, “h”), 1.08 (t, 2H, O-$CH_2$-C*H*$_2$-$N_3$, “p”).

* denotes *N*-Hydroxysuccinimide impurity (3.4H)

**Figure S2.6: $^{1}$H NMR spectrum of MTX-G3(COOH)$_{11.9}$(RGD)$_{4.1}$ dendron (6)**

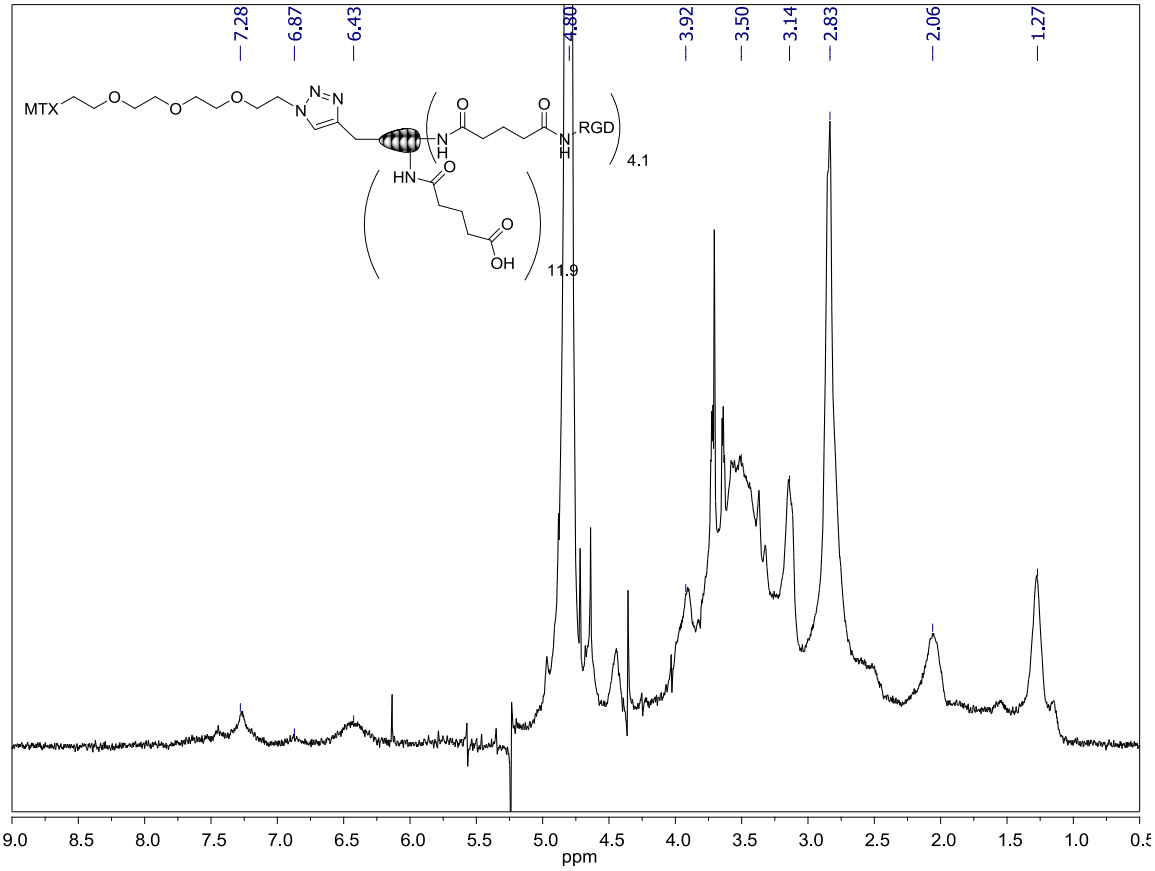


$^{1}$H NMR (500 MHz, $D_2O$)

Peaks were not resolved for this sample. MALDI, UPLC and *in vitro* functional assays were used to confirm the successful formation of the product.

**Figure S2.7: $^{1}$H NMR spectrum of Biotin-G3(COOH)$_{11.9}$(RGD)$_{4.1}$ dendron (7)**

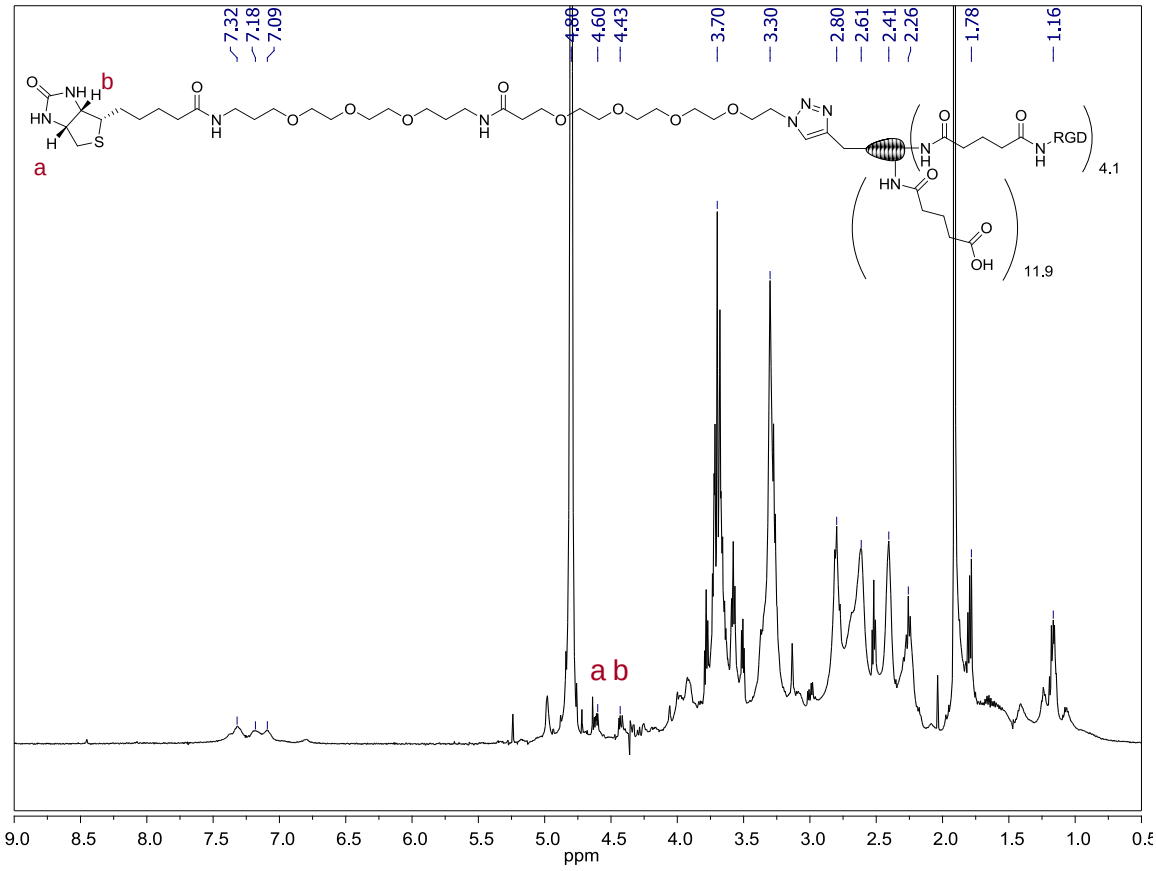


$^{1}$H NMR (400 MHz, $D_2O$): δ = 4.60 (1H, "a"), 4.43 (1H, "b"). The unassigned biotin peaks are overlapping with the aliphatic conjugated dendron peaks. The d-PEG spacer is overlapping in the dendron region (expected at 3.75-3.0)

An unknown impurity is present at 1.91.

**Figure S2.8: $^{1}$H NMR spectrum of azide-G2-PAMAM dendron (8)**

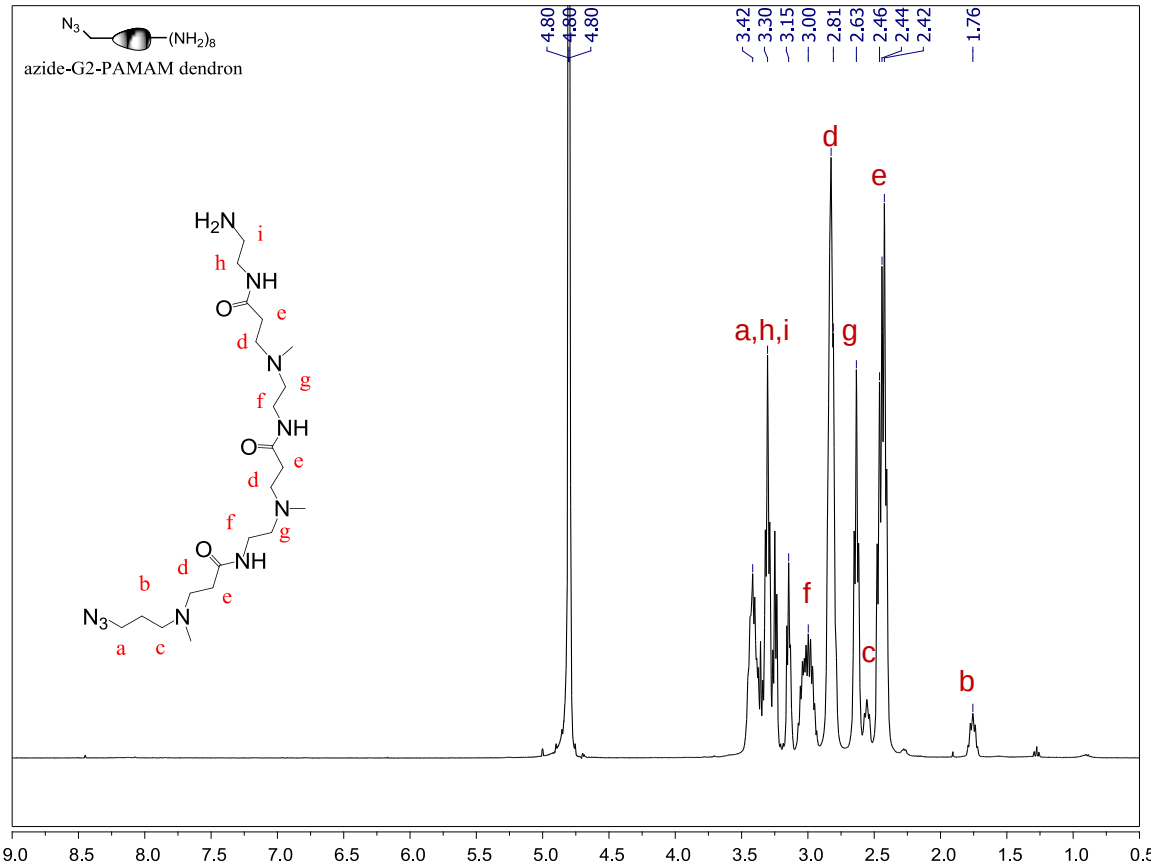


$^{1}$H NMR (400 MHz, $D_2O$): δ = 3.50-3.10 (34H, "a, h, and i"), 3.00 (12H, NH-C*H*$_2$-CH$_2$-N, "f"), 2.81 (28H, N-C*H*$_2$-CH$_2$-CO, "d"), 2.63 (12H, NH-CH$_2$-C*H*$_2$-N, "g"), 2.55 (2H, N$_3$-CH$_2$-CH$_2$-C*H*$_2$-N, "c"), 2.44 (28H, N-CH$_2$-C*H*$_2$-CO, "e"), 1.76 (2H, N$_3$-CH$_2$-C*H*$_2$-CH$_2$-N, "b").

**Figure S2.9: $^{1}$H NMR spectrum of azide-G2(AF)$_2$(OH)$_{24}$ dendron (9)**

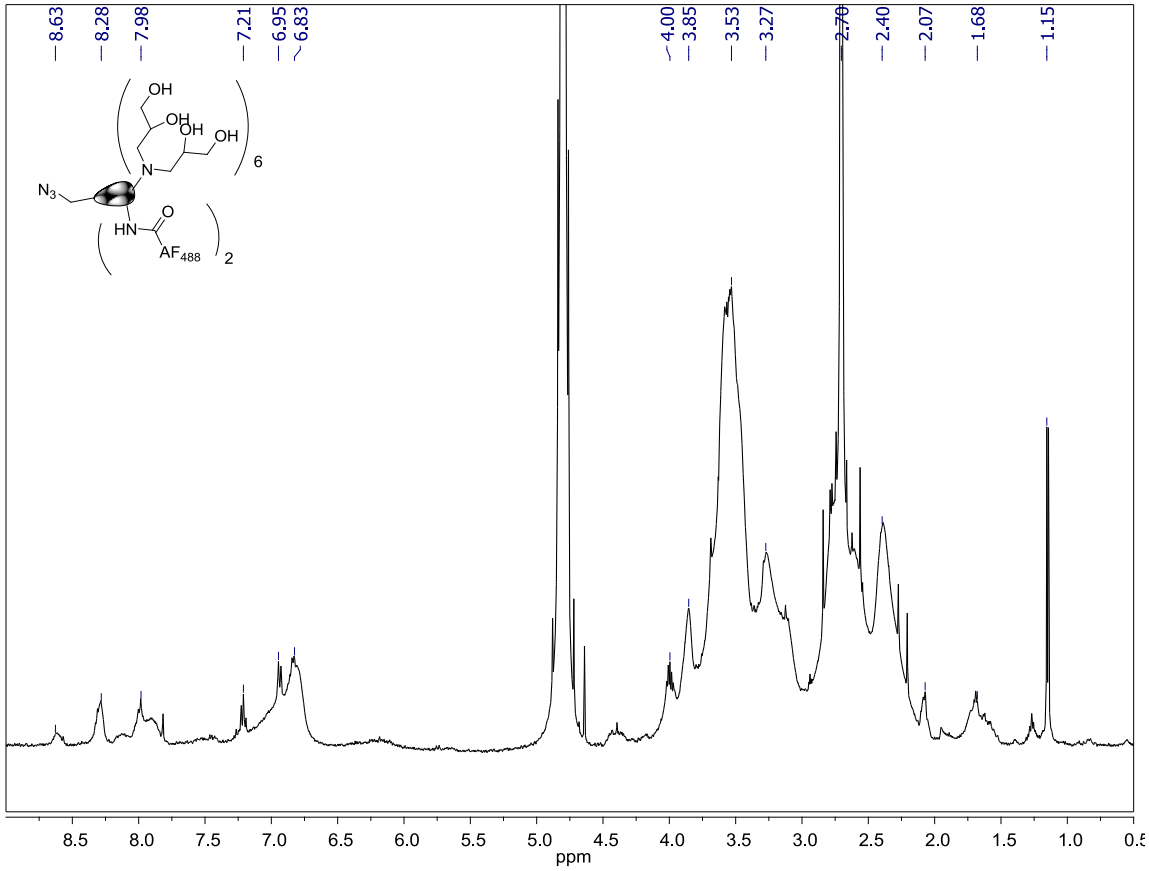


$^{1}$H NMR (500 MHz, $D_2O$)

Dendron peaks are indistinguishable between 4.0 and 1.0 ppm.

Sharp aromatic Alexa Fluor 488 peaks suggest that small free dye impurities were still present in this sample. The removal of detectable free dye after the attachment of this dendron to alkyne-G3(COOH)$_{11.9}$(RGD)$_{4.1}$ was confirmed via HPLC.

**Figure S2.10: $^{1}$H NMR spectrum of $(OH)_{24}(AF)_2G2\text{-}G3(COOH)_{11.9}(RGD)_{4.1}$ (10)**

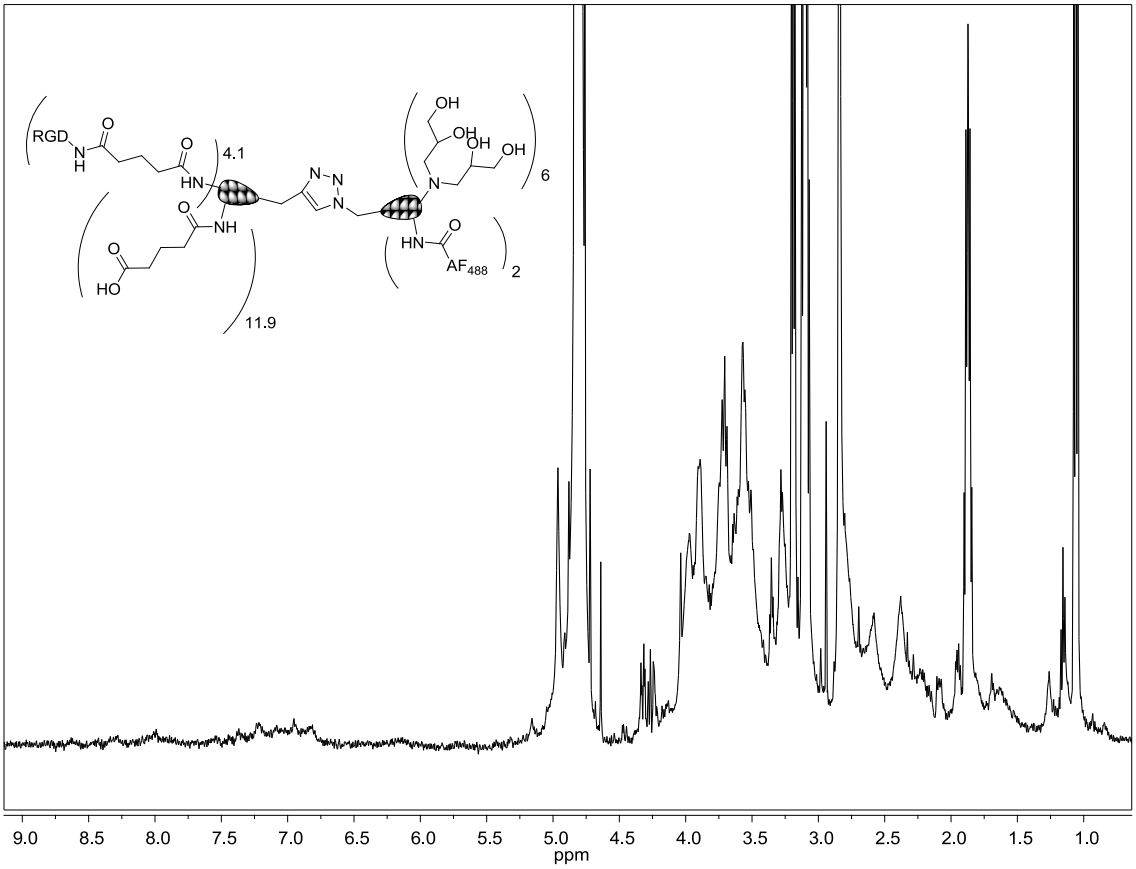


$^{1}$H NMR (500 MHz, $D_2O$)

The complexity and low concentration of the isolated co-dendron sample does not allow for proper assignments to be made. Aromatic RGD and Alexa Fluor 488 peaks are identifiable. MALDI, UPLC and *in vitro* experiments were used to confirm the successful formation of the product.

**Figure S2.11: HPLC Profile of alkyne-G3(COOH)$_{16}$ dendron (2)**

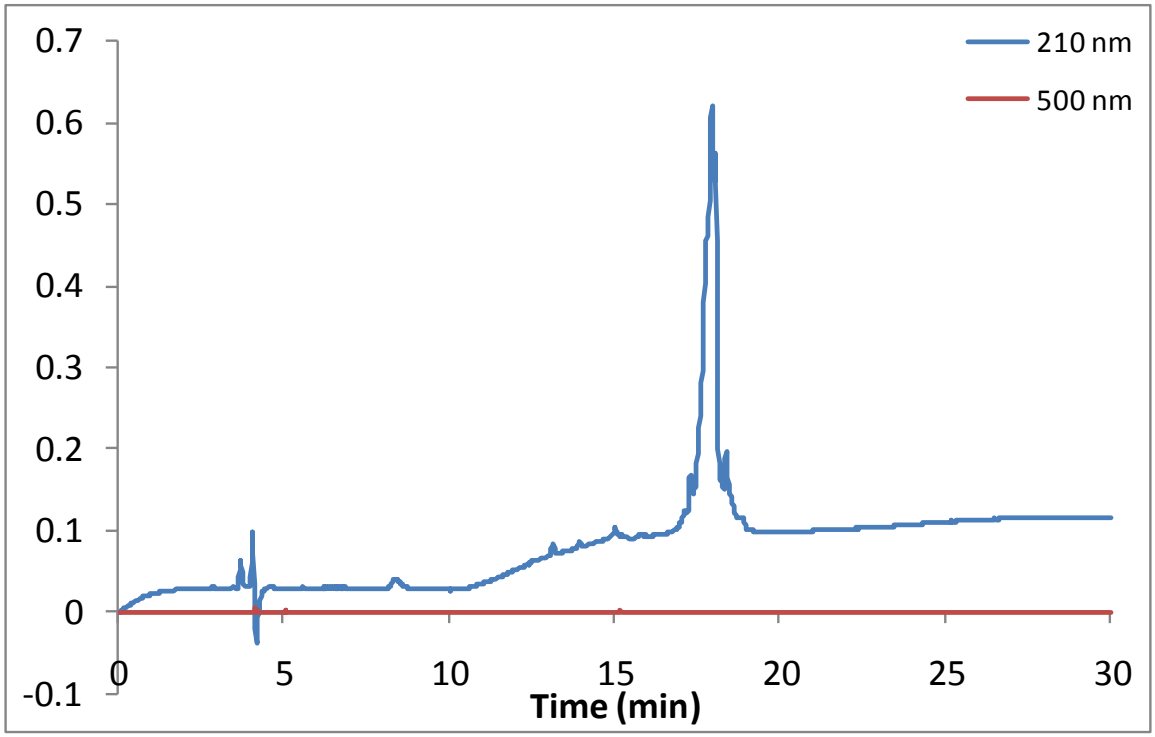


**Figure S2.12: HPLC Profile of alkyne-G3(COOH)$_{11.9}$(RGD)$_{4.1}$ (3)**

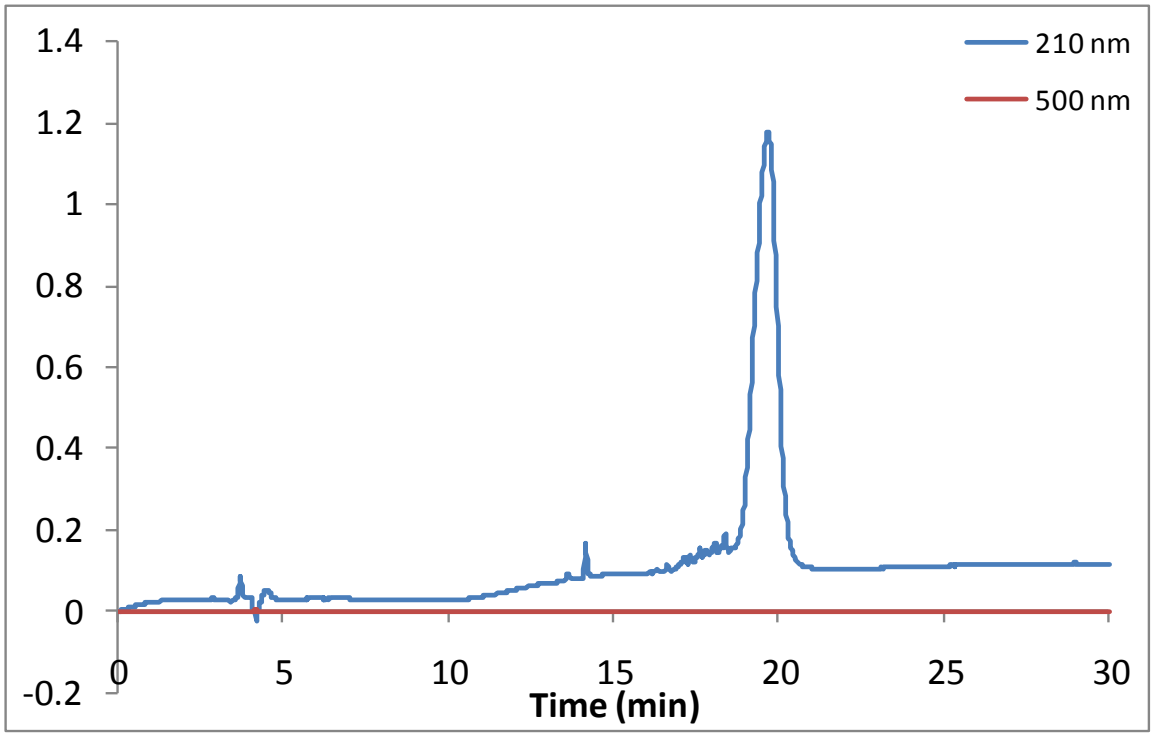

**Figure S2.13: HPLC Profile of AF-G3(COOH)$_{11.9}$(RGD)$_{4.1}$ dendron (4)**

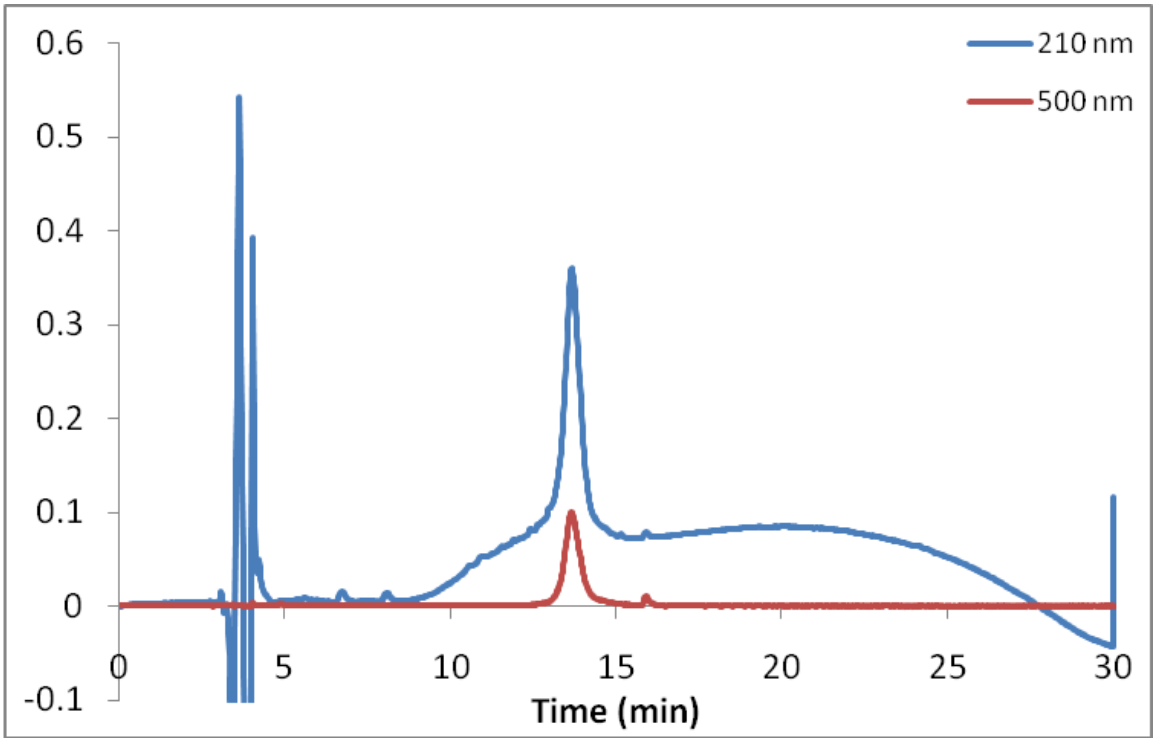


**Figure S2.14: UPLC Profile of MTX–azide (5)**

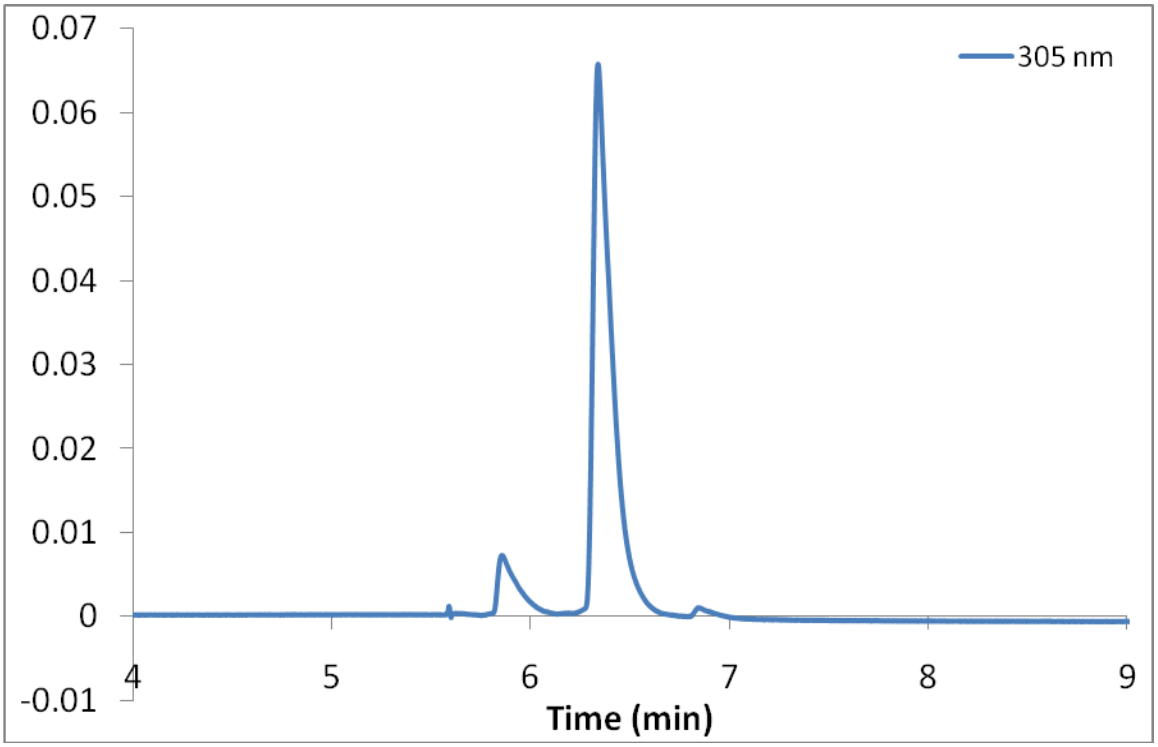

**Figure S2.15: UPLC Profile of MTX-G3(COOH)$_{11.9}$(RGD)$_{4.1}$ dendron (6)**

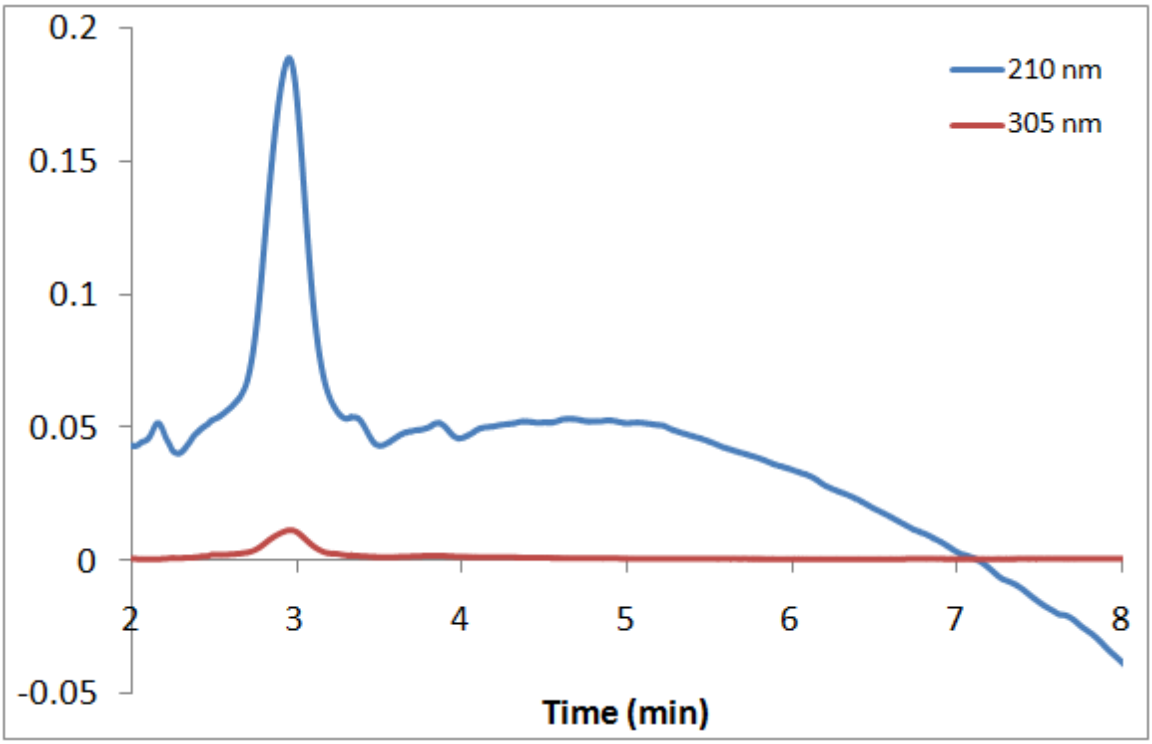


**Figure S2.16: UPLC Profile of Biotin-G3(COOH)$_{11.9}$(RGD)$_{4.1}$ dendron (7)**

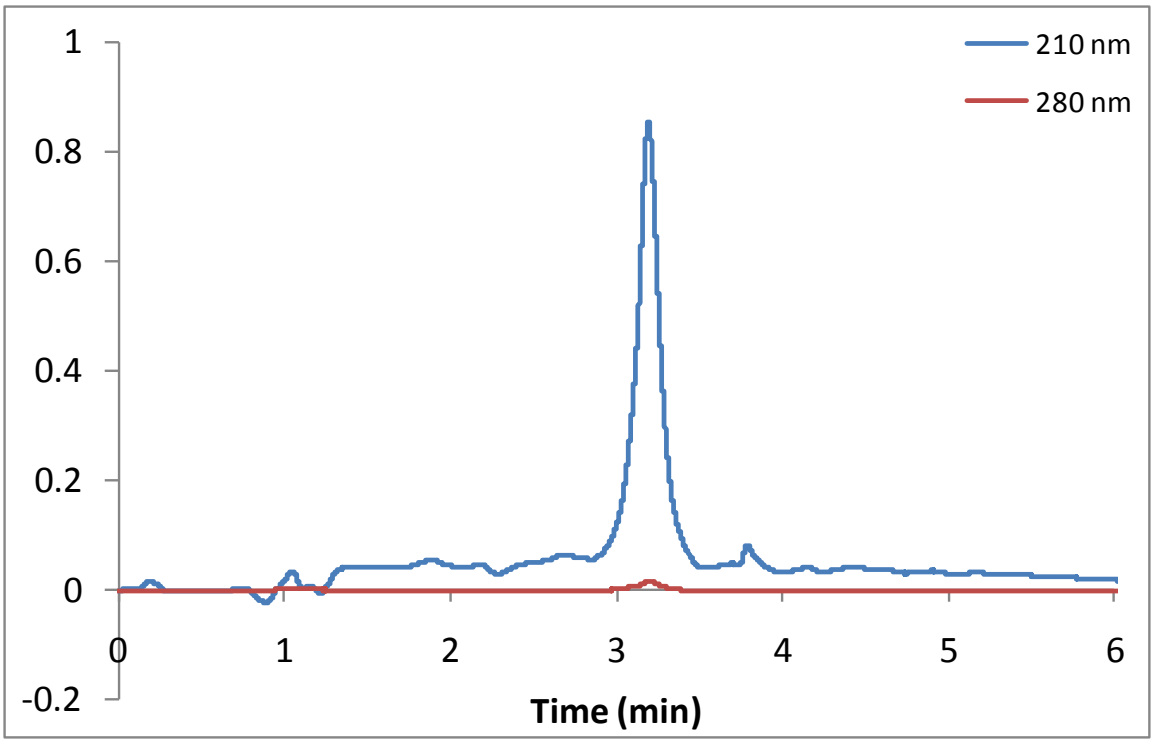

**Figure S2.17: HPLC Profile of azide-G2-PAMAM dendron (8)**

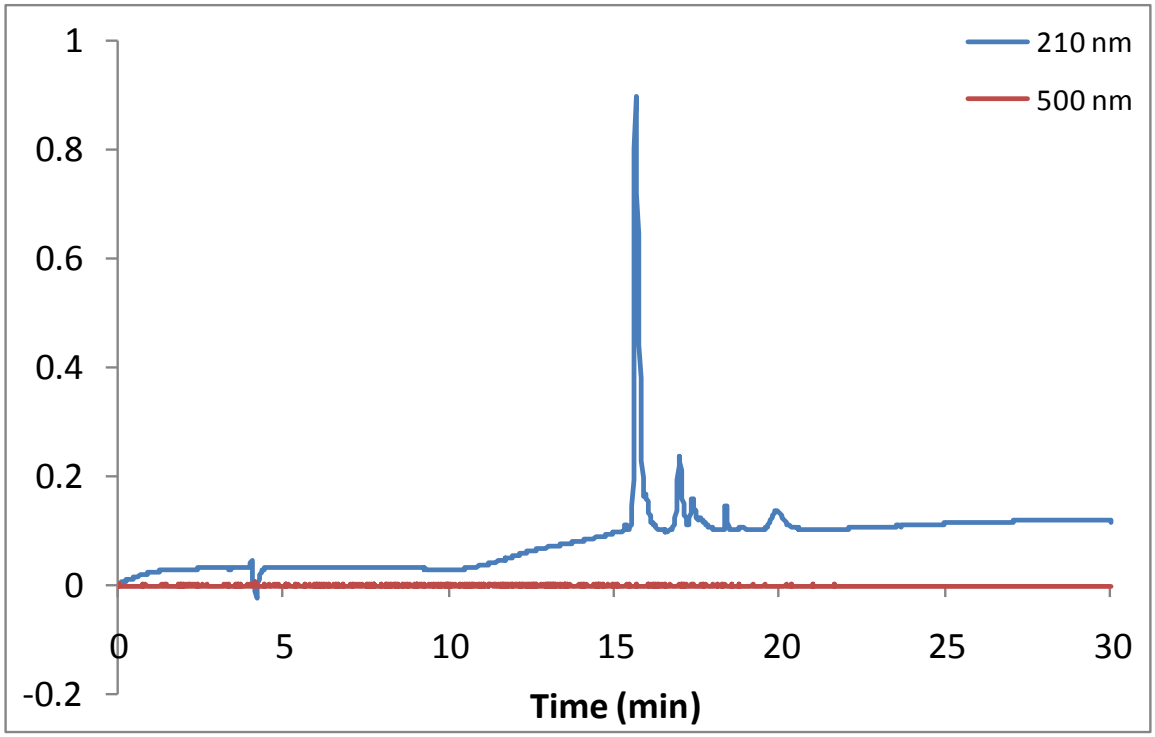


**Figure S2.18: UPLC Profile of azide-G2-$(AF)_2(OH)_{24}$ dendron (9)**

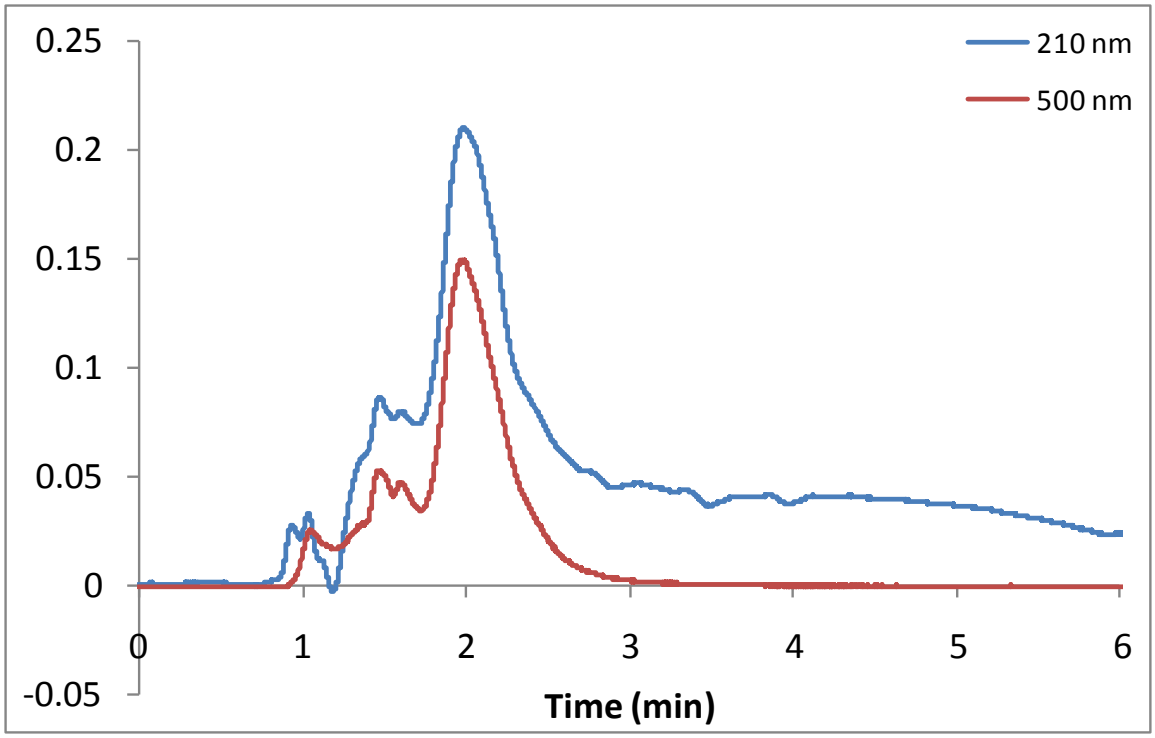

**Figure S2.19: UPLC and HPLC Profiles of $(OH)_{24}(AF)_2G2\text{-}G3(COOH)_{11.9}(RGD)_{4.1}$ (10)**

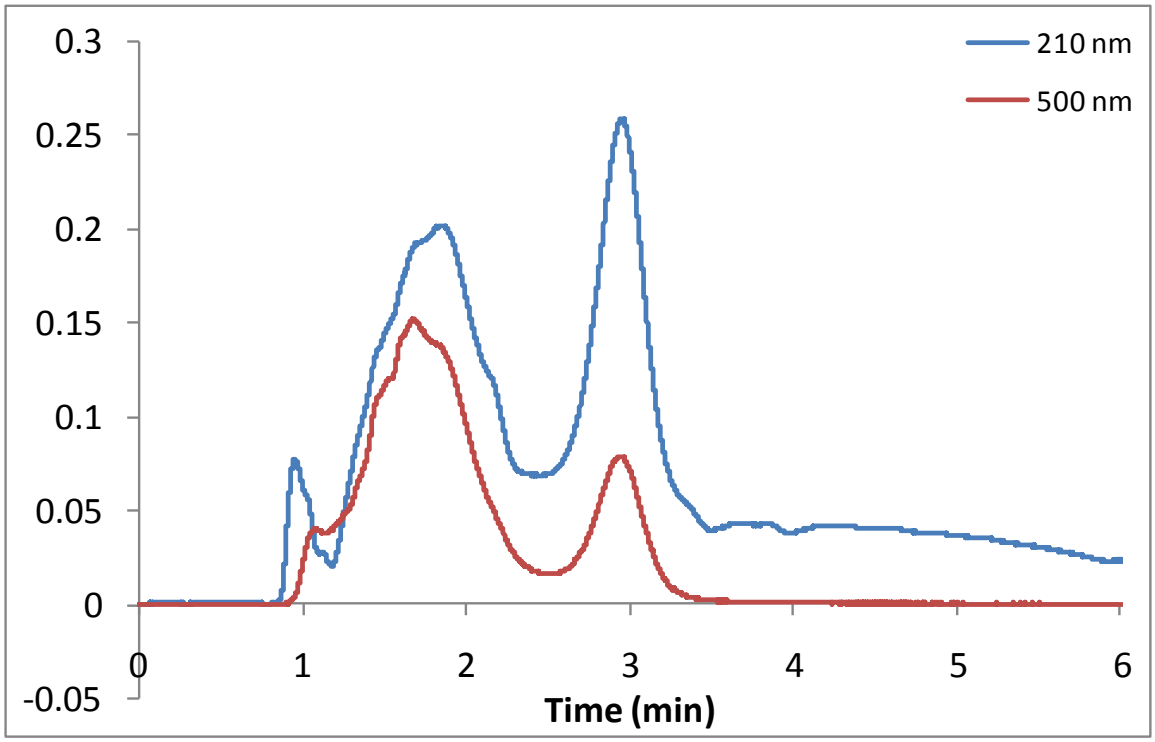


**HPLC (dotted lines show collected fraction)**

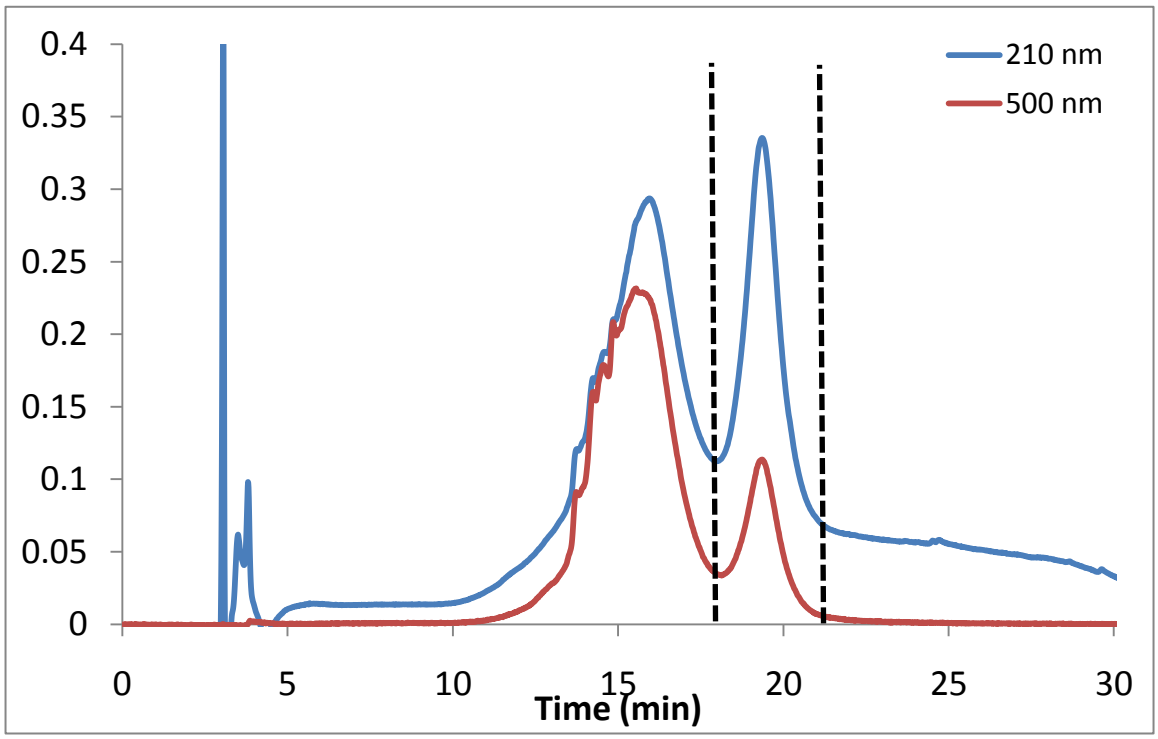

REFERENCES

(1) Mullen, D. G. (2010) Design Challenges in Nanoparticle-Based Platforms: Implications for Targeted Drug Delivery Systems. Dissertation, University of Michigan, Ann Arbor,

(2) Choi, Y., Thomas, T., Kotlyar, A., Islam, M. T. and Baker, J. R.,Jr. (2005) Synthesis and functional evaluation of DNA-assembled polyamidoamine dendrimer clusters for cancer cell-specific targeting. Chem.Biol. **12**, 35-43

(3) Goyal, P., Yoon, K. and Weck, M. (2007) Multifunctionalization of dendrimers through orthogonal transformations. Chemistry. **13**, 8801-8810

(4) Wu, P., Malkoch, M., Hunt, J. N., Vestberg, R., Kaltgrad, E., Finn, M. G., Fokin, V. V., Sharpless, K. B. and Hawker, C. J. (2005) Multivalent, bifunctional dendrimers prepared by click chemistry. Chem.Commun.(Camb). **(46)**, 5775-5777

(5) Shukla, R., Thomas, T. P., Peters, J., Kotlyar, A., Myc, A. and Baker Jr, J. R. (2005) Tumor angiogenic vasculature targeting with PAMAM dendrimer-RGD conjugates. Chem.Commun.(Camb). **(46)**, 5739-5741

(6) Hill, E., Shukla, R., Park, S. S. and Baker, J. R.,Jr. (2007) Synthetic PAMAM-RGD conjugates target and bind to odontoblast-like MDPC 23 cells and the predentin in tooth organ cultures. Bioconjug.Chem. **18**, 1756-1762

(7) Binder, W. H. and Kluger, C. (2006) Azide/alkyne-"click" reactions: Applications in material science and organic synthesis. Current Organic Chemistry. **10**, 1791

(8) Lee, J. W., Kim, J. H., Kim, H. J., Han, S. C., Kim, J. H., Shin, W. S. and Jin, S. H. (2007) Synthesis of symmetrical and unsymmetrical PAMAM dendrimers by fusion between azide- and alkyne-functionalized PAMAM dendrons. Bioconjug.Chem. **18**, 579-584

(9) Lee, J. W., Kim, J. H. and Kim, B. K. (2006) Synthesis of azide-functionalized PAMAM dendrons at the focal point and their application for synthesis of PAMAM-like dendrimers. Tetrahedron Letters. **47**, 2683-2686

(10) Brooks, P. C., Clark, R. A. and Cheresh, D. A. (1994) Requirement of vascular integrin alpha v beta 3 for angiogenesis. Science. **264**, 569-571

(11) Cleaver, O. and Melton, D. A. (2003) Endothelial signaling during development. Nat.Med. **9**, 661-668

(12) Baillie, C. T., Winslet, M. C. and Bradley, N. J. (1995) Tumour vasculature--a potential therapeutic target. Br.J.Cancer. **72**, 257-267

(13) Ruoslahti, E. (2002) Specialization of tumour vasculature. Nat.Rev.Cancer. **2**, 83-90

(14) Arap, W., Pasqualini, R. and Ruoslahti, E. (1998) Cancer treatment by targeted drug delivery to tumor vasculature in a mouse model. Science. **279**, 377-380

(15) Los, M. and Voest, E. E. (2001) The potential role of antivascular therapy in the adjuvant and neoadjuvant treatment of cancer. Semin.Oncol. **28**, 93-105

(16) Lee, J. W., Kim, B., Kim, H. J., Han, S. C., Shin, W. S. and Jin, S. (2006) Convergent synthesis of symmetrical and unsymmetrical PAMAM dendrimers. Macromolecules. **39**, 2418-2422

(17) Ornelas, C., Broichhagen, J. and Weck, M. (2010) Strain-promoted alkyne azide cycloaddition for the functionalization of poly(amide)-based dendrons and dendrimers. J.Am.Chem.Soc. **132**, 3923-3931

# Chapter 3:
# Efficient synthesis of compartmental platforms through thiol-based click chemistry coupling of dendrons

## Background

The work detailed in Chapter 2 demonstrates that biologically active material can be synthesized on a dendron platform utilizing the orthogonal focal point as a reactive site to create a molecule with a specific ratio of functional modules. However, there were issues related to use of the copper catalyst, which did not provide quantitative coupling in our polyamine system and was retained in the core of the dendrimer making the use of this material difficult in some biomedical applications due to metal toxicity. To address these problems we explored thiol-based click reactions (1-4), employing the thiol-ene and thiol-yne chemistry, as an alternative orthogonal reaction to functionalize dendron platforms. Thiol-based click chemistry follows a radical mechanism, where a radical initiator (photo or thermal) is introduced to a system with a thiol and either an alkene (thiol-ene) or alkyne (thiol-yne) (Figure 3.1).

Thiol-based click reactions have recently been shown to be useful for dendrimer synthesis (5), which traditionally involves the tedious purification of the newly formed dendrimer away from large excesses of monomer units. Thiol-ene reactions have been employed by the Hawker group to synthesize polyester dendrimers in near quantitative yield with minimal requirement for clean-up, while the Lowe group has used thiol-ene

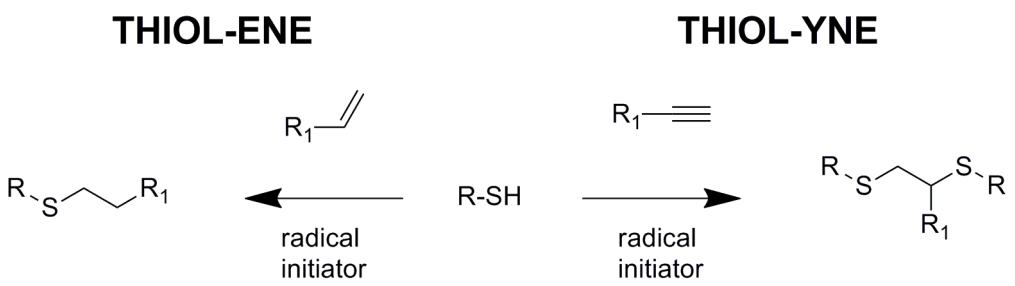


**Figure 3.1.** Thiol-click reaction. Thiol functional molecules follow a radical mechanism with the addition of a thermal or photoinitiator to react with available alkene (thiol-ene, left) or alkyne (thiol-yne, right) molecules.

and thiol-yne reactions in sequential growth steps of dendritic thioethers (6). To our knowledge, however no research has been performed on convergent coupling using thischemistry via the dendron's orthogonal focal point.

By adapting the strategy of click chemistry to the dendritic structure most commonly used in drug delivery research, we move closer to the goal of well-defined and reproducible platforms that can be easily tailored for specific biomedical applications. In addition, achieving high yield synthesis in the absence of a metal catalyst provides a more biocompatible route to synthesize modular dendrimers and dendrons for *in vivo* therapeutics. In this study, we first detail the functionalization of the orthogonal focal point of a polyester dendron via a thiol-yne reaction. The polyester backbone is an attractive model because it is readily available at high purity through commercial sources and it provides sharp, resolvable NMR spectra to monitor the reaction progress for reaction optimization. In addition, the polyester is non-toxic (7, 8) D) and its synthesis from cores containing orthogonal reactive sites is easily achieved.

In our thiol-yne systems, thiol functionalized molecules were reacted with the alkyne focal point of a generation 3 polyester dendron. A 1-dodecanethiol, a

hydrophobic molecule commonly used for self-assembly applications, was used as the model ligand.

After optimizing the reaction conditions with polyester dendrons, thiol-based click chemistry was then applied to PAMAM dendrons. We describe an efficient means of functionalizing an orthogonally reactive, commercially available PAMAM dendron. In the model system, an alkene or alkyne group is introduced at the focal point. These dendrons are then reacted with a thiol-functionalized ligand, 1-dodecanethiol or 2-phenylethanethiol. To show the applicability towards specific targeting, biotin was conjugated to the focal point of a dendron-RGD platform.

**Experimental procedures**

**General**: Polyester dendrons were purchased from the Polymer Factory (Sweden) and used without additional purification. PAMAM dendrons with hydroxyl focal points were purchased from Dendritech (Midland, MI). PAMAM dendrons with alkyne focal points were prepared as described in Chapter 2.

**Synthesis of (dodecane)$_2$-PE.G3-OH$_8$ (11).** Alkyne-PE.G3-OH$_8$ (0.0930 g, 0.103 mmol), 1-dodecanethiol (0.0941 g, 0.465 mmol), and 2,2-dimethoxy-2-phenyl acetophenone (0.0026 g, 0.47 mmol) were dissolved in anhydrous MeOH (1 mL) and purged with $N_2$ while stirring for 15 minutes. The reaction mixture was then exposed to UV-light from a sun lamp emitting 365 nm wavelength for 2 hours. All solvent was removed *in vacuo*, and the reaction material was dissolved in MeOH and purified on a

LH-20 Sephadex column. MS (MALDI): 1272.9 Da; calculated for $C_{62}H_{112}O_{22}S_2$: 1272.71 Da.

**Synthesis of (phenyl)$_2$-G3(NH$_2$)$_{16}$ (12).** Phenylethanethiol (0.0023 g, 0.016 mmol), alkyne-G3(NH$_2$)$_{16}$ **(1)** (0.0095 g, 0.0027 mmol), and 2,2-dimethoxy-2-phenyl acetophenone (0.0007 g, 0.003 mmol) were dissolved in anhydrous MeOH (2 mL) and purged with $N_2$ while stirring for 15 minutes. The reaction mixture was then exposed to UV-light from a sun lamp emitting 365 nm wavelength for 2 hours. All solvent was removed *in vacuo*, and the reaction material was dissolved in MeOH and purified on a LH-20 Sephadex column. MS (MALDI): 2500-4500 Da; calculated for $C_{169}H_{325}N_{61}O_{30}S_2$: 3753.5 Da.

**Synthesis of OH-G2(Boc)$_8$ (13).** Di-tert-butyl anhydride was added to a solution of OH-G2(NH$_2$)$_8$, in anhydrous chloroform while stirring. The reaction mixture was allowed to stir for 24 hours at room temperature. All solvent was removed *in vacuo*, and the reaction material was dissolved in MeOH and purified on a LH-20 Sephadex column. MS (MALDI): 2483.9 Da; calculated for $C_{114}H_{215}N_{29}O_{31}$: 2500.6 Da.

**Synthesis of alkene-G2(Boc)$_8$ (14).** 4-pentenoic anhydride (0.9970 g, 0.1944 mmol) was added to a solution of **13** (0.0486 g, 0.0194 mmol), pyridine (0.0154 g, 0.194 mmol) and DMAP (0.0024 g, 0.019 mmol) in anhydrous dichloromethane (4 mL) while stirring. The reaction mixture was allowed to stir for 24 hours at room temperature. All solvent was removed *in vacuo*, and the reaction material was dissolved in MeOH and

purified on a LH-20 Sephadex column. MS (MALDI): 2562.1 Da; calculated for $C_{120}H_{223}N_{29}O_{32}$: 2582.7 Da.

**Synthesis of (dodecane)-G2-(Boc)$_8$ (15).** **14** (0.0170 g, 0.00654 mmol), 1-dodecanethiol (0.0040 g, 0.0065 mmol), and 2,2-dimethoxy-2-phenyl acetophenone (0.0002 g, 0.0007 mmol) were dissolved in anhydrous MeOH (1 mL) and purged with $N_2$ while stirring for 15 minutes. The reaction mixture was then exposed to UV-light from a sun lamp emitting 365 nm wavelength for 2 hours. All solvent was removed *in vacuo*, and the reaction material was dissolved in MeOH and purified using a LH-20 Sephadex column. MS (MALDI): 2738.7 Da; calculated for $C_{130}H_{245}N_{29}O_{32}S$: 2756.8 Da.

**Synthesis of 2,2,5-trimethyl-1,3-dioxane-5-carboxylic anhydride (16).** N-(3-Dimethylaminopropyl)-N′-ethylcarbodiimide hydrochloride (0.6052 g, 3.157 mmol) in 2 mL anhydrous dichloromethane was added dropwise to a solution of 2,2,5-Trimethyl-1,3-dioxane-5-carboxylic acid (1.0 g, 5.7 mmol) in 4 mL anhydrous dichloromethane in an ice bath. The reaction mixture was allowed to stir for 24 hours. The solvent was removed *in vacuo*, the reaction material was redissolved in 2 mL dichloromethane, and precipitated in 250 mL ice-cold hexanes. The solution was filtered and the solvent evaporated to give a clear oil. The product was used without further purification (85% anhydride material by NMR).

**Synthesis of OH-G3(An)$_{16}$ (17).** **16** (0.2246 g, 0. mmol) dissolved in anhydrous MeOH (2 mL) was added to a solution of OH-G3($NH_2$)$_{16}$ (0.0750 g, 0.0213 mmol) and

triethylamine (0.0516 g, 0.510 mmol) in anhydrous MeOH (3 mL) while stirring. The reaction mixture was allowed to stir for 24 hours at room temperature. All solvent was removed *in vacuo*, and the reaction material was dissolved in MeOH and purified on a LH-20 Sephadex column. MS (MALDI): 5500-6500 Da, maximum at 5878.1 Da; calculated for $C_{283}H_{505}N_{61}O_{79}$: 6022.8 Da.

**Synthesis of alkene-G3(An)$_{16}$ (18).** 4-pentenoic anhydride (0.0228 g, 0.125 mmol) was added to a solution of **17** (0.0556 g, 0.0125 mmol), pyridine (0.0099 g, 0.13 mmol) and DMAP (0.0015 g, 0.013 mmol) in anhydrous DMSO (1 mL) while stirring. The reaction mixture was allowed to stir for 24 hours at room temperature. All solvent was removed *in vacuo*, and the reaction material was dissolved in MeOH and purified on a LH-20 Sephadex column. MS (MALDI): 5500-6500 Da, maximum at 5947.1 Da; calculated for $C_{288}H_{511}N_{61}O_{80}$: 6104.8 Da.

**Synthesis of phenyl-G3(An)$_{16}$ (19).** Phenylethanethiol (0.0005 g, 0.003 mmol), **18** (0.0056 g, 0.0011 mmol), and 2,2-dimethoxy-2-phenyl acetophenone (0.0003 g, 0.001 mmol) were dissolved in anhydrous MeOH (1 mL) and purged with $N_2$ while stirring for 15 minutes. The reaction mixture was then exposed to UV-light from a sun lamp emitting 365 nm wavelength for 2 hours. All solvent was removed *in vacuo*, and the reaction material was dissolved in MeOH and purified on a LH-20 Sephadex column. MS (MALDI): 5000-7000 Da; calculated for $C_{296}H_{521}N_{61}O_{80}S$: 6242.85 Da.

**Synthesis of biotin$_2$-G3(COOH)$_{11.9}$(RGD)$_{4.1}$ (20).** Biotinylated tri(ethylene glycol) undecane thiol (Nanoscience Instruments) (0.0015 g, 2.4 μmol), alkyne-G3(COOH)$_{11.9}$(RGD)$_{4.1}$ **(3)** (0.0007 g, 0.1 μmol), and 2,2-dimethoxy-2-phenyl acetophenone (0.0003 g, 1 μmol) were dissolved in anhydrous MeOH (1 mL) and purged with $N_2$ while stirring for 15 minutes. The reaction mixture was then exposed to UV-light from a sun lamp emitting 365 nm wavelength for 2 hours. All solvent was removed *in vacuo*, and the reaction material was dissolved in MeOH and purified on a LH-20 Sephadex column. MS (MALDI): 5000-12000 Da.

**Flow Cytometry.** Cells were incubated with **20** at 0°C for 1 hours followed by exposure to 2000 nM of NeutrAvidin-Dylight 488 for 15 minutes. Cells were washed with 5mL of PBS, spun at 150 G for 7 minutes, and re-suspended in 2 mL of PBS with BSA prior to being examined. Cells were examined quantitatively for dendron uptake via a flow cytometer (Beckman Coulter Epics XL-MCL). The FL1 fluorescence of 10000 cells was measured and the mean fluorescence of cells was quantified.

**Results and Discussion**

Thiol click chemistry reaction conditions were evaluated using polyester dendrons with an alkyne focal point. In general, the thiol click reactions were performed using a photoinitiator and applying UV light for 2 hours. Initial attempts made without inert gas purging provided less than quantitative conversions. High conversions were achieved only after bubbling $N_2$ through the reaction vessel for 15 minutes. Model thiol-yne reactions were performed on polyester or PAMAM dendrons with alkyne focal points.

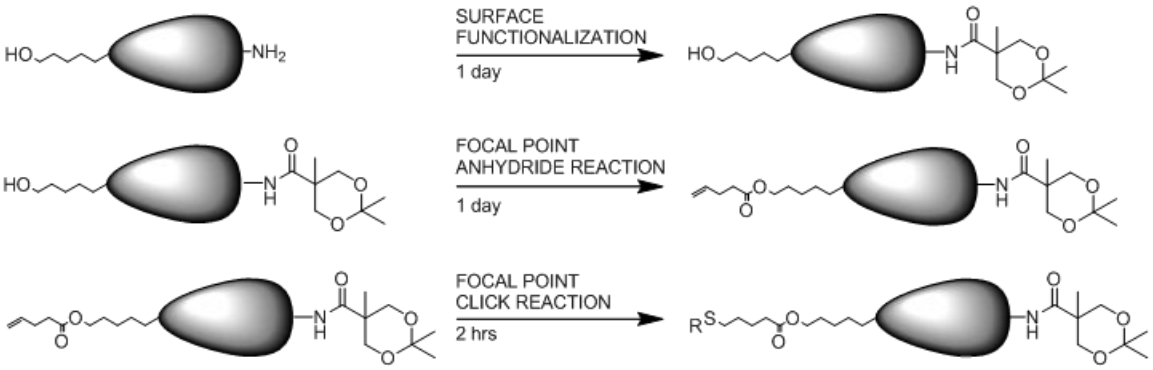


**Figure 3.2.** General reaction scheme for thiol-ene reaction of commercial PAMAM dendrons. The surface amines are modified to allow for the conversion of the hydroxyl focal point to an alkene group via an anhydride reaction. The thiol-ene reaction is performed by introducing a thiol-functional molecules and a photoinitiator and exposing the stirred mixture to UV light.

The thiol-ene reactions were evaluated using commercially available PAMAM dendrons (Figure 3.2). The orthogonality of the dendron platform allows for the surface amines to be modified allowing for the eventual esterification of the less reactive hydroxyl focal point to yield an alkene terminal group. We initially used Boc protecting groups to easily react the surface amines, however we previously found that the deprotection conditions hydrolyzed the focal point. As an alternative, an acetonide-protecting group was chosen because it can be easily removed by an ion exchange chromatography, leaving the focal point ester intact.

The esterification of the focal point was performed by reacting 4-pentenoic anhydride with the dendron. This reaction provides several useful NMR signals allowing for easy monitoring of the thiol-ene reaction (Figure 3.3). The esterification of the focal point causes the triplet associated with the methylene protons nearest the hydroxyl focal point to shift from 3.55 ppm to 4.13 ppm. Additionally, the alkene will have peaks at 5.08 ppm and 5.89 ppm. A successful thiol-ene click reaction can be monitored by the

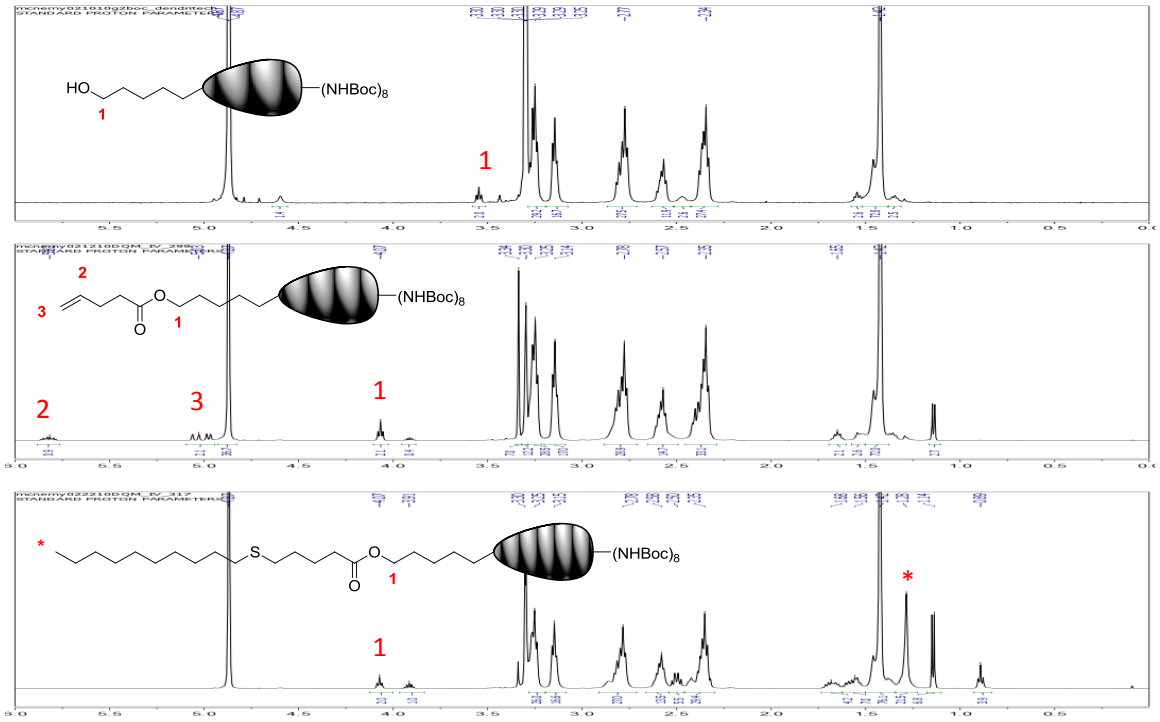


**Figure 3.3.** NMR spectra of dendron products with distinguishable handles to trace reaction progress. Top) Commercially available PAMAM dendron, with methylene protons (1) adjacent to the focal point at 3.53 ppm. Middle) Alkene-functionalized PAMAM dendron, with alkene protons at 5.03 ppm (2) and 5.81 ppm (3) and the methylene protons (1) shifting to 4.07 ppm. Bottom) PAMAM dendron after a successful thiol-ene reaction. Alkene protons have disappeared after reaction with the thiol-functional molecule.

disappearance of the alkene peaks while the methylene nearest the hydroxyl remains unchanged.

In contrast, thiol-yne click reactions lack easily distinguishable NMR signals to monitor reaction progress. The disappearance of the alkyne proton and subsequent appearance of new methylene and single proton peaks can be observed between 2.5 and 3.5 ppm with the polyester dendrons; however overlapping signals in this region with PAMAM dendrons makes reaction progress harder to follow.

In general, dendrons were mixed with an excess of thiol in the presence of a UV-initiator, 2,2-dimethoxy-2-phenyl acetophenone (DMPA), and reacted by exposure to UV

light for 2 hours. The purified products were characterized by NMR and showed near quantitative conversion of the dendron focal point by the thiol-ene reaction. Repeated attempts to remove free thiol by column purification were inconsistently effective, sometimes leaving a small percentage of this impurity.

To demonstrate the use of thiol click chemistry for applications such as specific targeting, thiol-functionalized biotin was conjugated to the alkyne focal point of a dendron-RGD platform (described in detail in Chapter 2). U87MG cells were treated with **20** followed by the addition of a secondary detection agent, NeutrAvidin-DyLight 488. Cells treated with the bifunctional dendron platform showed increased uptake compared to non-targeted biotin (Figure 3.4).

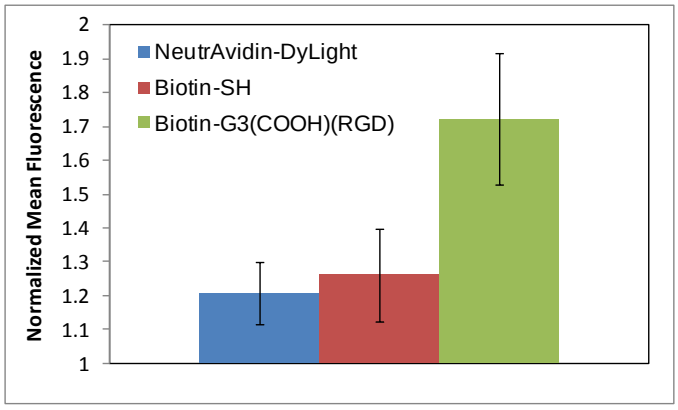


**Figure 3.4. U**ptake and targeting of 1 µM binary dendrons to U87MG cells after the thiol-ene reaction determined via flow cytometry. Mean fluorescence values are normalized against mean fluorescence of untreated cells.

The thiol-ene and thiol-yne click reactions provided significantly improved yields compared to the CuAAC without the need to remove a toxic metal catalyst. Despite these successes, thiol click chemistry has drawbacks when applied to PAMAM delivery platforms. First, the degree of orthogonality of the thiol-ene reaction is not as high as in alkyne-azide reactions: this is because alkenes may react with available amines in the

reaction mixture (undergoing the same Michael addition that proceeds during the traditional PAMAM growth step), and thiol bridging may occur. These incompatibilities hinder the ability to grow dendrons from thiol or alkene-containing focal points. Instead, the orthogonal site must be introduced to the focal point after dendron synthesis has been accomplished as seen in this model study. This limits the potential surface groups that are incompatible with the thiol click reactions. Additionally, the UV light needed for photoinitiated reactions prevents the successful conjugation of some functional groups, such as dyes due to photobleaching. Thermo-initiators may provide a suitable alternative approach, providing that reaction temperatures are not high enough to degrade the dendron backbone. However, thiol click chemistry remains a useful tool and could be adapted for applications such as the functionalization of surfaces with dendrons.

**Acknowledgments:** Jolanta F. Kukowska-Latallo, Ankur M. Desai, Baohua Huang, and James R. Baker Jr. made essential contributions to the work in this chapter.

## Chapter 3 Appendix

**Figure S3.1: $^{1}$H NMR spectrum of alkyne-PE.G3-OH**

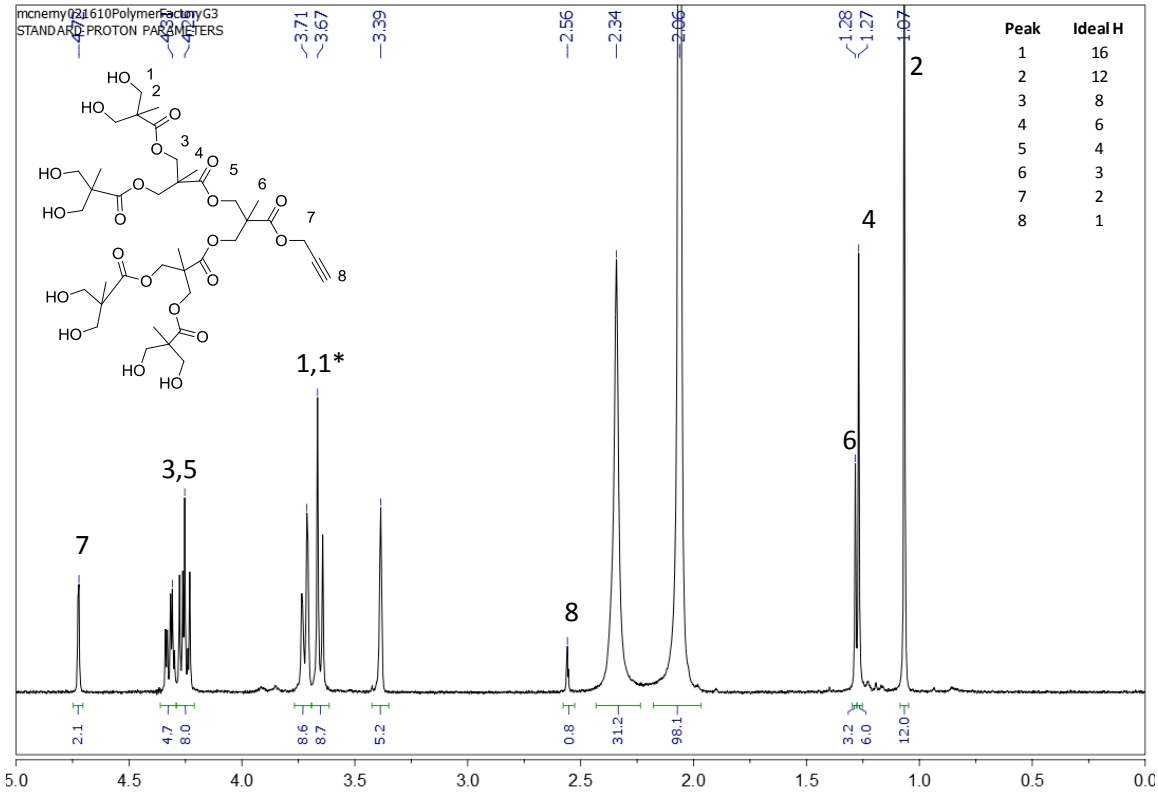


$^{1}$H NMR (500 MHz, $CDCl_3$): δ = 4.72 (s, 2H, O-C*H*$_2$-C-CH), 4.38-4.20 (m, 12H, O-C*H*$_2$-C), 3.75-3.70 (d, 8H, OH-C*H*$_2$-C), 3.70-3.60 (d, 8H, OH-C*H*$_2$-C), 2.56 (s, 1H, $CH_2$-C-C*H*), 1.28 (s, 3H, C*H*$_3$-C), 1.27 (s, 6H, C*H*$_3$-C), 1.07 (s, 12H, C*H*$_3$-C).

**Figure S3.2: $^{1}$H NMR spectrum of (Dodecane)$_2$-PE.G3-OH$_8$.**

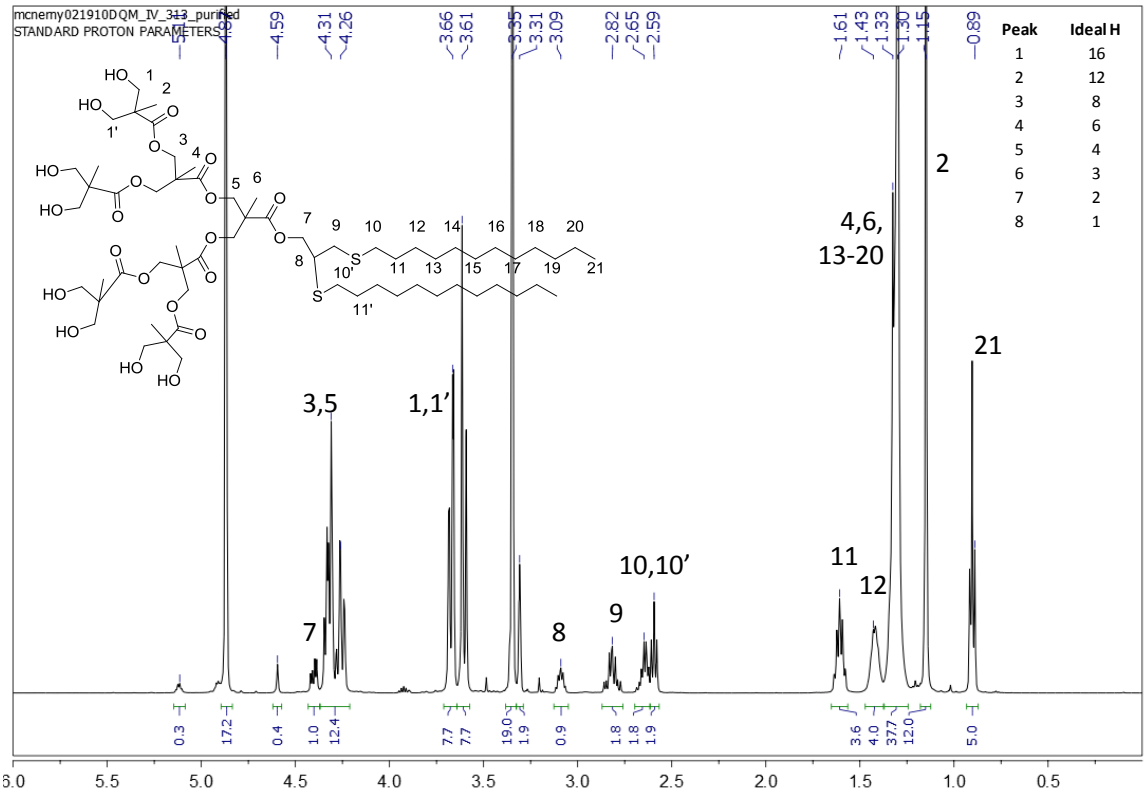


$^{1}$H NMR (500 MHz, MeOH-d): δ = 4.40 (m, 2H, O-C*H*$_2$-CH), 4.38-4.20 (m, 12H, O-C*H*$_2$-C), 3.75-3.65 (d, 8H, OH-C*H*$_2$-C), 3.65-3.55 (d, 8H, OH-C*H*$_2$-C), 3.08 (qt, 1H, CH$_2$-C*H*-CH$_2$), 2.82 (m, 2H, CH$_2$-CH-C*H*$_2$-S), 2.65-2.55 (m, 1H, S-C*H*$_2$-CH$_2$), 1.61 (qt, 4H, S-CH$_2$-C*H*$_2$), 1.43 (qt, 4H, S-CH$_2$-CH$_2$-C*H*$_2$), 1.35-1.25 (m, 41H), 1.15 (t, 12H, C*H*$_3$-C), 0.89 (t, 6H, C*H*$_3$-CH$_2$).

**Figure S3.3: $^{1}$H NMR spectrum of OH-G3$(NH_2)_{16}$**

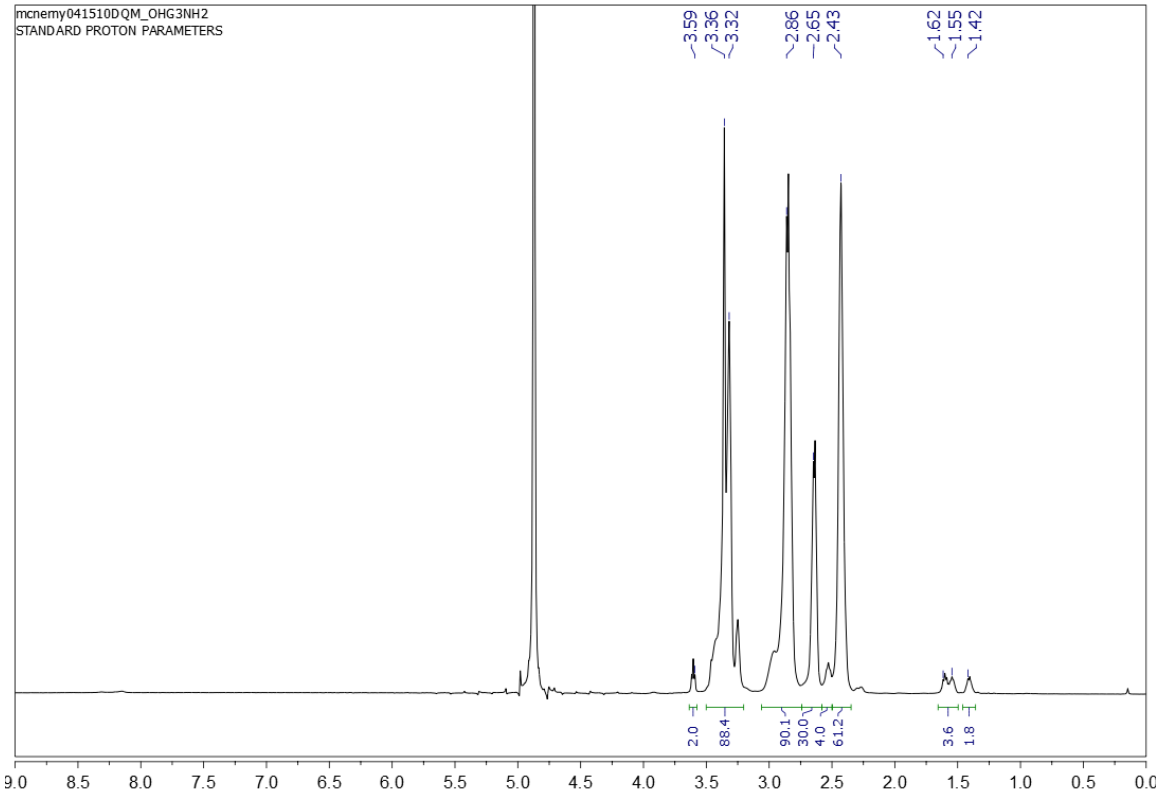


$^{1}$H NMR (500 MHz, MeOH-d): δ = 3.59 (t, 2H, OH-C*H*$_2$-CH$_2$), 3.43-3.20 (m, 64H, NH-C*H*$_2$-CH$_2$-NH$_2$, NH-C*H*$_2$-CH$_2$-N), 2.86 (m, 60H, N-C*H*$_2$-CH$_2$-CO, 28H, NH-CH$_2$-C*H*$_2$-NH$_2$), 2.65 (t, 28H, NH-CH$_2$-C*H*$_2$-N), 2.43 (m, 60H, N-CH$_2$-C*H*$_2$-CO), 1.65-1.42 (m, 6H, pentanol focal point).

**Figure S3.4: $^{1}$H NMR spectrum of (Phenyl)$_2$-G3(NH$_2$)$_{16}$.**

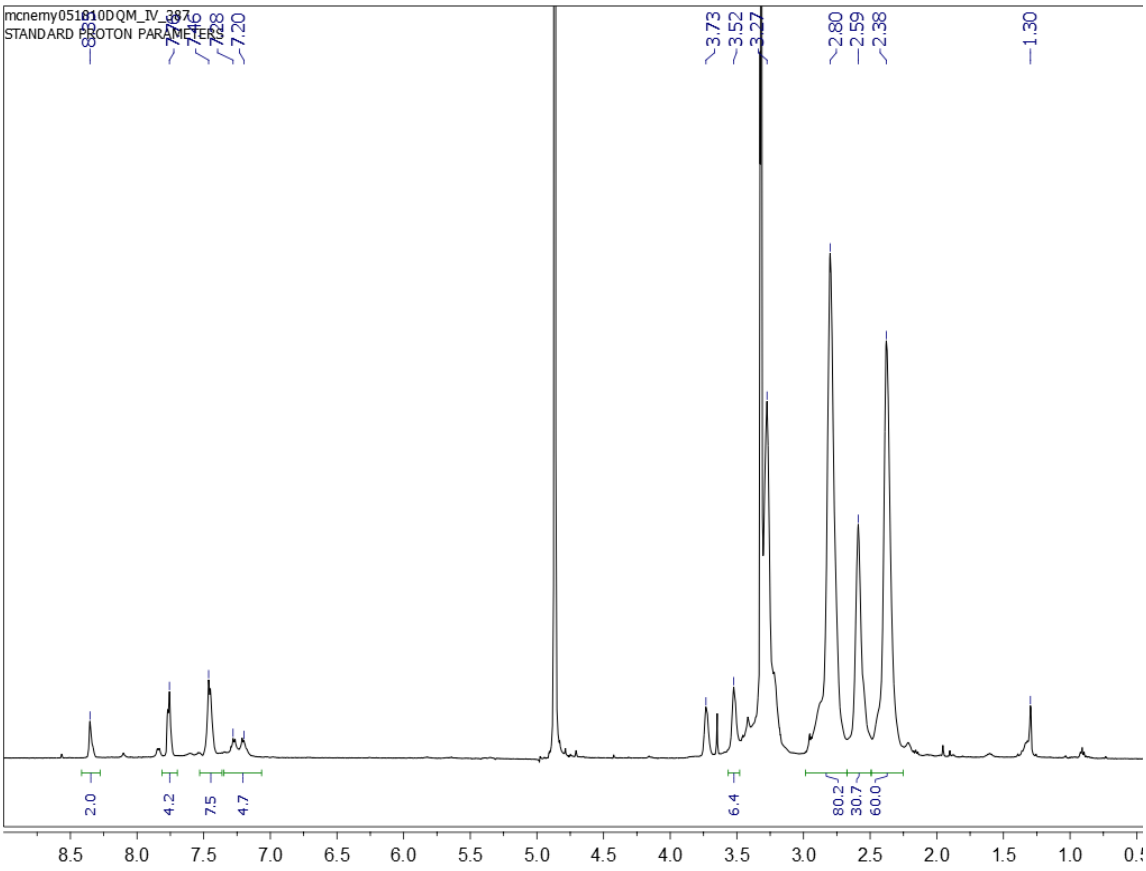


$^{1}$H NMR (500 MHz, MeOH): δ = 8.30 (b, 2H, CH aromatic), 7.75 (b, 2H, CH aromatic), 7.30-7.20 (b, 4H, CH aromatic), 3.52 (s, 2H, N-C*H*$_2$-CH), 3.43-3.20 (m, 64H, NH-C*H*$_2$-CH$_2$-NH$_2$, NH-C*H*$_2$-CH$_2$-N), 2.80 (m, 60H, N-C*H*$_2$-CH$_2$-CO, 28H, NH-CH$_2$-C*H*$_2$-NH$_2$), 2.59 (t, 28H, NH-CH$_2$-C*H*$_2$-N), 2.38 (m, 60H, N-CH$_2$-C*H*$_2$-CO, “d”).

* Thiol proton from free 2-phenylethanethiol impurity present at 1.30.

**Figure S3.5: $^{1}$H NMR spectrum of OH-G2(Boc)$_8$.**

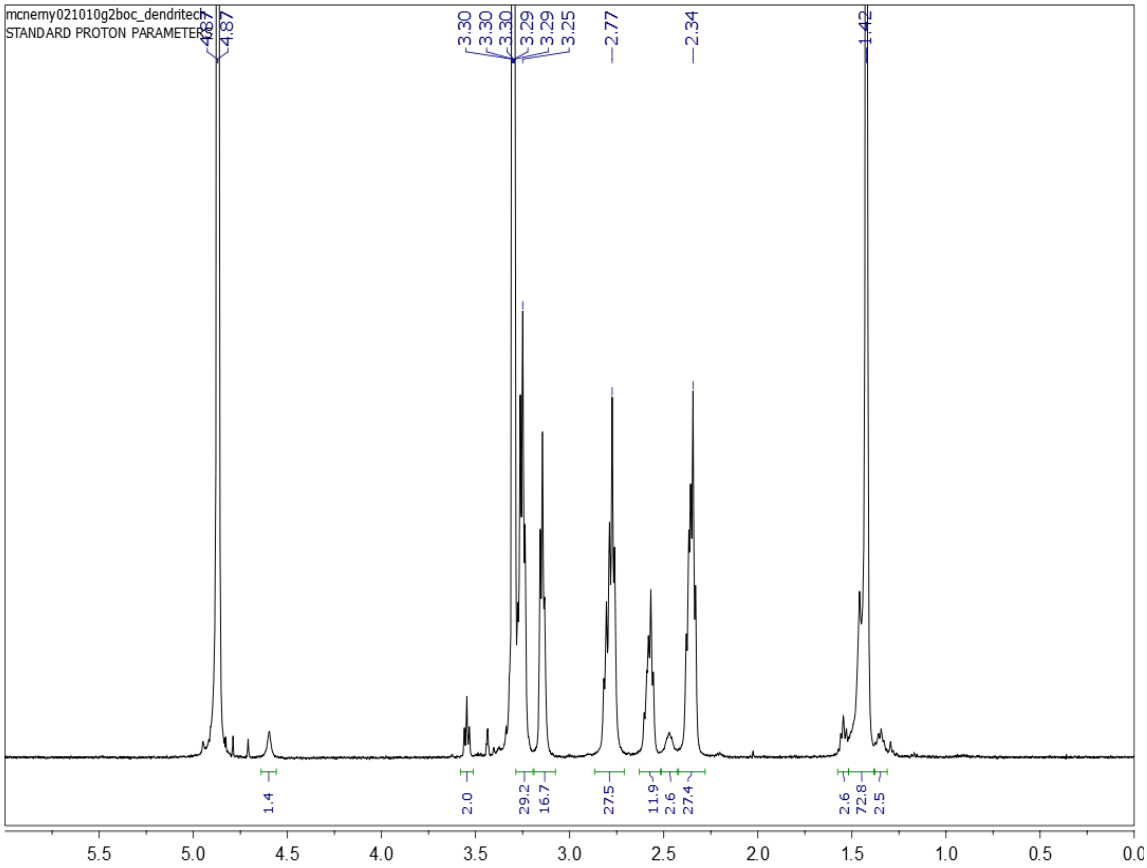


$^{1}$H NMR (500 MHz, MeOH-d): δ = 3.53 (t, 2H, OH-C*H*$_2$-CH$_2$), 3.43-3.20 (m, 32H, NH-C*H*$_2$-CH$_2$-NH$_2$, NH-C*H*$_2$-CH$_2$-N), 2.77 (m, 28H, N-C*H*$_2$-CH$_2$-CO, 28H, NH-CH$_2$-C*H*$_2$-NH$_2$), 2.60 (t, 12H, NH-CH$_2$-C*H*$_2$-N), 2.50 (qt, 2H, pentanol focal point), 2.34 (m, 28H, N-CH$_2$-C*H*$_2$-CO), 1.65-1.42 (m, 6H, pentanol focal point), 1.42 (s, 72H, C*H*$_3$-C).

**Figure S3.6: $^{1}$H NMR spectrum of Alkene-G2(Boc)$_8$.**

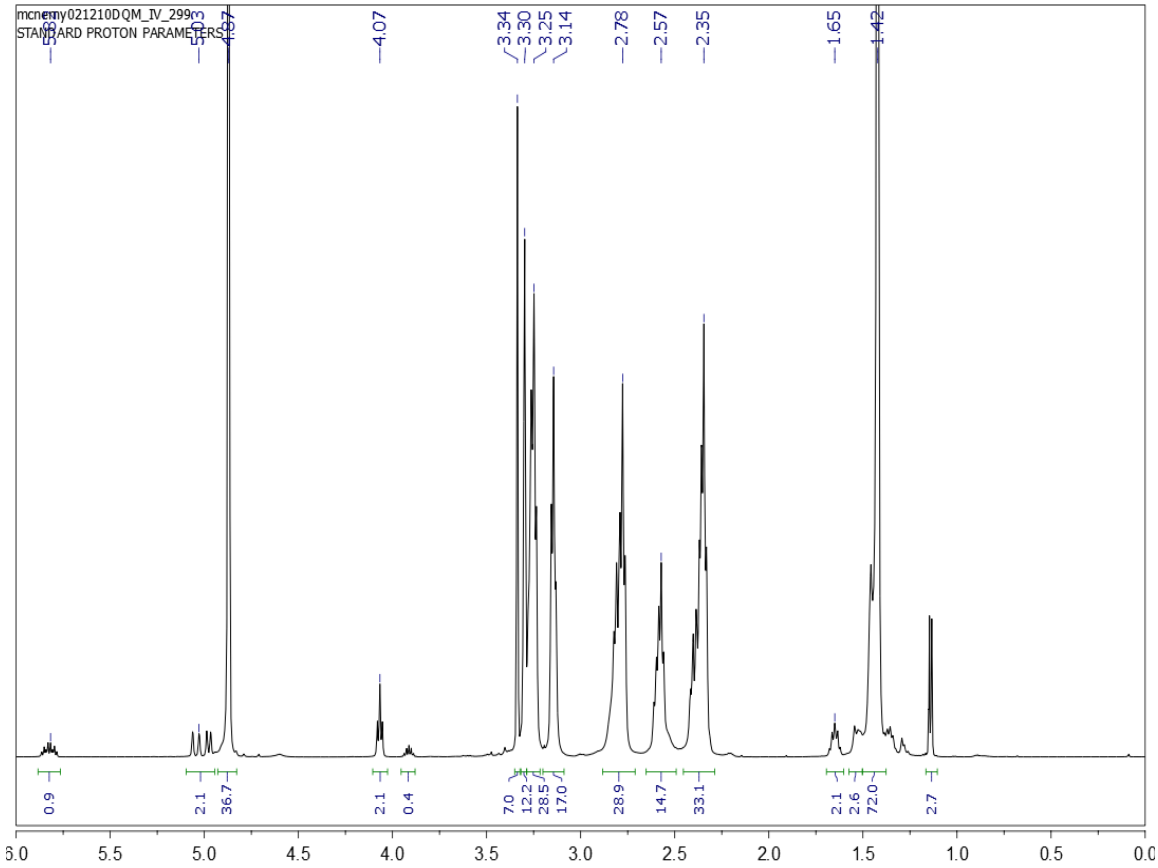


$^{1}$H NMR (500 MHz, MeOH-d): δ = 5.82 (m, 1H, $CH_2$-C*H*-$CH_2$), 5.03 (m, 2H, C*H*$_2$-CH-$CH_2$), 4.07 (t, 2H, CO-O-C*H*$_2$-$CH_2$), 3.43-3.20 (m, 32H, NH-C*H*$_2$-$CH_2$-$NH_2$, NH-C*H*$_2$-$CH_2$-N), 2.77 (m, 28H, N-C*H*$_2$-$CH_2$-CO, 28H, NH-$CH_2$-C*H*$_2$-$NH_2$), 2.60 (t, 12H, NH-$CH_2$-C*H*$_2$-N), 2.50 (qt, 2H, pentanol focal point), 2.34 (m, 28H, N-$CH_2$-C*H*$_2$-CO), 1.65-1.42 (m, 6H, pentanol focal point), 1.42 (s, 72H, C*H*$_3$-C).

**Figure S3.7: $^{1}$H NMR spectrum of (Dodecane)-G2-(Boc)$_8$.**

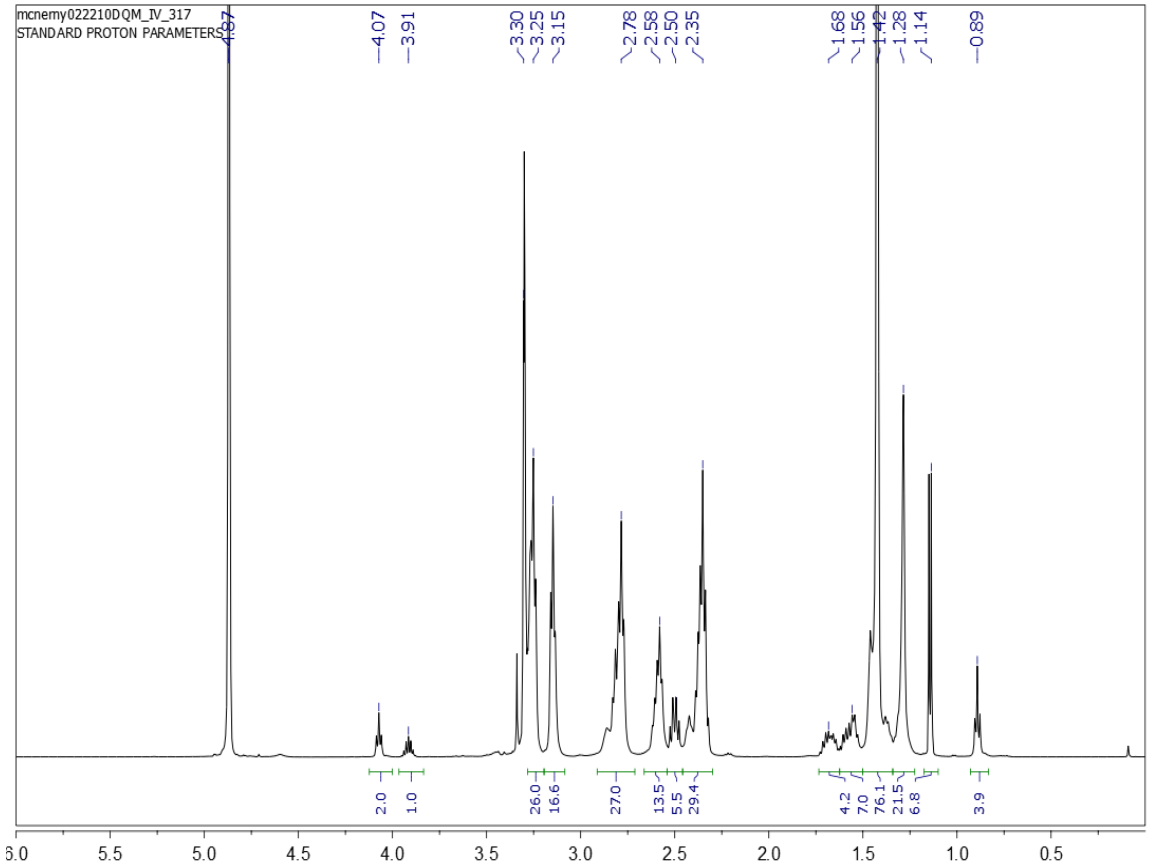


$^{1}$H NMR (500 MHz, MeOH-d): δ = 4.07 (t, 2H, CO-O-C*H*$_2$-CH$_2$), 3.43-3.20 (m, 32H, NH-C*H*$_2$-CH$_2$-NH$_2$, NH-C*H*$_2$-CH$_2$-N), 2.77 (m, 28H, N-C*H*$_2$-CH$_2$-CO, 28H, NH-CH$_2$-C*H*$_2$-NH$_2$), 2.60 (t, 12H, NH-CH$_2$-C*H*$_2$-N), 2.50 (qt, 2H, pentanol focal point), 2.34 (m, 28H, N-CH$_2$-C*H*$_2$-CO), 1.65-1.42 (m, 6H, pentanol focal point), 1.42 (s, 72H, C*H*$_3$-C), ), 1.68 (qt, 2H, S-CH$_2$-C*H*$_2$), 1.56 (qt, 2H, S-CH$_2$-CH$_2$-C*H*$_2$), 1.35-1.25 (m, 16H), 1.14 (s, 3H, C*H*$_3$-C), 0.89 (t, 6H, C*H*$_3$-CH$_2$).

* NMR integration suggests 1 EQ of free dodecanethiol.

**Figure S3.8: $^{1}$H NMR spectrum of 2,2,5-trimethyl-1,3-dioxane-5-carboxylic anhydride**

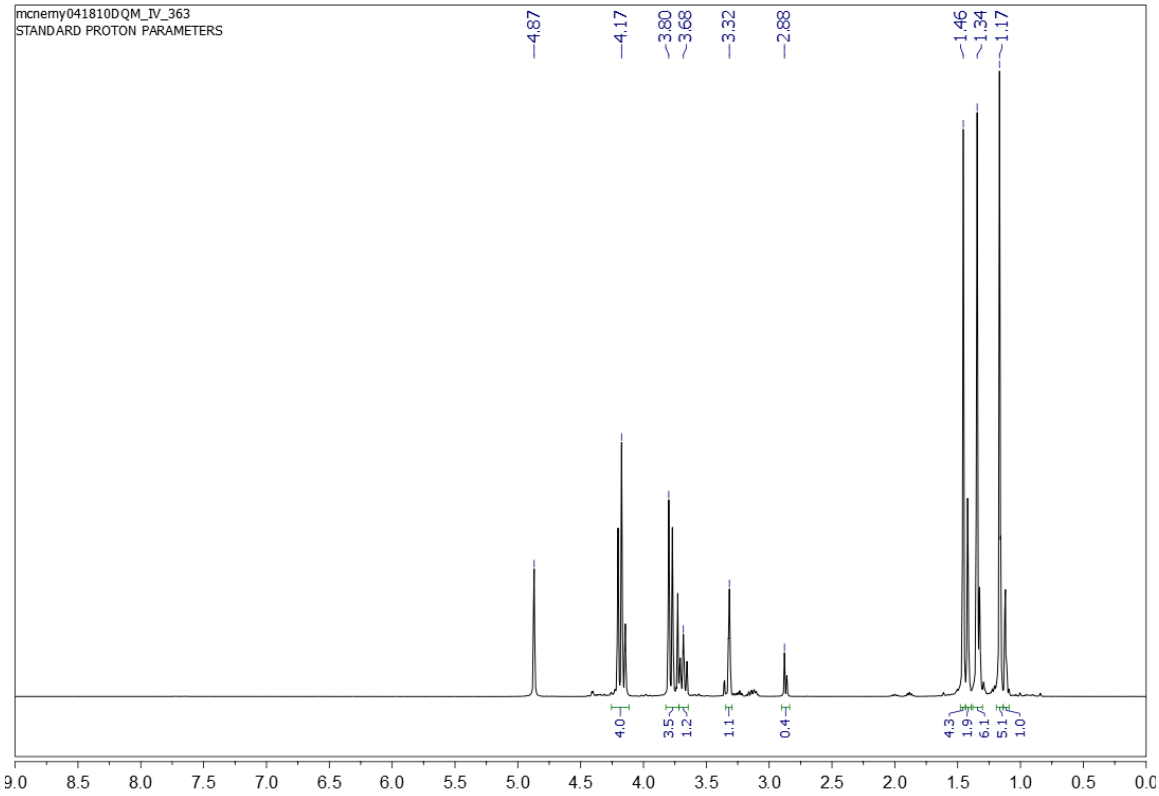


$^{1}$H NMR (500 MHz, MeOH-d): δ = 4.17 (m, 4H, O-CH*H*-C), 3.80 (m, 4H, O-C*H*H-C), 1.46 (s, 6H, C$H_3$-C-$(O)_2$), 1.34 (s, 6H, C$H_3$-C-$(O)_2$), 1.17 (s, 6H, C$H_3$-C-$C_3$).

**Figure S3.8: $^{1}$H NMR spectrum of OH-G3(An)$_{16}$**

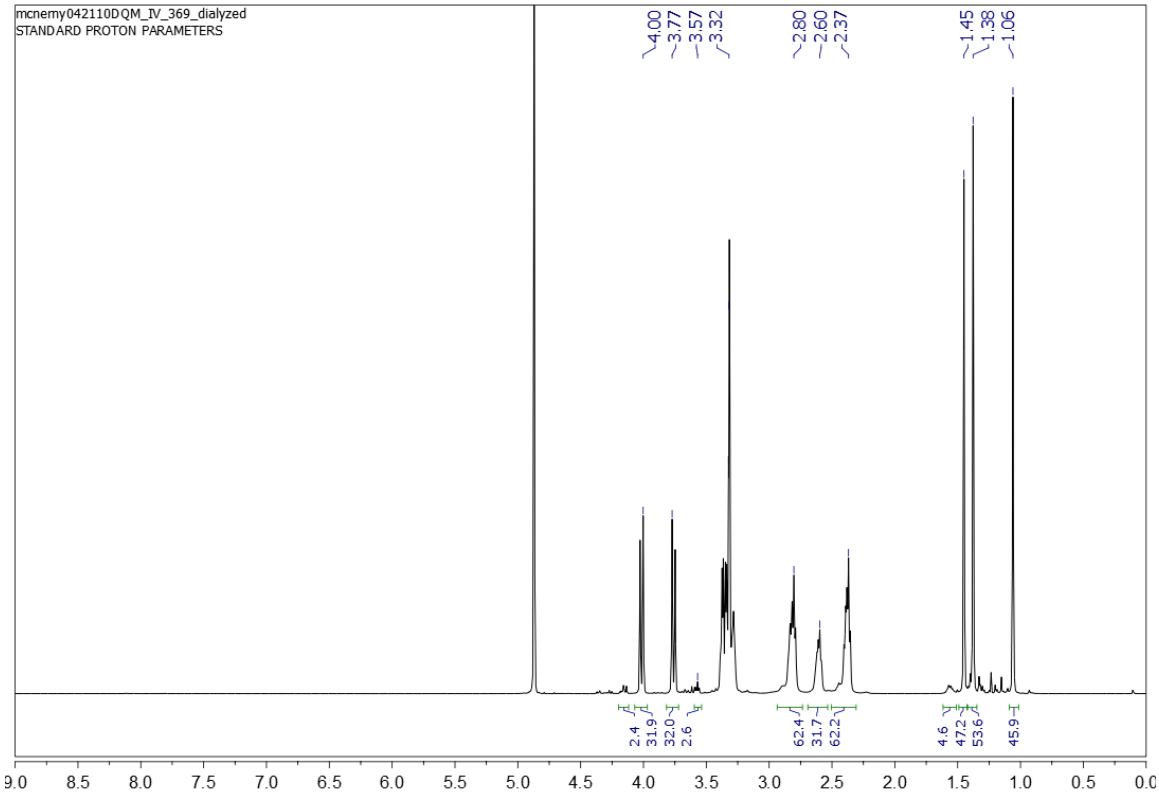


$^{1}$H NMR (500 MHz, MeOH-d): δ = 4.00 (m, 32H, O-CH*H*-C), 3.77 (m, 32H, O-C*H*H-C), 3.59 (t, 2H, OH-C*H*$_2$-CH$_2$), 3.43-3.20 (m, 64H, NH-C*H*$_2$-CH$_2$-NH$_2$, NH-C*H*$_2$-CH$_2$-N), 2.86 (m, 60H, N-C*H*$_2$-CH$_2$-CO, 28H, NH-CH$_2$-C*H*$_2$-NH$_2$), 2.65 (t, 28H, NH-CH$_2$-C*H*$_2$-N), 2.43 (m, 60H, N-CH$_2$-C*H*$_2$-CO), 1.65-1.42 (m, 6H, pentanol focal point), 1.46 (s, 48H, C*H*$_3$-C-(O)$_2$), 1.38 (s, 48H, C*H*$_3$-C-(O)$_2$), 1.06 (s, 48H, C*H*$_3$-C-C$_3$).

**Figure S3.9: $^{1}$H NMR spectrum of alkene-G3(An)$_{16}$**

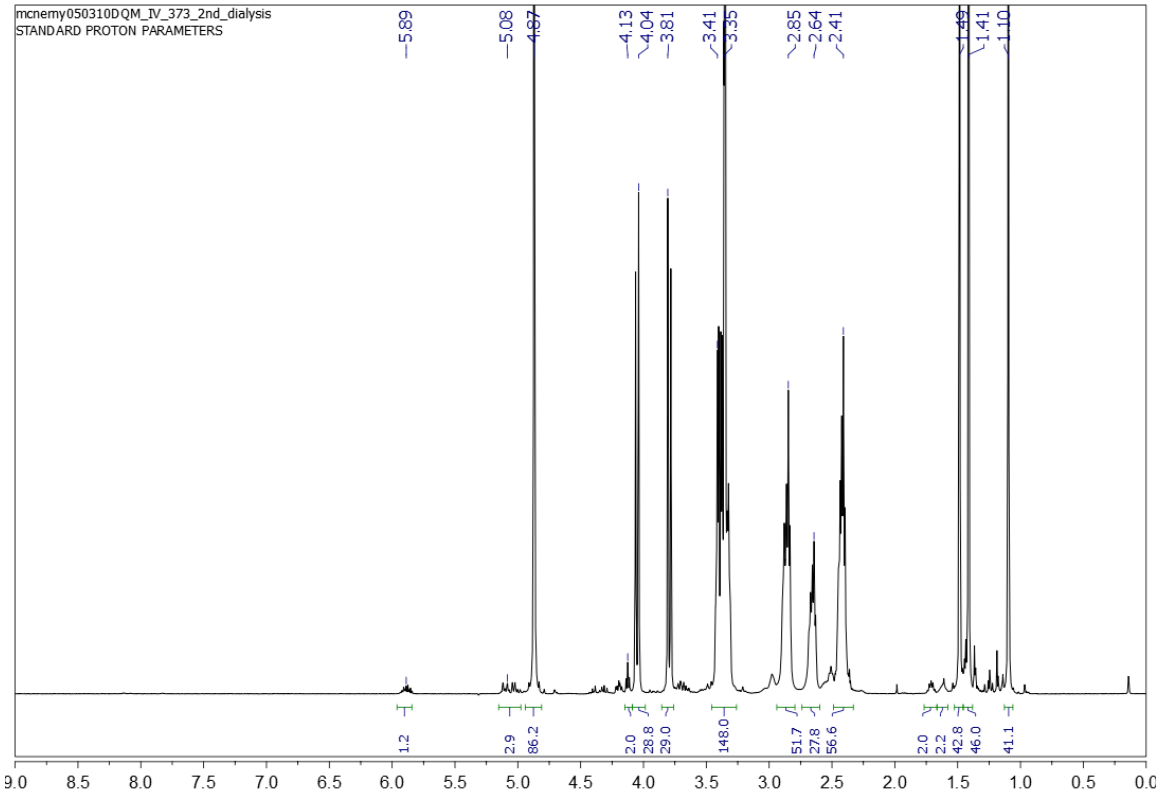


$^{1}$H NMR (500 MHz, MeOH-d): δ = 5.82 (m, 1H, $CH_2$-C*H*-$CH_2$), 5.03 (m, 2H, C*H*$_2$-CH-$CH_2$), 4.07 (t, 2H, CO-O-C*H*$_2$-$CH_2$), 4.00 (m, 32H, O-CH*H*-C), 3.77 (m, 32H, O-C*H*H-C), 3.43-3.20 (m, 64H, NH-C*H*$_2$-$CH_2$-$NH_2$, NH-C*H*$_2$-$CH_2$-N), 2.86 (m, 60H, N-C*H*$_2$-$CH_2$-CO, 28H, NH-$CH_2$-C*H*$_2$-$NH_2$), 2.65 (t, 28H, NH-$CH_2$-C*H*$_2$-N), 2.43 (m, 60H, N-$CH_2$-C*H*$_2$-CO), 1.65-1.42 (m, 6H, pentanol focal point), 1.46 (s, 48H, C*H*$_3$-C-(O)$_2$), 1.38 (s, 48H, C*H*$_3$-C-(O)$_2$), 1.06 (s, 48H, C*H*$_3$-C-C$_3$).

**Figure S3.10: $^{1}$H NMR spectrum of phenyl-G3(An)$_{16}$**

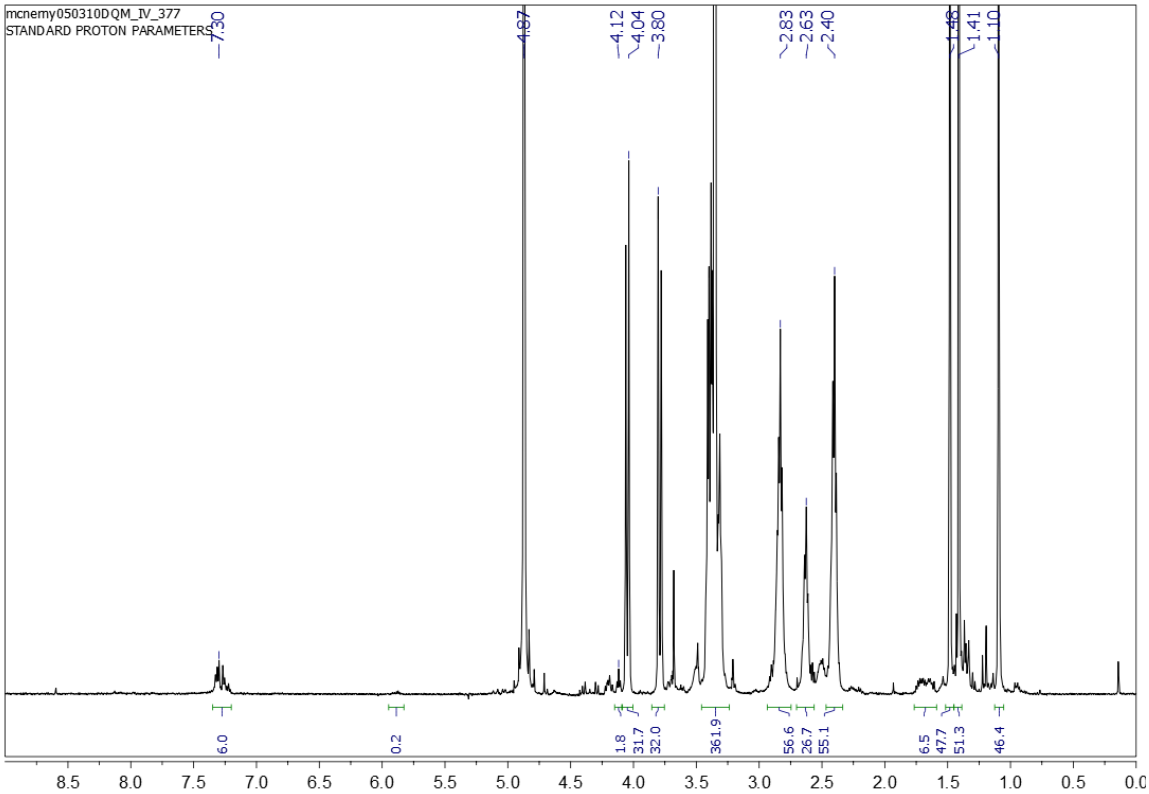


$^{1}$H NMR (500 MHz, MeOH-d): δ = 7.30-7.20 (b, 4H, CH aromatic), 4.07 (t, 2H, CO-O-C*H*$_2$-CH$_2$), 4.00 (m, 32H, O-CH*H*-C), 3.77 (m, 32H, O-C*H*H-C), 3.43-3.20 (m, 64H, NH-C*H*$_2$-CH$_2$-NH$_2$, NH-C*H*$_2$-CH$_2$-N), 2.86 (m, 60H, N-C*H*$_2$-CH$_2$-CO, 28H, NH-CH$_2$-C*H*$_2$-NH$_2$), 2.65 (t, 28H, NH-CH$_2$-C*H*$_2$-N), 2.43 (m, 60H, N-CH$_2$-C*H*$_2$-CO), 1.65-1.42 (m, 6H, pentanol focal point), 1.46 (s, 48H, C*H*$_3$-C-(O)$_2$), 1.38 (s, 48H, C*H*$_3$-C-(O)$_2$), 1.06 (s, 48H, C*H*$_3$-C-C$_3$).

**Figure S3.11: $^{1}$H NMR spectrum of biotin-G3(COOH)(RGD).**

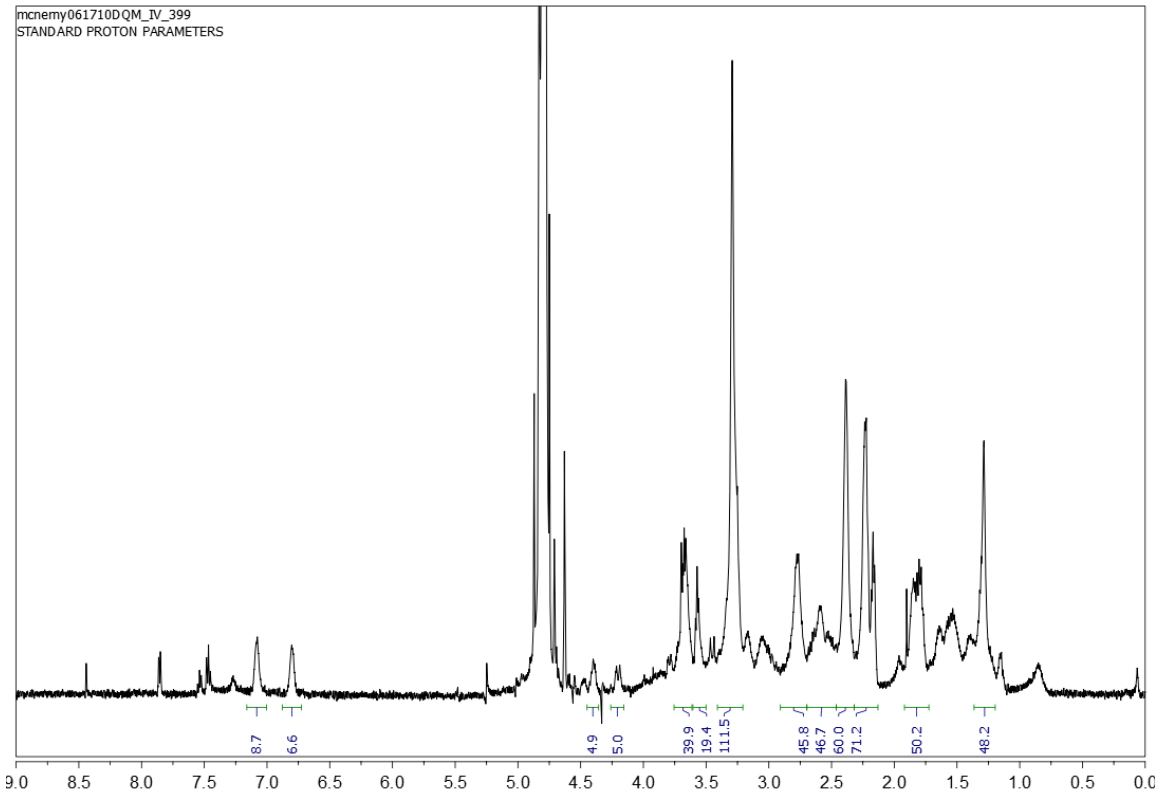


$^{1}$H NMR (500 MHz, MeOH-d):

Dendron backbone: 3.42 (s, 2H, N-C*H*$_2$-CH), 3.30 (m, 92H, NH-C*H*$_2$-CH$_2$-NH$_2$, NH-C*H*$_2$-CH$_2$-N, NH-CH$_2$-C*H*$_2$-NH$_2$), 2.80 (m, 60H, N-C*H*$_2$-CH$_2$-CO), 2.62 (b, 28H, NH-CH$_2$-C*H*$_2$-N), 2.41 (b, 60H, N-CH$_2$-C*H*$_2$-CO), 2.24 (b, 48H, CO-C*H*$_2$-CH$_2$-CH$_2$-CO-OH, CO-CH$_2$-CH$_2$-C*H*$_2$-CO-OH, 2.10-1.75 (m, 48H).

Conjugated RGD: 7.2-6.80 (16.4 H, aromatic RGD protons), 4.40 (8.2H), 4.20 (8.2H), 3.72 (8.2H), 3.10, 1.70 (8.2H), 1.53 (8.2H), 1.35 (8.2H) 1.17 (16.4H). Additional peaks are overlapping with peaks from the dendron backbone.

Biotin: 4.40-4.20 (4H).

REFERENCES

(1) Hoyle, C. E., Lowe, A. B. and Bowman, C. N. (2010) Thiol-click chemistry: A multifaceted toolbox for small molecule and polymer synthesis. Chem.Soc.Rev. **39**, 1355-1387

(2) Yu, B., Chan, J. W., Hoyle, C. E. and Lowe, A. B. (2009) Sequential thiol-ene/thiol-ene and thiol-ene/thiol-yne reactions as a route to well-defined mono and bis end-functionalized poly(*N*-isopropylacrylamide). Journal of Polymer Science Part A: Polymer Chemistry. **47**, 3544-3557

(3) Hoyle, C. E. and Bowman, C. N. (2010) Thiol-ene click chemistry. Angew.Chem.Int.Ed Engl. **49**, 1540-1573

(4) Hensarling, R. M., Doughty, V. A., Chan, J. W. and Patton, D. L. (2009) "Clicking" polymer brushes with thiol-yne chemistry: Indoors and out. J.Am.Chem.Soc. **131**, 14673-14675

(5) Killops, K. L., Campos, L. M. and Hawker, C. J. (2008) Robust, efficient, and orthogonal synthesis of dendrimers via thiol-ene "click" chemistry. J.Am.Chem.Soc. **130**, 5062-5064

(6) Chan, J. W., Hoyle, C. E. and Lowe, A. B. (2009) Sequential phosphine-catalyzed, nucleophilic Thiol−Ene/Radical-mediated Thiol−Yne reactions and the facile orthogonal synthesis of polyfunctional materials. J.Am.Chem.Soc. **131**, 5751-5753

(7) Padilla De Jesus, O. L., Ihre, H. R., Gagne, L., Frechet, J. M. and Szoka, F. C.,Jr. (2002) Polyester dendritic systems for drug delivery applications: In vitro and in vivo evaluation. Bioconjug.Chem. **13**, 453-461

(8) Ihre, H. R., Padilla De Jesus, O. L., Szoka, F. C.,Jr and Frechet, J. M. (2002) Polyester dendritic systems for drug delivery applications: Design, synthesis, and characterization. Bioconjug.Chem. **13**, 443-452

# Chapter 4:
# Orthogonal coupling of dendron platforms via strain-promoted alkyne-azide cycloaddition

## Background

Shortly after the Sharpless group popularized click chemistry through the copper-catalyzed alkyne-azide cycloaddition (1), efforts to find metal-free analogs that avoided *in vivo* cytotoxicity began. An alternative approach pioneered by the Bertozzi group lowers the activation of the [3+2] cycloaddition through the ring strain of cyclooctynes (2, 3). The strained alkynes orthogonally react with azides to form triazoles under ambient conditions. Ring-strain click chemistry has been successfully employed for the *in vivo* labeling of cells (4, 5), however, wide-spread application of this technique was limited due to the tedious, multi-step, low yield reactions required to synthesize the cyclooctynes.

Work by the Shultz and Weck groups pioneered the synthesis of cyclooctynes in 3 high-yield reactions (6, 7), facilitating ring-strain click chemistry in many applications. The Weck group successfully employed ring-strain click chemistry to the terminal azide groups of polyamine dendrons by reacting with a 3 molar excess of cyclooctyne achieving near quantitative yields. The ring-strain cycloaddition may be more attractive than thiol-based click chemistry (detailed in Chapter 3) due to its higher degree of orthogonality and the ease of introducing either cyclooctyne or azide moieties compared to the thiol or alkene.

In this study, we explored the use of ring-strain click chemistry to orthogonally couple dendrons through their focal point. Similar to the work described in Chapter 3, polyester dendrons were used as a model to first evaluate reaction conditions and identify the NMR signals that result from a successful click reaction between azide and cyclooctyne groups. Subsequently, PAMAM dendrons with an azide focal-point were reacted with the cyclooctyne model. Finally, synthesis of PAMAM dendrons was attempted from a cyclooctyne focal point.

**Experimental procedures**

**General**: Polyester dendrons were purchased from Polymer Factory (Sweden) and used without additional purification. PAMAM dendrons with azide focal points were prepared as described in Chapter 2.

**Synthesis of 8,8-dibromobicyclo[5.1.0]octane (21).** Cycloheptene (1.00 g, 10.4 mmol) and potassium tert-butoxide (1.34 g, 12.0 mmol) were added to anhydrous pentane (26 ml) and cooled to 0°C. A solution of bromoform (6.63 g, 10.4 mmol) in anhydrous hexane (26 ml) was added drop-wise over a period of 3 h at 0°C under argon. After complete addition the burnt orange mixture turned brown and was warmed to room temperature and stirred overnight. After addition of water and neutralization with conc. HCl, the aqueous layer was extracted with pentane (3 x 30 ml). The combined organic layers were washed with water (3 x 30 ml) and dried over $Na_2SO_4$. Evaporation of the solvent under high vacuum gave the product (1.3246 g, 47.65 %) as a brown oil.

**Synthesis of methyl 10-((Z)-2-bromocyclooct-2-enyloxy)decanoate (22). 21** (0.80 g, 3 mmol) and methyl 10-hydroxydecanoate (7.25 g, 36 mmol, 12 eq) were dissolved in anhydrous $MeNO_2$ (14.95 ml) in an aluminum foil wrapped flask under nitrogen. $AgClO_4$ (1.86 g, 9 mmol) was added and the resulting suspension was stirred at room temperature under argon for 30 min. After addition of pentane (80 ml) and filtration, the solvent was evaporated under reduced pressure. Flash column chromatography (cHex/EtOAc) afforded the product (0.34 g, 29.2 %) as a light yellow oil.

**Synthesis of 10-(cyclooct-2-ynyloxy)decanoic acid (23). 22** (0.34 g, 0.087 mmol) was dissolved in anhydrous DMSO (3.97 ml) and heated to 60 °C. DBU (0.26 mL) was added, the resulting solution was stirred for 15 min, and more DBU (1.05 mL) was added. The mixture was stirred at 60 °C overnight and then cooled to room temperature. Water (0.87 ml) followed by sodium methoxide (0.189 g, 0.35 mmol) was added to the muddy brown mixture, and the resulting suspension was stirred for 1 h. After acidification to pH 1 with 1 M HCl, the aqueous phase was extracted with EtOAc (5 x 100 ml) and the combined organic layers were dried over $Na_2SO_4$ and evaporated under reduced pressure. Flash column chromatography (cHex/EtOAc 9:1, 1 % HOAc) afforded the product (0.121 g, 46.93 %) as a light yellow oil. MS (ESI MS-): 292.8 Da; calculated for $C_{18}H_30O_3$: 294.2 Da.

**Synthesis of COOH-PE.G3-OH (24).** Azide-PE.G3-OH (0.0100 g, 0.00531 mmol) and **23 (**0.0078 g, 0.027 mmol) were dissolved in 2:1 methanol/water (2 mL).

The solution was stirred at room temperature for 24 hours. The solvents were removed and the product was washed twice with EtOAc in order to remove excess cyclooctyne. MS (MALDI): 1230-1275 Da; calculated for $C_{59}H_{99}N_3O_{25}$: 1249.7 Da.

**Synthesis of COOH-G2($NH_2$)$_8$ (25).** Azide-G2($NH_2$)$_8$ **(8)** (0.0085 g, 0.0050 mmol) and **23** (0.0074 g, 0.025 mmol) were dissolved in 2:1 methanol/water (2 mL). The reaction mixture was allowed to stir for 24 hours at room temperature. All solvent was removed *in vacuo*, and the reaction material was washed with EtOAc to remove excess cyclooctyne. MS (MALDI): 1900-2020 Da; calculated for $C_{91}H_{180}N_{32}O_{17}$: 1993.4 Da.

**Synthesis of N-(2-aminoethyl)-10-(cyclooct-2-yn-1-yloxy)decanamide (26).** 1-(3-(dimethylamino)propyl)-3-ethylcarbodiimide HCl (EDC) (0.0649 g, 0.339 mmol) was allowed to react with **23** (0.0500 g, 0.169 mmol) in anhydrous $CH_2Cl_2$ (5 mL) for 2 hours to form an active ester. Ethylenediaime (1.0179 g, 16.936 mmol) in anhydrous $CH_2Cl_2$ (5 mL) was added dropwise to the EDC and cyclooctyne solution and stirred for 2 days at room temperature. Flash column chromatography (MeOH/$CHCl_3$ 20:80) afforded the product as a light yellow oil. MS (ESI MS+): 337.3 Da; calculated for $C_{20}H_{36}N_2O_2$: 336.3 Da.

**Synthesis of Cyclooctyne-G(-0.5) (27).** **26** (0.0250 g, 0.0737 mmol) in 1:1 methanol/$CH_2Cl_2$ (2 mL) was added dropwise to a stirred solution of methyl acrylate (0.0507 g, 0.589 mmol) in methanol (1 mL) under nitrogen in an ice bath. The mixture was allowed to warm to room temperature and stirred for 5 days. The solvent was

removed under reduced pressure at 40°C using a rotary evaporator and the resulting colorless oil dried under vacuum to give the final product. MS (ESI MS+): 509.3 Da; calculated for $C_{28}H_{48}N_2O_6$: 508.4 Da.

**Synthesis of Cyclooctyne-G0 (28).** **27** (0.0300 g, 0.0590 mmol) in chloroform (0.5 mL) was added dropwise to a solution of ethylenediamine (0.8867 g, 14.75 mmol) in methanol (1 mL) in an ice bath. The mixture was allowed to warm to room temperature and stirred for 5 days. The solvent was removed under reduced pressure at 40°C using a rotary evaporator and the resulting colorless oil dried under vacuum to give the final product. MS (ESI MS+): 273.2 Da, 357.3 Da, 459.3 Da, 565.4 Da; calculated for $C_{30}H_{56}N_6O_4$: 564.4 Da.

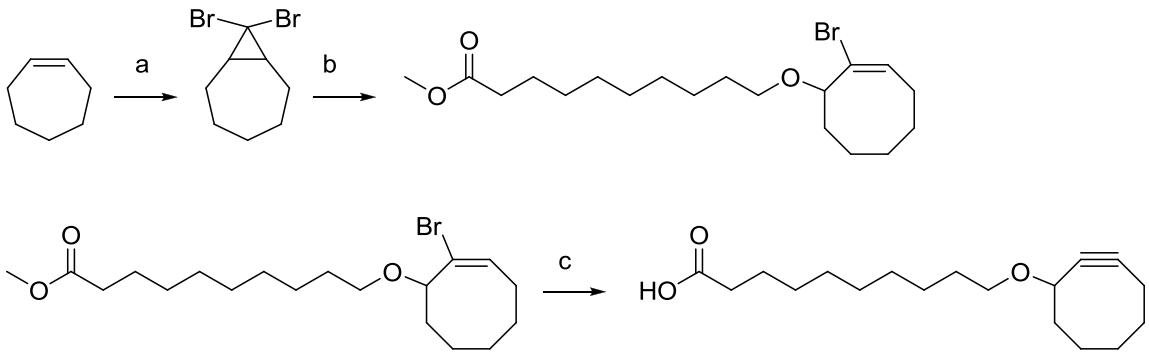


**Figure 4.1.** Synthesis scheme for the cyclooctyne used for ring-strain reactions with dendrons. a) potassium tert-butoxide, pentane, bromoform, hexane, 0°C to room temperature, overnight, b) methyl 10-hydroxydecanoate, $MeNO_2$, $AgClO_4$, 30 min, c) DMSO, DBU, 60°C overnight, water, sodium methoxide, 1 hr, acidification with 1 M HCl.

**Results and Discussion**

Strain-promoted alkyne-azide cycloadditions were explored as an alternative to copper-catalyzed click chemistry to orthogonally functionalize the focal point of dendron platforms. The cyclooctyne (Figure 4.1) was synthesized by using a protocol modified

from Shultz (7). The cyclooctyne was successfully reacted with both polyester and PAMAM dendrons (Figure 4.2) with azide focal points; the dendron additionally helped solubilize the hydrophobic cyclooctyne ligand. Work up of the reaction was minimal; the solvents were removed using a rotary evaporator and the product was washed with EtOAc to remove excess cyclooctyne. Progress of the cycloaddition was determined by $^{1}H$ NMR using the integration the four triazole regioisomers peaks between 4.2 and 4.8 ppm that are formed upon a successful click reaction (Figure 4.3). The multiple characteristic signals of the triazole formation provide a useful advantage compared to the copper-catalyzed variant, where a single proton peak is located in the sometimes crowded aromatic region of the spectra.

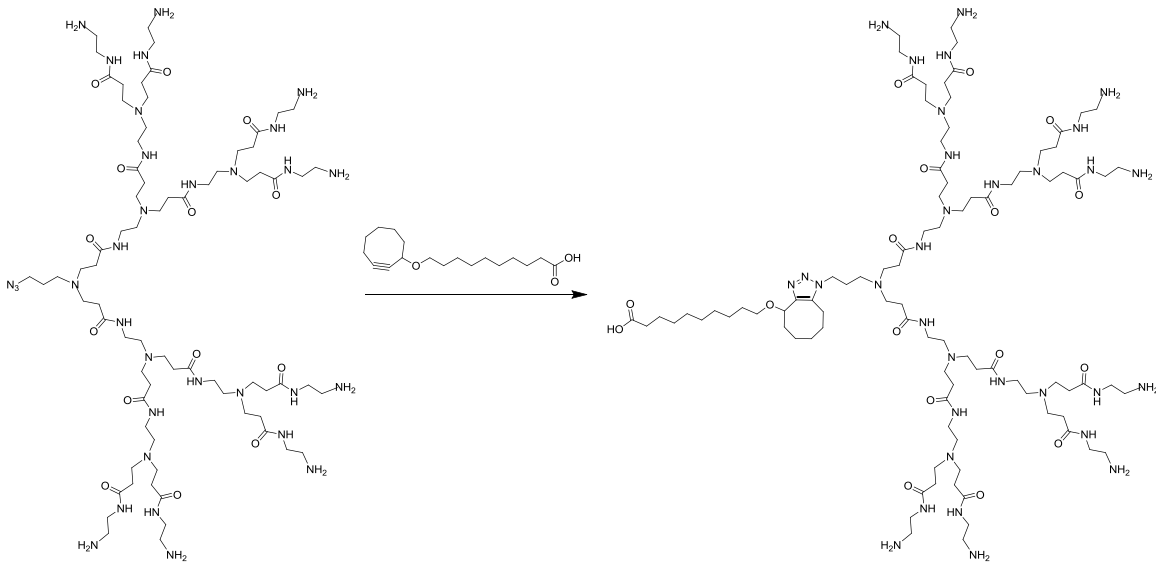

**Figure 4.2.** Generation 2 PAMAM dendron with an azide focal point was reacted with 10-(Cyclooct-2-ynyloxy)decanoic acid to quantitatively yield dendron with a carboxyl focal point. The azide and ring-strained alkyne form a triazole ring following a successful click reaction.

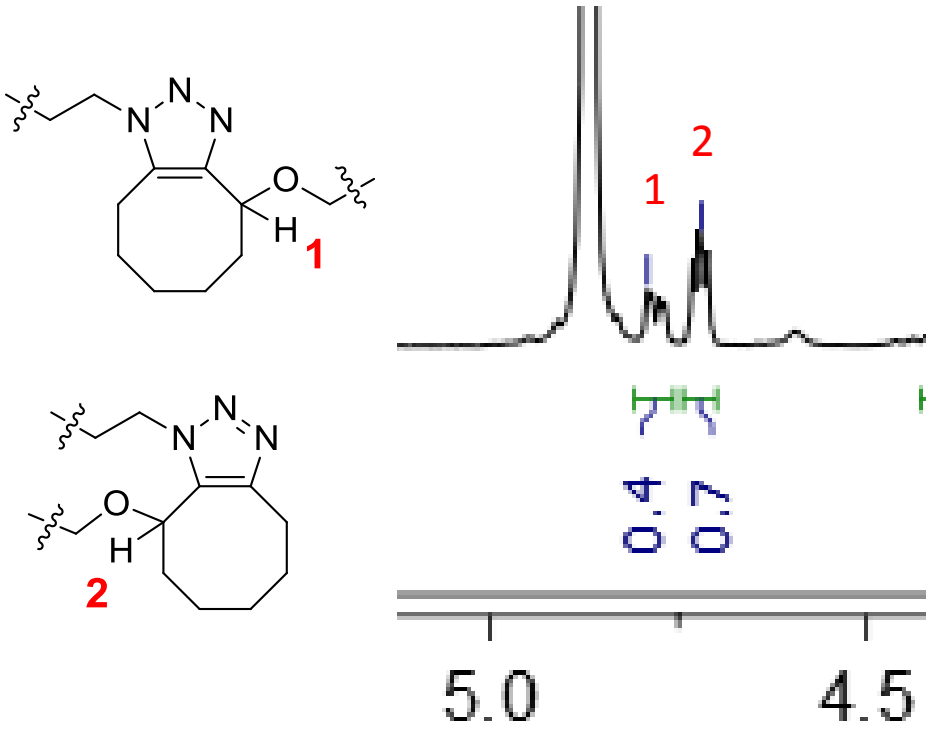


**Figure 4.3.** NMR peaks of isomer products from the ring-strain alkyne-azide cycloaddition.

The high conversion and ease of monitoring the orthogonal strain-promoted cycloaddition reaction makes it a highly attractive system for future dendron design. We began to synthesize PAMAM dendrons with a cyclooctyne focal point with the intent of creating hybrid modular structures of previously unobtainable scalability (Figure 4.4). **23** was reacted with ethylenediamine to yield the core of the dendron. Traditional dendrimer synthesis employs repeating growth steps using methyl acrylate and ethylenediamine; unfortunately, when the amidation step to synthesize generation 0 dendron, **28**, was performed it caused the formation of a significant percentage of side products. According to the $^{1}$H spectra, greater than 50% of the reaction product had lost its ring-strained alkyne. Future work is needed to examine the molecular events of these side reactions and if they can be minimized. These side reactions severely restrict the ability

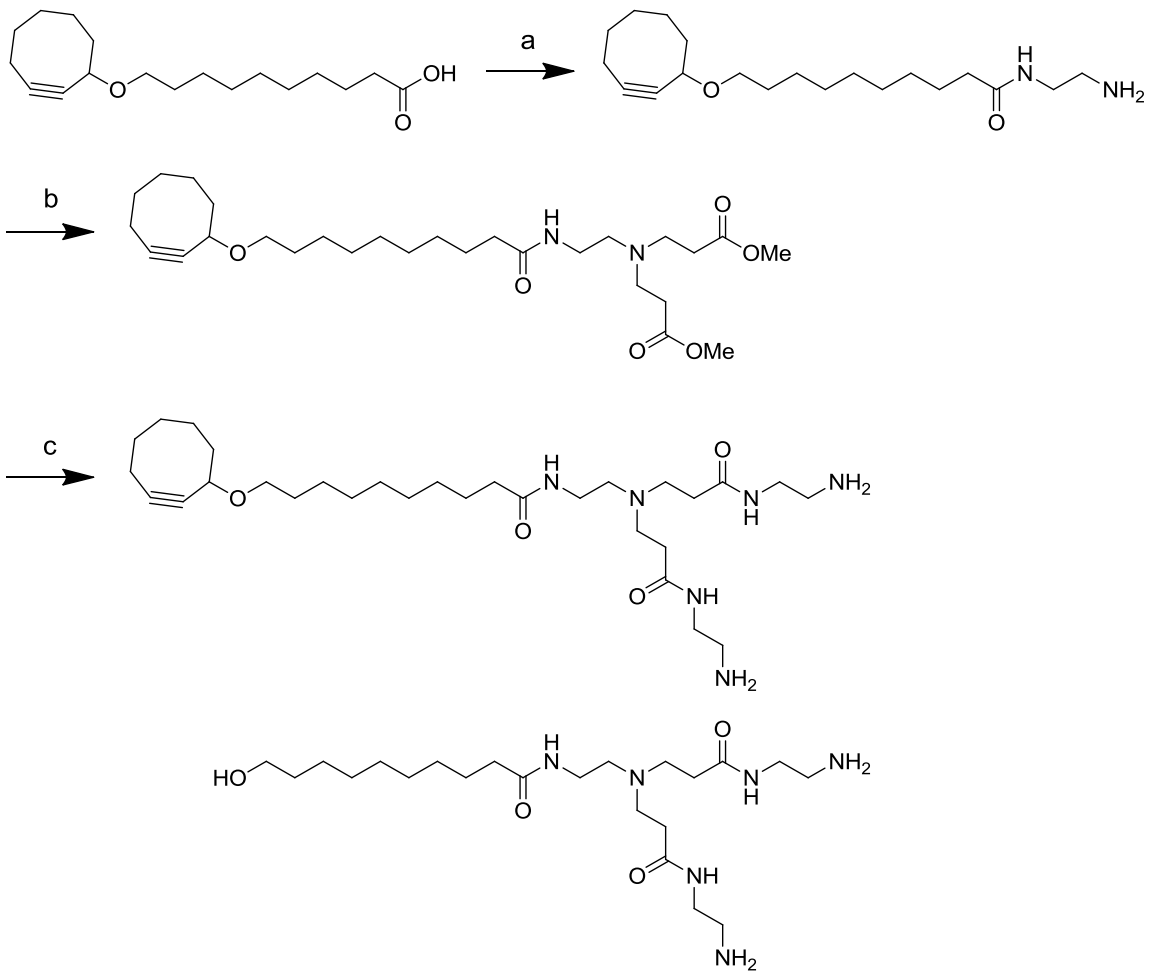


**Figure 4.4.** Growth of PAMAM dendrons from a cyclooctyne core. Significant side products formed during the synthesis of generation 0 material. a) EDC, ethylene diamine, $CHCl_3$, 2 days, b) methyl acrylate, $MeOH/CHCl_2$, 4 days, c) ethylene diamine, $MeOH/CHCl_2$, 7 days. The final amidation step yielded several side products, including a dendron with the cycloocctyne cleaved from the focal point.

to synthesize higher generation dendrons from a cyclooctyne core using tradition growth schemes.

Despite this setback, the high efficiency and orthogonality of the ring-strain cycloaddtion warrants additional exploration as a means to assemble dendritic platforms. The discovery of alternative mechanisms to introduce azide or cyclooctyne moieties into

dendron would allow for the synthesis of Janus dendrimers and thus should remain an important focus of future research.

**Acknowledgments:** Emily C. Salans, Ankur M. Desai, Baohua Huang, Hong Zong and James R. Baker Jr. made essential contributions to the work in this chapter.

## Chapter 4 Appendix

**Figure S4.1: $^{1}$H NMR spectrum of 10-(Cyclooct-2-ynyloxy)decanoic acid.**

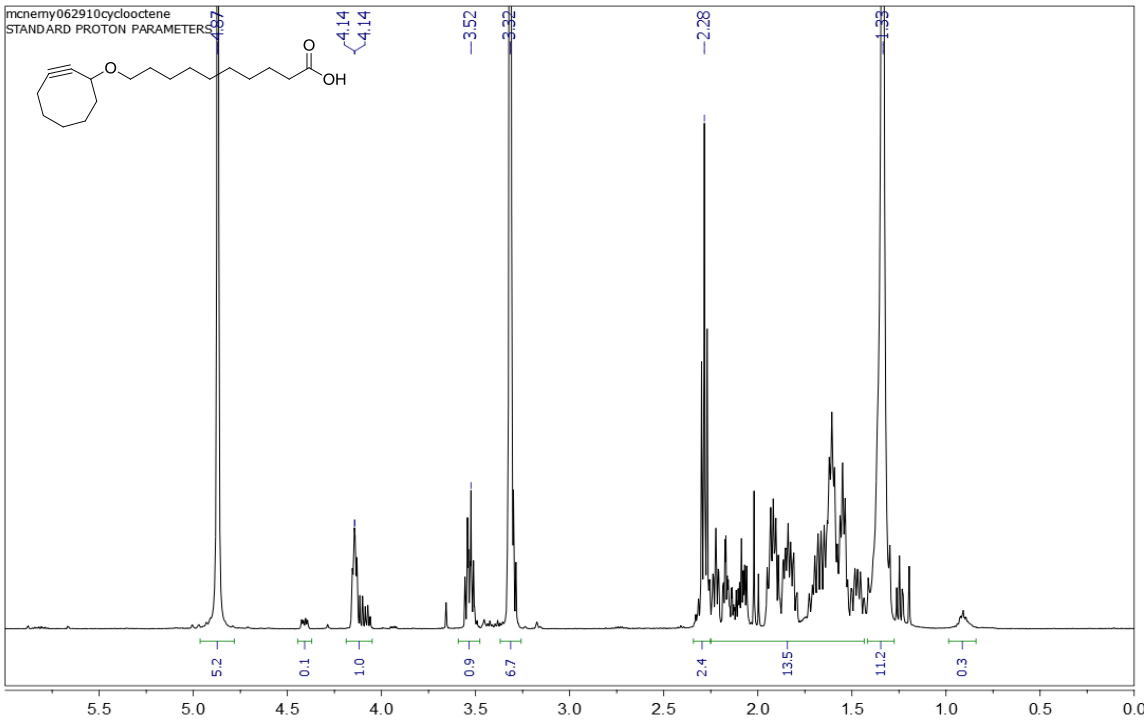


$^{1}$H NMR (500 MHz, MeOH-d): δ = 4.13-4.17 (m, 1H, C*H*$_{propargyl}$), 3.52 (dt, 1H, C*H*H), 3.29 (dt, 1H, OCH*H*), 2.28 (t, 2 H, C*H*2(CO)OH), 2.22-2.28 (m, 1H, C*H*H$_{propargyl}$), 2.08-2.19 (m, 2H, OCHC*H*H,CH*H*$_{propargyl}$), 1.89-1.98 (m, 2H, OCHCH*H*, OCH(CH$_2$)$_3$C*H*H), 1.77-1.86 (m, 2H, OCHCH$_2$C*H*H, OCH(CH$_2$)$_3$CH*H*), 1.53-1.73 (m, 6H, CH(CH$_2$)$_2$C*H*$_2$, OCH$_2$C*H*$_2$, C*H*$_2$CH$_2$(CO)OH), 1.39-1.47 (m, 1H, OCHCH$_2$CH*H*), 1.33 (bs, 10H, C*H*$_2$C*H*$_2$C*H*$_2$C*H*$_2$C*H*$_2$(CH$_2$)$_2$(CO)OH).

**Figure S4.2: $^{1}$H NMR spectrum of azide-PE.G3-OH.**

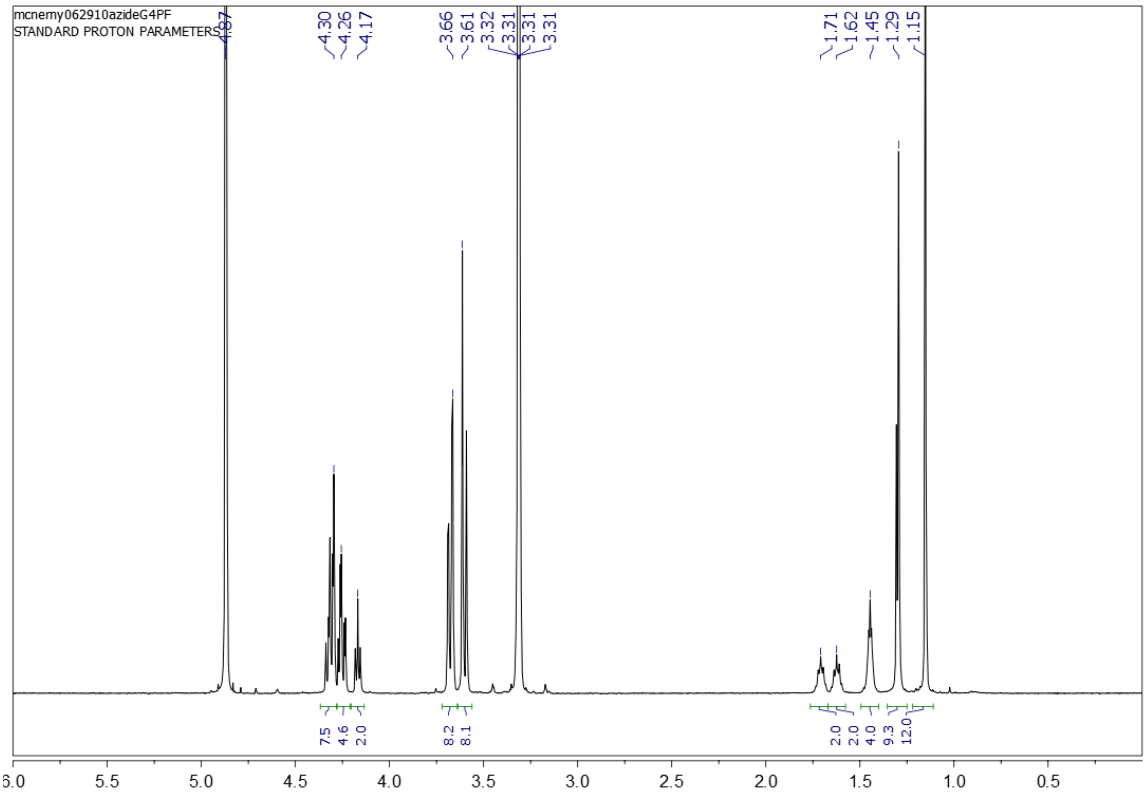


$^{1}$H NMR (500 MHz, MeOH-d): δ = 4.38-4.20 (m, 12H, O-C*H*$_2$-C), 4.17 (s, 2H, O-C*H*$_2$-CH$_2$), 3.75-3.65 (d, 8H, OH-C*H*$_2$-C), 3.65-3.55 (d, 8H, OH-C*H*$_2$-C), 1.71 (qt, 2H, O-CH$_2$-C*H*$_2$-CH$_2$), 1.62 (qt, 2H, O-CH$_2$-CH$_2$-C*H*$_2$), 1.45 (m, 4H, C*H*$_2$-C*H*$_2$-CH$_2$-N$_3$), 1.30 (s, 3H, C*H*$_3$-C), 1.29 (s, 6H, C*H*$_3$-C), 1.15 (s, 12H, C*H*$_3$-C).

**Figure S4.3: $^{1}$H NMR spectrum of COOH-PE.G3-OH.**

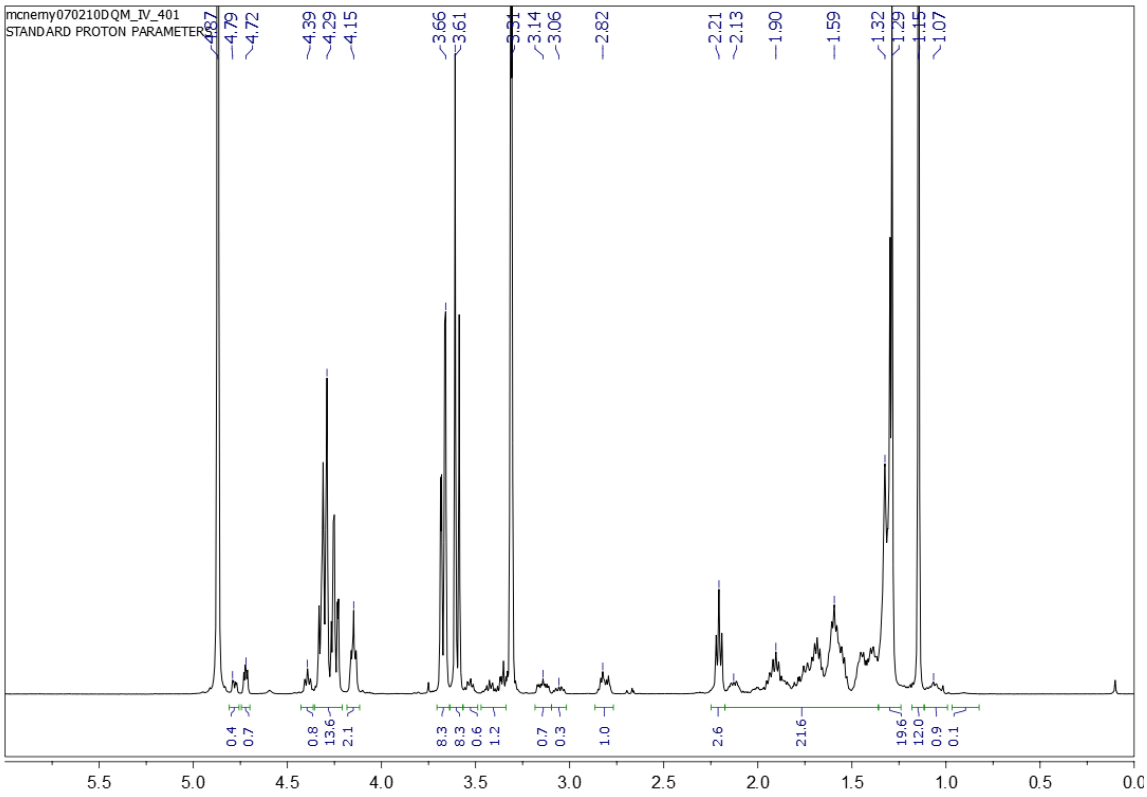


$^{1}$H NMR (500 MHz, MeOH-d):

Conjugated cyclooctyne δ = 3.52 (dt, 1H, C*H*H), 3.29 (dt, 1H, OCH*H*), 2.28 (t, 2H, C*H*2(CO)OH), , 1.89-1.98 (m, 2H, OCHCH*H*, OCH$(CH_2)_3$C*H*H), 1.77-1.86 (m, 2H, OCHC$H_2$C*H*H, OCH$(CH_2)_3$CH*H*), 1.53-1.73 (m, 6H, CH$(CH_2)_2$C$H_2$, OC$H_2$C$H_2$, C$H_2$C$H_2$(CO)OH), 1.39-1.47 (m, 1H, OCHC$H_2$CH*H*), 1.33 (bs, 10H, C$H_2$C$H_2$C$H_2$C$H_2$C$H_2$$(CH_2)_2$(CO)OH).

Dendron: δ = 4.38-4.20 (m, 12H, O-C$H_2$-C), 4.17 (s, 2H, O-C$H_2$-$CH_2$), 3.75-3.65 (d, 8H, OH-C$H_2$-C), 3.65-3.55 (d, 8H, OH-C$H_2$-C), 1.71 (qt, 2H, O-$CH_2$-C$H_2$-$CH_2$), 1.62 (qt, 2H, O-$CH_2$-$CH_2$-C$H_2$), 1.45 (m, 4H, C$H_2$-C$H_2$-$CH_2$-$N_3$), 1.30 (s, 3H, C$H_3$-C), 1.29 (s, 6H, C$H_3$-C), 1.15 (s, 12H, C$H_3$-C).

Triazole formation: 4.79, 4.72 (1H), 4.39 (1H)

**Figure S4.4: $^{1}$H NMR spectrum of Azide-G2$(NH_2)_8$.**

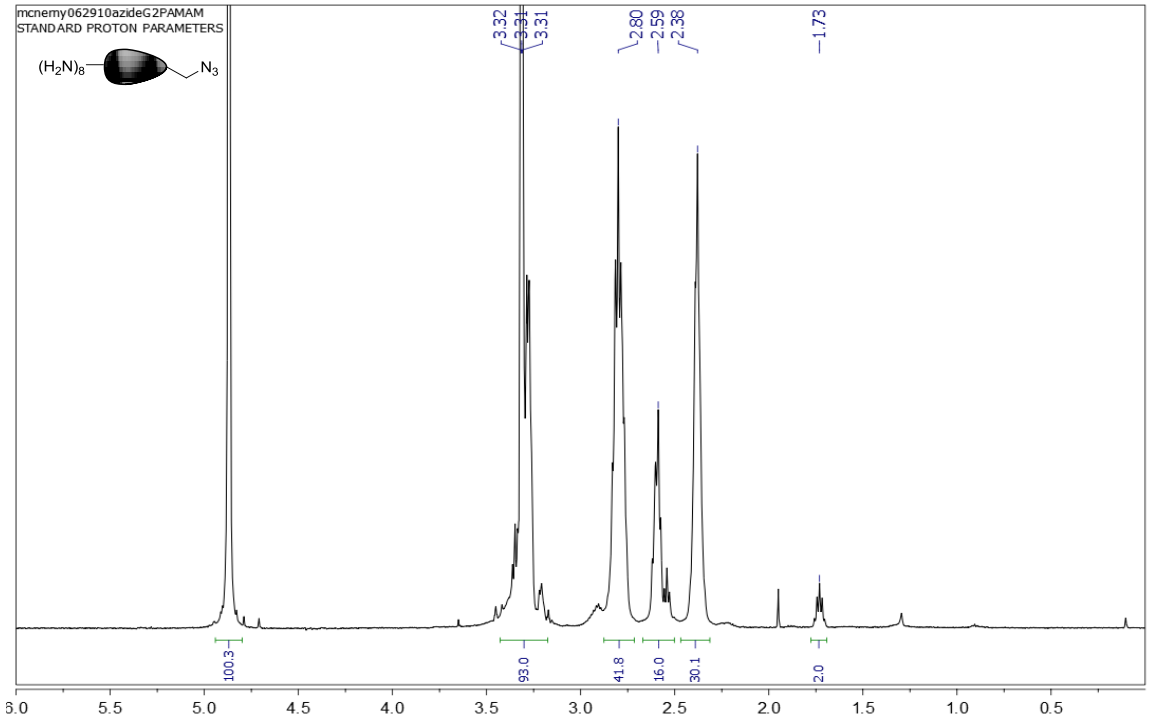


$^{1}$H NMR (500 MHz, MeOH-d): δ = 3.50-3.10 (34H, NH-C*H*$_2$-CH$_2$-NH$_2$, NH-C*H*$_2$-CH$_2$-N), 2.81 (28H, N-C*H*$_2$-CH$_2$-CO, 12H, NH-C*H*$_2$-CH$_2$-N), 2.59 (12H, NH-CH$_2$-C*H*$_2$-N), 2.55 (2H, N$_3$-CH$_2$-CH$_2$-C*H*$_2$-N), 2.38 (28H, N-CH$_2$-C*H*$_2$-CO, "e"), 1.73 (2H, N$_3$-CH$_2$-C*H*$_2$-CH$_2$-N).

**Figure S4.5: $^{1}$H NMR spectrum of COOH-G2$(NH_2)_8$.**

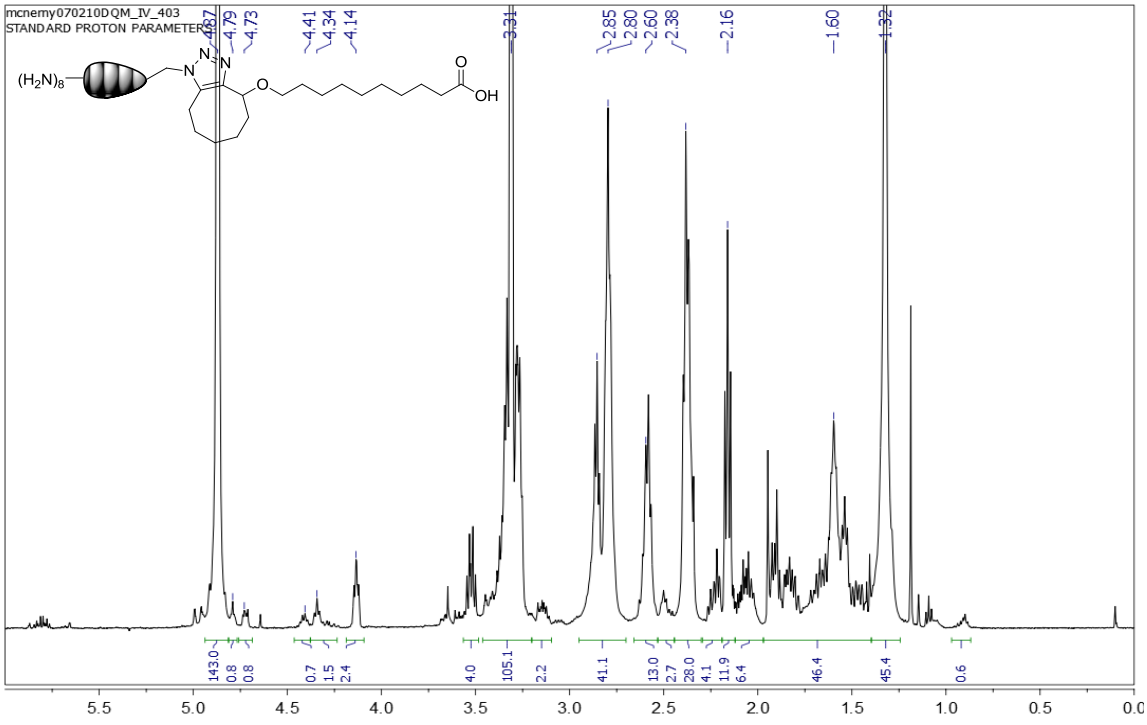


$^{1}$H NMR (500 MHz, MeOH-d):

Conjugated cyclooctyne δ = 3.52 (dt, 1 H, C*H*H), 3.29 (dt, 1H, OCH*H*), 2.28 (t, 2 H, C*H*2(CO)OH), , 1.89-1.98 (m, 2H, OCHCH*H*, OCH$(CH_2)_3$C*H*H), 1.77-1.86 (m, 2H, OCHC$H_2$C*H*H, OCH$(CH_2)_3$CH*H*), 1.53-1.73 (m, 6H, CH$(CH_2)_2$C$H_2$, OC$H_2$C$H_2$, C$H_2$C$H_2$(CO)OH), 1.39-1.47 (m, 1H, OCHC$H_2$CH*H*), 1.33 (bs, 10H, C$H_2$C$H_2$C$H_2$C$H_2$C$H_2$$(CH_2)_2$(CO)OH).

Dendron δ = 3.50-3.10 (34H, NH-C$H_2$-C$H_2$-$NH_2$, NH-C$H_2$-C$H_2$-N), 2.81 (28H, N-C$H_2$-C$H_2$-CO, 12H, NH-C$H_2$-C$H_2$-N), 2.59 (12H, NH-C$H_2$-C$H_2$-N), 2.55 (2H, $N_3$-C$H_2$-C$H_2$-C$H_2$-N), 2.38 (28H, N-C$H_2$-C$H_2$-CO, "e"), 1.73 (2H, $N_3$-C$H_2$-C$H_2$-C$H_2$-N).

Triazole formation: 4.79, 4.73 (1H), 4.41, 4.34 (1H)

**Figure S4.6: $^{1}$H NMR spectrum of N-(2-aminoethyl)-10-(cyclooct-2-yn-1-yloxy)decanamide.**

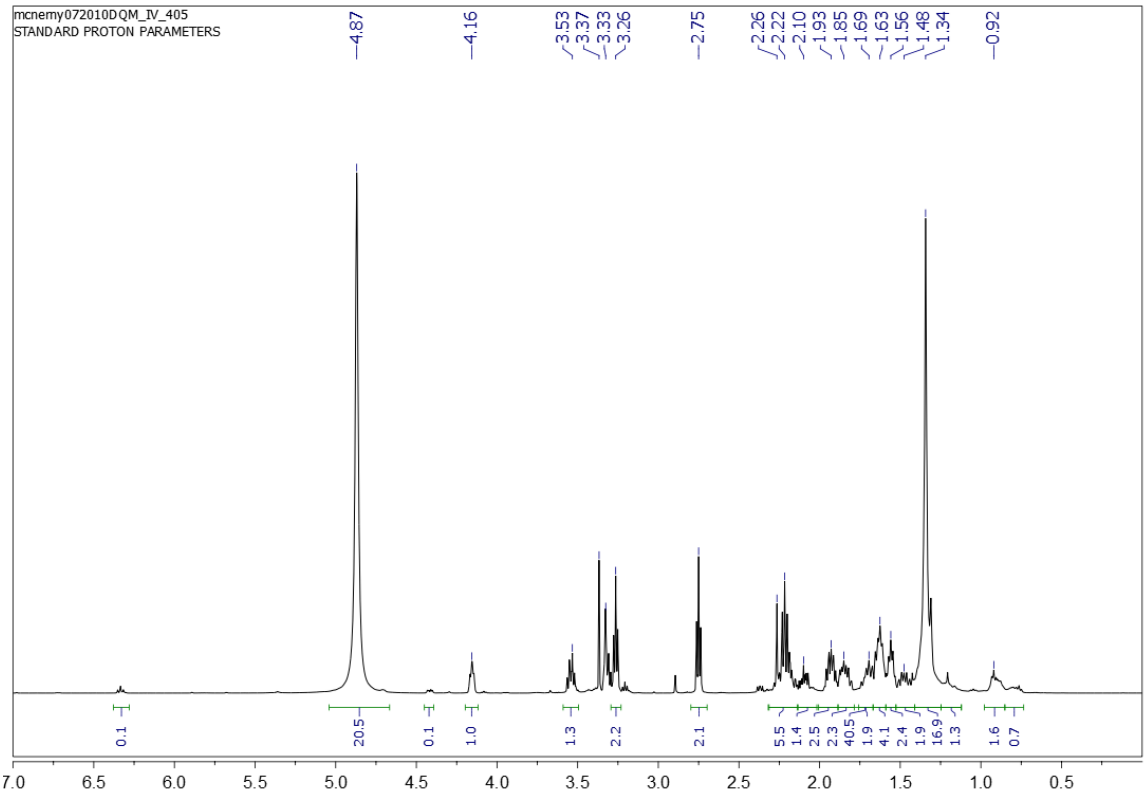


$^{1}$H NMR (500 MHz, MeOH-d): δ = 4.13-4.17 (m, 1H, C*H*$_{propargyl}$), 3.52 (dt, 1H, C*H*H), 3.29 (dt, 1H, OCH*H*), 3.26 (t, 2H, NH-C*H*$_2$-CH$_2$-NH$_2$), 2.75 (t, 2H, NH-CH$_2$-C*H*$_2$-NH$_2$), 2.15 (t, 2H, C*H*2(CO)NH), 2.22-2.28 (m, 1H, C*H*H$_{propargyl}$), 2.08-2.19 (m, 2H, OCHC*H*H,CH*H*$_{propargyl}$), 1.89-1.98 (m, 2H, OCHCH*H*, OCH(CH$_2$)$_3$C*H*H), 1.77-1.86 (m, 2H, OCHCH$_2$C*H*H, OCH(CH$_2$)$_3$CH*H*), 1.53-1.73 (m, 6H, CH(CH$_2$)$_2$C*H*$_2$, OCH$_2$C*H*$_2$, C*H*$_2$CH$_2$(CO)OH), 1.39-1.47 (m, 1H, OCHCH$_2$CH*H*), 1.33 (bs, 10H, C*H*$_2$C*H*$_2$C*H*$_2$C*H*$_2$C*H*$_2$(CH$_2$)$_2$(CO)OH).

**Figure S4.7: $^{1}$H NMR spectrum of Cyclooctyne-G(-0.5).**

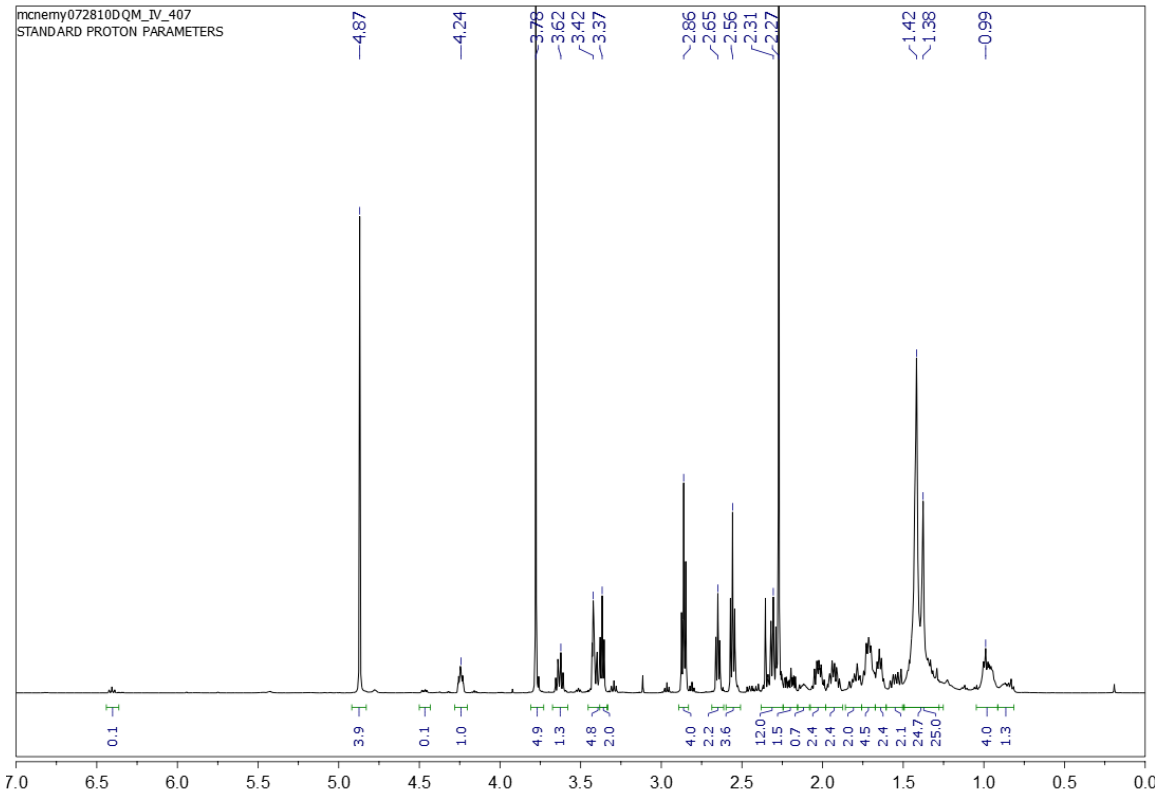


$^{1}$H NMR (500 MHz, MeOH-d): δ = 4.24 (m, 1H, C*H*$_{propargyl}$), 3.78 (s, 6H, $CH_3$-O-CO), 3.22 (dt, 1H, C*H*H), 3.42 (dt, 1H, OCH*H*), 3.37 (t, 2H, NH-C*H*$_2$-$CH_2$-$NH_2$), 2.86 (t, 4H, N-C*H*$_2$-$CH_2$-COO), 2.65 (t, 2H, NH-$CH_2$-C*H*$_2$-N), 2.56 (t, 4H, N-$CH_2$-C*H*$_2$-COO), 2.15 (t, 2H, C*H*2(CO)NH), 2.22-2.28 (m, 1H, C*H*H$_{propargyl}$), 2.08-2.19 (m, 2H, OCHC*H*H,CH*H*$_{propargyl}$), 1.89-1.98 (m, 2H, OCHCH*H*, OCH$(CH_2)_3$C*H*H), 1.77-1.86 (m, 2H, OCHC$H_2$C*H*H, OCH$(CH_2)_3$CH*H*), 1.53-1.73 (m, 6H, CH$(CH_2)_2$C*H*$_2$, $OCH_2$C*H*$_2$, C*H*$_2$$CH_2$(CO)OH), 1.39-1.47 (m, 1H, OCHC$H_2$CH*H*), 1.42 (bs, 10H, C*H*$_2$C*H*$_2$C*H*$_2$C*H*$_2$C*H*$_2$$(CH_2)_2$(CO)OH).

**Figure S4.8: $^{1}$H NMR spectrum of Cyclooctyne-G0.**

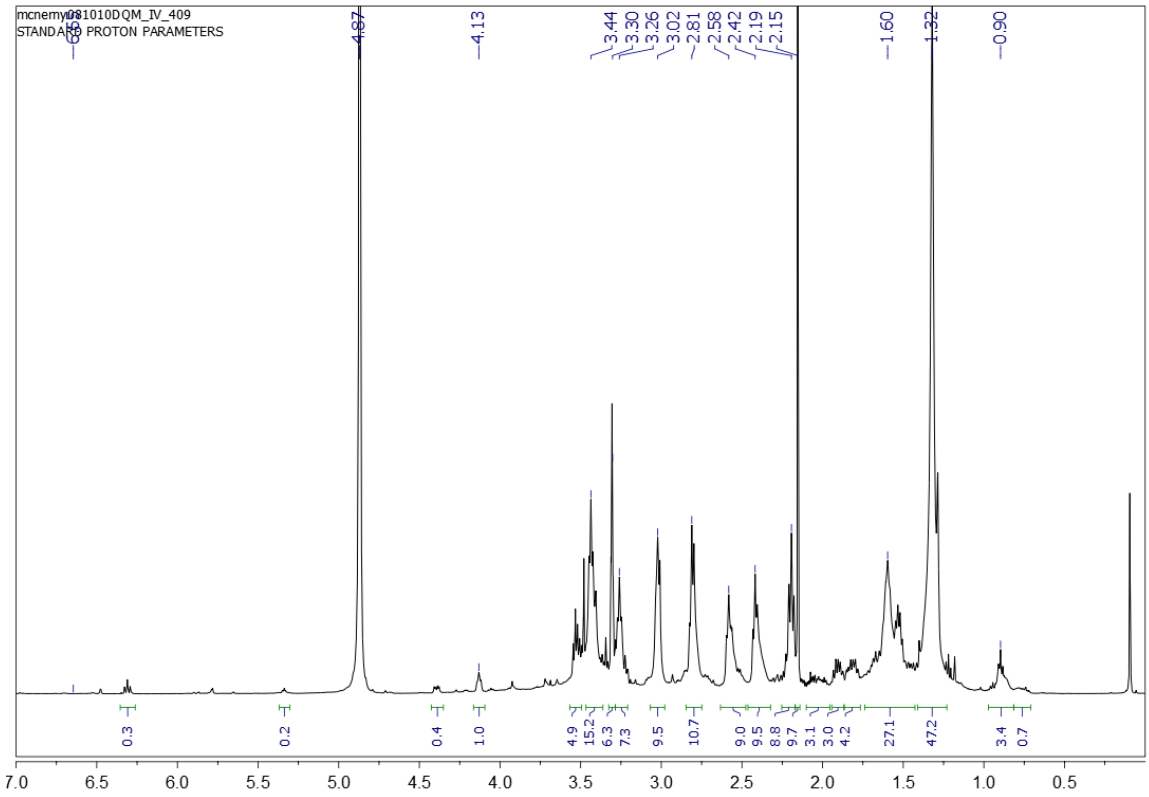


**Note significant loss of cyclooctyne proton at 4.13**

**Figure S4.8: HPLC of alkyne-PE.G3-OH and COOH-PE.G3-OH**

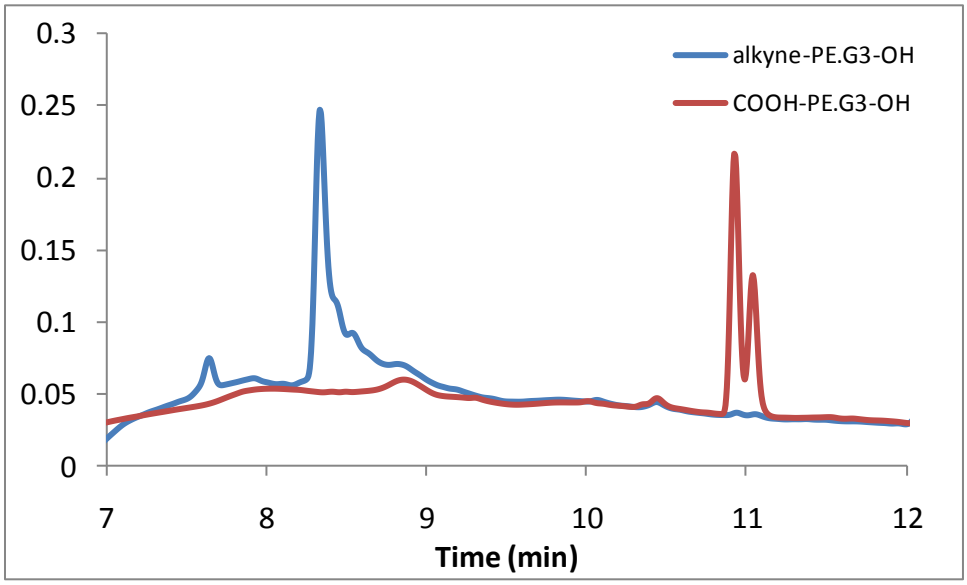

REFERENCES

(1) Kolb, H. C., Finn, M. G. and Sharpless, K. B. (2001) Click chemistry: Diverse chemical function from a few good reactions. Angew.Chem.Int.Ed Engl. **40**, 2004-2021

(2) Agard, N. J., Prescher, J. A. and Bertozzi, C. R. (2004) A strain-promoted [3 + 2] azide-alkyne cycloaddition for covalent modification of biomolecules in living systems. J.Am.Chem.Soc. **126**, 15046-15047

(3) Jewett, J. C., Sletten, E. M. and Bertozzi, C. R. (2010) Rapid cu-free click chemistry with readily synthesized biarylazacyclooctynones. J.Am.Chem.Soc. **132**, 3688-3690

(4) Jewett, J. C. and Bertozzi, C. R. (2010) Cu-free click cycloaddition reactions in chemical biology. Chem.Soc.Rev. **39**, 1272-1279

(5) Chang, P. V., Prescher, J. A., Sletten, E. M., Baskin, J. M., Miller, I. A., Agard, N. J., Lo, A. and Bertozzi, C. R. (2010) Copper-free click chemistry in living animals. Proc.Natl.Acad.Sci.U.S.A. **107**, 1821-1826

(6) Ornelas, C., Broichhagen, J. and Weck, M. (2010) Strain-promoted alkyne azide cycloaddition for the functionalization of poly(amide)-based dendrons and dendrimers. J.Am.Chem.Soc. **132**, 3923-3931

(7) Neef, A. B. and Schultz, C. (2009) Selective fluorescence labeling of lipids in living cells. Angew.Chem.Int.Ed Engl. **48**, 1498-1500

# Chapter 5:
# Conclusions and future directions

## Thesis findings

Poly(amidoamine) (PAMAM) dendritic platforms have been explored extensively for diagnostic and therapeutic applications that take advantage of their ability to (A) conjugate a wide variety of functional groups including targeting and drug moieties, (B) increase payloads by conjugating multiple copies of bioactive ligands to the many arms of the branched structure, and (C) solubilize hydrophobic molecules. Unfortunately, despite the low polydispersity of the dendritic backbone these platforms have been slow to reach clinicians due to difficulties in characterizing multifunctional devices and problems with the synthesis of these materials at larger scales. Recent work exploring ligand distribution on stochastic dendrimer platforms shows the synthesis of these molecules often results in a wide population distribution width in a single product mixture. If the biologically functional molecules are only a small portion of this population or, even worse, if a percentage of material has an undesirable behavior, then it is unlikely the material will perform as desired in biomedical applications.

Orthogonal or modular pathways to construct multifunctional dendritic devices could overcome the limitations of conventional dendrimer platforms by providing greater degree of specificity and flexibility in reaction conditions. Monofunctionalized materials can be individually characterized and smaller modular units can reduce or replace stochastic distributions to ensure quality and improve reproducibility. The work detailed

in this thesis shows for the first time that biologically functional platforms can be synthesized from PAMAM dendrons via orthogonal conjugation chemistries. Additionally, we explore various orthogonal click chemistry strategies to broaden the utility of the platform and dendritic materials.

Our initial studies with PAMAM dendrons utilized CuAAC to create biologically functional binary devices capable of specifically targeting integrin-expressing cell lines. The RGD-functionalized PAMAM dendron maintained the binding specificity and multivalency of previous dendrimers models (1, 2) while creating an orthogonally coupled scaffold that is more uniform than other approaches. A wide variety of azide-functional molecules, AlexaFluor 488, biotin, methotrexate or a second dye-conjugated dendron, were successfully coupled to the alkyne focal point. However, problems remain with this approach since CuAAC requires extensive purification to remove the potentially toxic copper catalyst. CuAAC was also shown to display less than quantitative reaction efficiencies and it is hypothesized that this reaction is hindered by complexation of the catalyst with the polyamine structures.

We explored alternative click chemistry reactions that would avoid the use of metal catalysts, specifically thiol-ene and thiol-yne reactions, discussed in Chapter 3, and ring-strain alkyne-azide cycloadditions, addressed in Chapter 4. For the thiol-ene reaction, a single alkene group was inserted by modifying the focal point of commercially available PAMAM dendrons. The thiol-yne reaction was used on the alkyne focal point dendron first detailed in Chapter 2. Both thiol-based click reactions provided near-quantitative yields in our model systems. Unfortunately, excess free ligand used in the coupling reactions was difficult to remove from generation 2 and 3 dendrons employing

our standard purification techniques: size exclusion chromatography and dialysis. The inability to remove free ligand using these techniques and the high loss of product during dialysis was seen at a much higher rate using the commercial material than with our higher quality in-house dendron used in Chapter 2, possibly suggesting small molecular weight dendron contaminants. Purification remains a vexing problem with dendrons, as it is with other dendritic platforms. Regardless, the successful adaptation of thiol click chemistry is a significant step towards scalable modular platforms.

The ring-strain alkyne-azide cycloaddition explored in Chapter 4 also provided near-quantitative synthesis of dendron platforms by attaching a cyclooctyne ligand to azide-focal point dendrons. The high degree of orthogonality and ease of monitoring the reaction progress makes this perhaps the most exciting class of click chemistry for future dendron platforms. Model PAMAM dendrons were synthesized from a cyclooctyne core, though progress was halted at generation 0 due to significant formation of side products during the amidation step. Additional work is necessary to determine if these side products can be eliminated or minimized or if alternative means of introducing the cyclooctyne can be devised.

**Future of PAMAM dendron platform design**

The synthesis of PAMAM dendritic platforms remains a laborious, time-intensive practice. Due to this fact, commercially available dendrons with a hydroxyl focal point were used in the majority of work in Chapter 3 as we explored alternative orthogonal coupling mechanisms. The structure of the commercial dendron was less than ideal for orthogonal functionalization because any ester reaction of the focal point would be prone

to hydrolysis and the reactive surface amines of the dendron would need to be capped to allow the hydroxyl to be modified. These problems limit the applicability of the commercial dendron by restricting the functional groups and chemistry that are compatible with the platform. However, this material successfully allowed us to screen different coupling mechanisms, a task that would have taken much longer than the timeframe of this thesis had dendrons been synthesized from the appropriate asymmetrical cores without any prior knowledge of the success of the orthogonal reaction.

Now that this information is available, specifically tailored dendrons can be confidently synthesized. We propose several logical designs, but surely additional approaches will be possible.

*Thiol-ene PAMAM dendron platforms*

PAMAM dendrons used for thiol-ene reactions will likely be the least versatile of the click reactions explored. Because alkene groups are reacted during the Michael addition growth steps of the dendron, any focal point alkene must be inserted following the completion of dendron synthesis. A proposed platform (Figure 5.1) would call for a mono-protected diamine core, followed by traditional repeating growth steps. The terminal amines would be hydroxylated, followed by deprotection of the focal point. The alkene can then be introduced through an amide bond. Alternatively, the amines can be appropriately functionalized and neutralized prior to deprotection and focal point modification, provided the surface ligand is neither sensitive to the deprotection conditions nor has competing reactive sites.

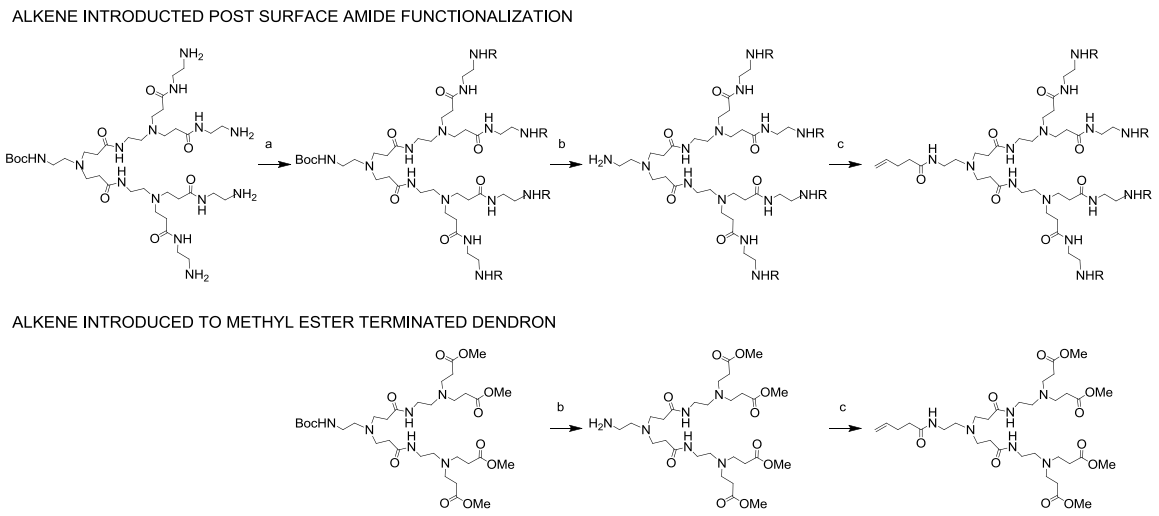


**Figure 5.1.** Proposed synthesis scheme of PAMAM dendrons for thiol-ene click chemistry. The alkene functional group is inserted at the dendron focal point after modification of the surface amines of full-generation dendrons (top) or to half-generation dendrons (bottom). a) surface modification of primary amines, b) deprotection of the NH-Boc group at the dendron focal point, c) insertion of the alkene group to the focal point via an anhydride reaction.

Another potential approach would be to reduce cystamine core dendrimers to afford dendrons with thiol focal points for reactions with alkene-functionalized materials. However, this approach is not as attractive since it has been reported in literature (3) and seen from in own observations that cystamine core dendrimers have numerous defect structures.

*Ring-strain PAMAM dendron platforms*

The most logical platform, however, would be to synthesize the dendron from a cyclooctyne core as described in Chapter 4. Unfortunately, the application of this approach was limited as a percentage of the strained ring was lost during the amidation step. Further work will investigate the stability of the cyclooctyne throughout the dendron growth process to determine if reaction conditions can be altered to minimize defects. If stability is proven a concern or side products are not minimized during the

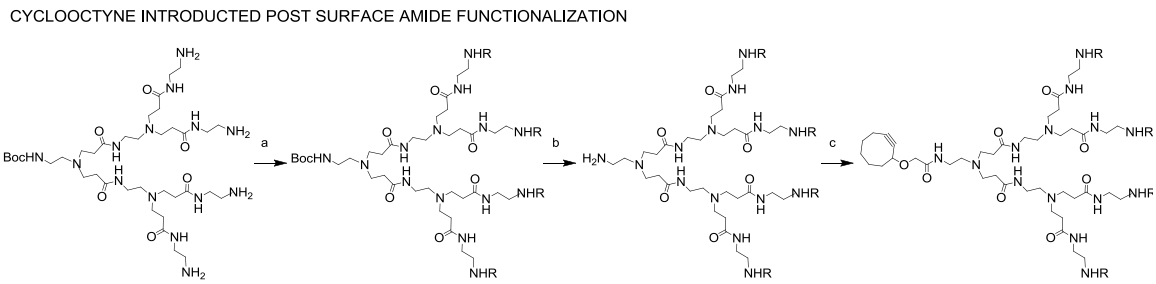


**Figure 5.2.** Proposed synthesis scheme of PAMAM dendrons for ring-strain click chemistry. The cyclooctyne functional group is inserted at the dendron focal point after modification of the surface amines of full-generation dendrons. a) surface modification of primary amines, b) deprotection of the NH-Boc group at the dendron focal point, c) insertion of the cyclooctyne group to the focal point via an EDC-coupling reaction.

amidation step, the cyclooctyne should be introduced once the surface amines of the dendron have been appropriately modified (Figure 5.2).

*Convergent dendron synthesis*

I hypothesize that ring-strain systems also have the potential to be designed from convergent means. Convergent synthesis would bypass the exposure of the cyclooctyne to repeated amidation steps and would likely assist in maintaining the structure. The proposed synthetic scheme (Figure 5.3) constructs PAMAM dendrons from smaller building blocks and selective deprotection of trifluoromethyl modified amines and tert-butyl protected esters. The deprotection reactions are selective and avoid the use of any metal catalysts. Briefly, a cyclooctyne core is built to an ester-terminated generation -0.5 dendron. The other building blocks start with mono-protecting ethylene diamine with ethyl trifluoracetate, followed by a Michael addition reaction with tert-butyl acrylate. The amine can be deprotected under basic conditions while the carboxylic acid can be made available under acidic conditions.

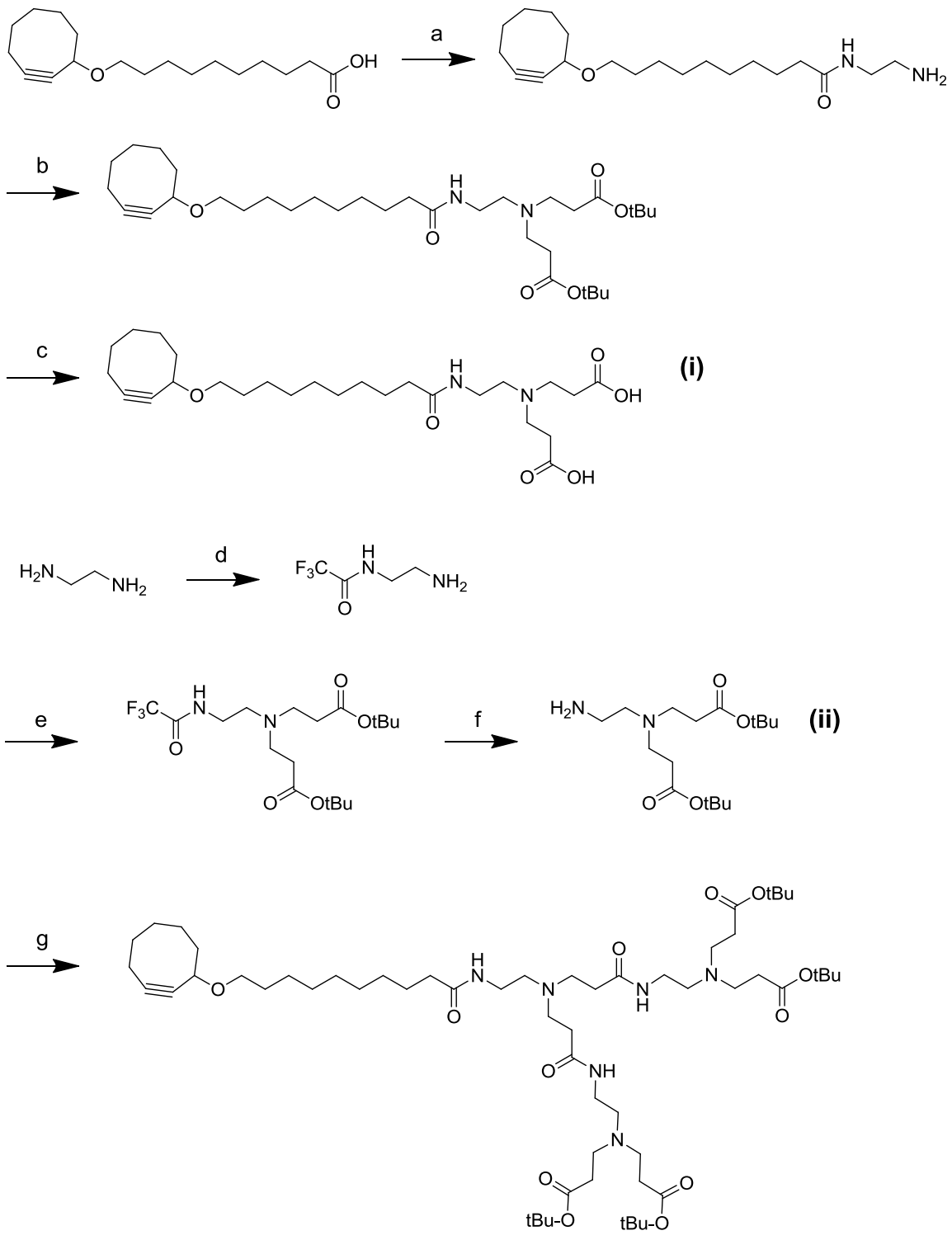


**Figure 5.3.** Proposed convergent synthesis scheme of PAMAM dendrons for ring-strain click chemistry. A cyclooctyne-G(-0.5) dendron is used as the core. a) EDC, ethylene diamine, MeOH/$CHCl_3$, b) tert-butyl acrylate, MeOH, c) formic acid, d) ethyl trifluoroacetate, MeCN, e) tert-butyl acrylate, MeOH, f) NaOH, g) EDC, (i), MeOH.

*Generation: purification / solubility / conversion / removal of distributions*

The appropriate dendron generation of the platform for individual applications is a variable that would benefit from additional research. The bulk of research during this thesis project was performed using generation 3 material. Without a wealth of prioliterature on functionalized PAMAM dendrons or a large supply of material, generation 3 was chosen because it was assumed to solubilize appropriate numbers of functional ligands while still leaving the focal point available. It was determined later that generation 3 was inadequate to solubilize the traditional folic acid/methotrexate therapeutic system, which remains the stable test bed for dendrimer research within the institute. Thus, more hydrophilic RGD was used as a targeting ligand in Chapter 2.

No universal claims can be made as to the appropriate dendron generation as they vary with intended use. However, important criteria should be considered, regardless of application. These criteria include the ability to solubilize the appropriate payload, easily separate the product from impurities, whether by size or solubility, and to quantitatively react the focal point or be able to selectively remove unreacted dendron.

Finally, the distributions of the synthetic products that result from these synthetic strategies should be explored (Figure 5.4). For example, conjugating 4 folic acid to a generation 4 dendron with 32 terminal arms is more feasible than conjugating 4 folic acid to a generation 1 dendron with 4 terminal arms since the generation 1 conjugate will be largely insoluble. However, the synthesis of this generation 4 conjugate will bear a distribution of products with different numbers of folates, from zero to potentially 32; each component will likely have different binding affinities and biological activity. Perhaps chromatographic techniques will improve to the point where components of the

distribution may be isolated for all ligands, as opposed to a select few. Until then, an attractive alternative is to use the generation 1 material without any distribution and solubilize the product through a hydrophilic linker or the coupling of an additional larger hydrophilic dendron module. Smaller generation materials, like the one suggested above, can also offer insight into possible local ligand concentration effects and whether site blocking occurs on multivalent targeting platforms.

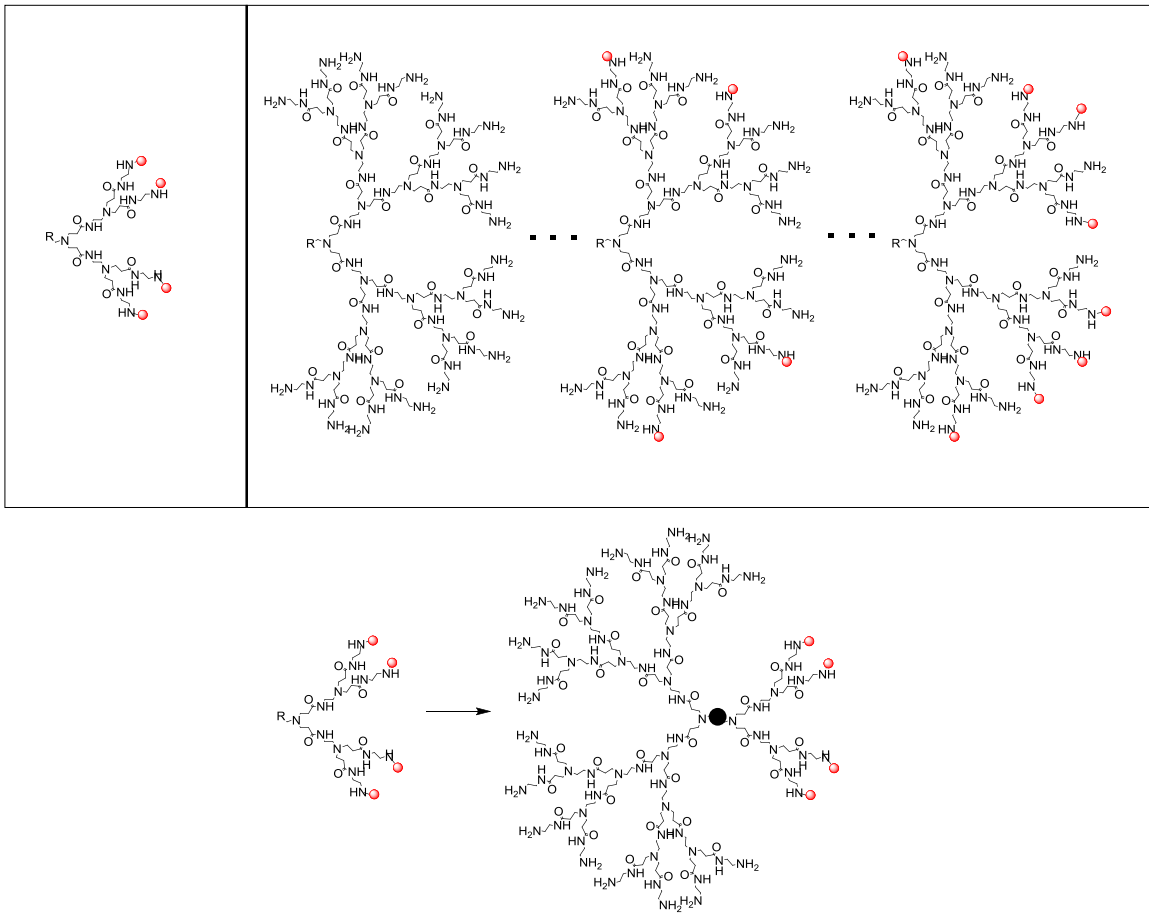

**Figure 5.4.** Proposed generalized dendrons for exploring the role of distributions in functional materials. Smaller dendrons with stoichiometric additions of ligands (top left) would be compared to a dendron distribution synthesized by stochastic coupling of ligands (top right). Solubility of the smaller dendrons could be enhanced by coupling to larger hydrophilic dendron modules (bottom).

## Applications

The original aim of this thesis was to create a wide library of conjugates; this was altered once it was discovered how critical it was to develop orthogonal focal point coupling schemes with quantitative yields. The final thesis largely focuses on approaches to specifically synthesize modular devices, which now hopefully opens doors for functional materials to be made for specific applications.

The most obvious application is to proceed with the design of a library of targeted therapeutics, since individually conjugated modules can be specifically coupled. Dendrons with either the necessary targeting agent or therapeutic to treat a specific malignancy could be joined using the orthogonal methods discussed in this thesis, opening the doors for studies that personalized cancer therapy for specific tumors.

Modular dendrimers can also be designed to be biphasic, creating a class of material with self assembly properties. Recently published work by Percec et al. (4) showed amphiphilic Janus dendrimers can self-assemble into a variety of controlled vesicles. This study used a large library of dendrimers grown from asymmetric cores to provide tunable molecular structure and physical properties. The branched architecture of the dendrimers provides increased control of the size and structure of hydrophobic and hydrophilic regions, allowing for tunable shape, stability, and functionality of its assemblies. Similar libraries could be synthesized from orthogonal coupling through a dendron focal point and applied as to biomembrane for therapeutic activities.

Finally, one area briefly explored is the functionalization of surfaces with dendrons (see Chapter 5 Appendix). A potential application would be to use dendrons

coupled at their focal point to create islands of controlled size and density (Figure 5.5). This could prove important for cellular adhesion studies and activities examining cell behavior, such as proliferation and differentiation, that are affected by localized adhesion proteins (5,6).

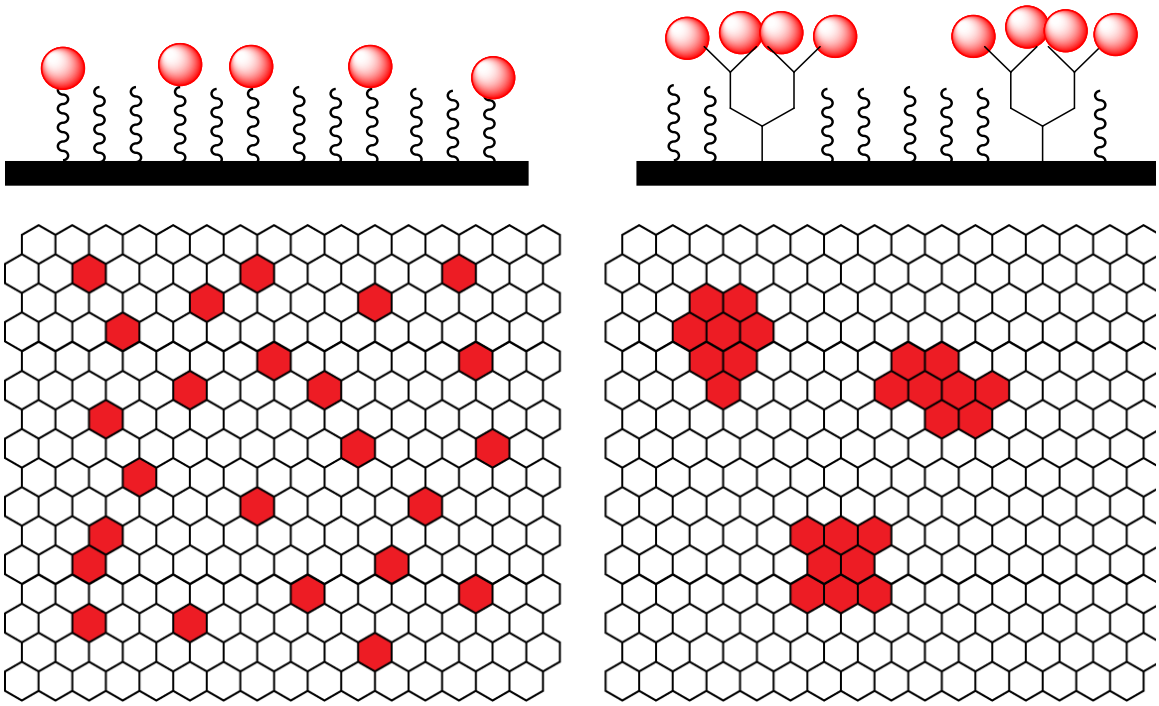

**Figure 5.5.** Representation of local ligand density manipulation on surfaces using dendron islands. Monomeric ligands are randomly distributed (left) while ligands attached to dendron platforms result in an increased local concentration (right).

**Final remarks**

It should be acknowledged that PAMAM backbones, while exhibiting superior biological compatibility compared to other dendritic backbones, may not be the most appropriate for modular coupling due to the difficulties introducing orthogonal groups to a PAMAM dendron focal point. The eventual modular, dendritic material that meets commercial demand will exhibit similar or improved biological activity compared to traditional PAMAM backbones while having a simplistic and scalable synthesis protocol

capable of quantitative orthogonal coupling. However, the orthogonal coupling strategies discussed and developed in this thesis can be applied to a wide variety of modular platforms beyond PAMAM dendrons. Thus, the impact of this thesis extends far beyond the limits of any single material and provides an approach applicable to nearly any modular polymeric system.

## Chapter 5 Appendix

As part of the development and testing of a photonic crystal biosensor, PAMAM dendron was synthesized with a precise number of biotin (one) to its focal point. Briefly, in the experimental setup, biotin is attached to a modified silica surface. Streptavidin is then flowed over the cell, forming a monolayer upon binding with biotin. The biotin-conjugated dendron was then run, attaching to the remaining available sites on the streptavidin monolayer. The biotin-dendron was shown to specifically bind to the streptavidin.

The photonic crystal total-internal-reflection sensor was successful in detecting molecules of a wide range of molecular weights (244 Da to 150,000 Da) with high sensitivity (7).

**Biotin-G3 synthesis**. A mixture of biotin-dPEG$_{3+4}$-azide (0.0029 g, 0.0040 mmol) and alkyne-G3-(NH$_2$)$_{16}$ (0.0105 g, 0.00198 mmol) in 1:1 DMSO/H$_2$O (1 mL) in the presence of copper(II) sulfate (0.0099 g, 0.040 mmol) and sodium ascorbate (0.0314 g, 0.158 mmol) was stirred for 36 hours at room temperature. The solution was purified on a G-25 Sephadex column and lyophilized.

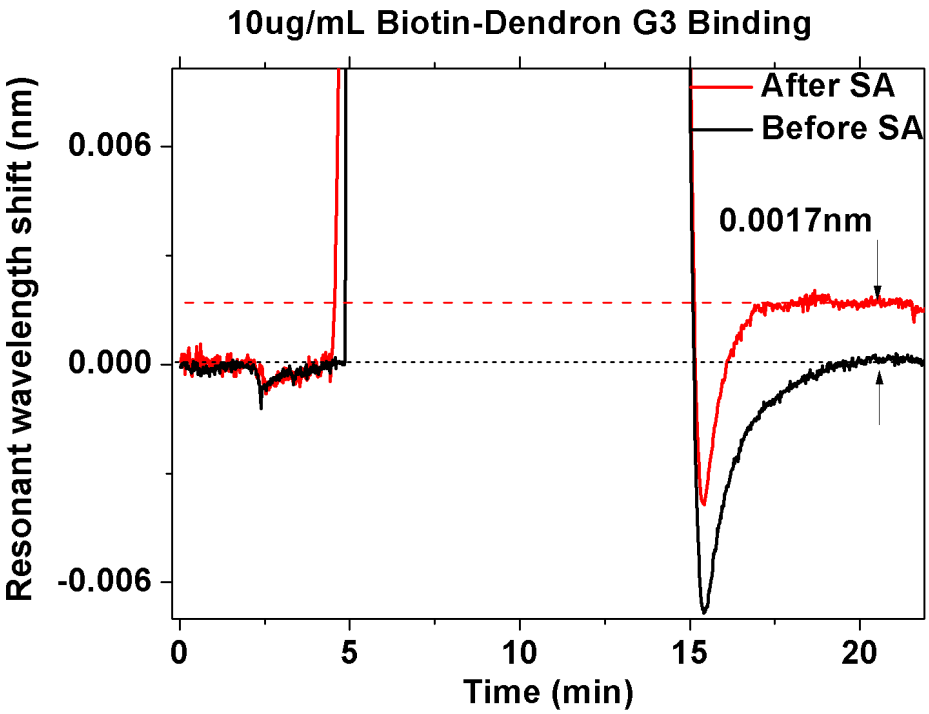
10ug/mL Biotin-Dendron G3 Binding
Resonant wavelength shift (nm)
0.006
0.000
-0.006
0
5
10
15
20
Time (min)
After SA
Before SA
0.0017nm

REFERENCES

(1) Shukla, R., Thomas, T. P., Peters, J., Kotlyar, A., Myc, A. and Baker Jr, J. R. (2005) Tumor angiogenic vasculature targeting with PAMAM dendrimer-RGD conjugates. Chem.Commun.(Camb). **(46)**, 5739-5741

(2) Hill, E., Shukla, R., Park, S. S. and Baker, J. R.,Jr. (2007) Synthetic PAMAM-RGD conjugates target and bind to odontoblast-like MDPC 23 cells and the predentin in tooth organ cultures. Bioconjug.Chem. **18**, 1756-1762

(3) Huang, B. and Tomalia, D. A. (2005) Dendronization of gold and CdSe/cdS (core-shell) quantum dots with Tomalia type, thiol core, functionalized poly(amidoamine) (PAMAM) dendrons. J Lumin. **111**, 215-223

(4) Percec, V., Wilson, D. A., Leowanawat, P., Wilson, C. J., Hughes, A. D., Kaucher, M. S., Hammer, D. A., Levine, D. H., Kim, A. J., Bates, F. S., Davis, K. P., Lodge, T. P., Klein, M. L., DeVane, R. H., Aqad, E., Rosen, B. M., Argintaru, A. O., Sienkowska, M. J., Rissanen, K., Nummelin, S. and Ropponen, J. (2010) Self-assembly of janus dendrimers into uniform dendrimersomes and other complex architectures. Science. **328**, 1009-1014

(5) Comisar, W. A., Kazmers, N. H., Mooney, D. J. and Linderman, J. J. (2007) Engineering RGD nanopatterned hydrogels to control preosteoblast behavior: A combined computational and experimental approach. Biomaterials. **28**, 4409-4417

(6) Comisar, W. A., Hsiong, S. X., Kong, H. J., Mooney, D. J. and Linderman, J. J. (2006) Multi-scale modeling to predict ligand presentation within RGD nanopatterned hydrogels. Biomaterials. **27**, 2322-2329

(7) Guo, Y., Ye, J.Y., Divin, C., Huang, B., Thomas, T. P., Baker, J. R.,Jr., and Norris, T. B., (2010) Real-Time Biomolecular Binding Detection Using a Sensitive Photonic Crystal Biosensor. Anal.Chem. **82**, 5211-5218